# 1

# General Introduction and Background of Photofunctional Nanomaterials in Biomedical Applications

*Chunxia Li*[1] *and Jun Lin*[2]

[1] *Shandong University, School of Chemistry and Chemical Engineering, Institute of Frontier Chemistry, Binhai Road, Qingdao 266237, P.R. China*
[2] *Chinese Academy of Sciences, Changchun Institute of Applied Chemistry, State Key Laboratory of Rare Earth Resource Utilization, Renmin Avenue, Changchun 130022, P.R. China*

## 1.1 Introduction to Nanomaterials

From the perspective of human history, the history of human knowledge of the world is the history of the development of scale and materials. With the continuous development of science and technology, human cognition of the world has long exceeded the single macroscopic world, and the emergence of nanotechnology in 1984 has directly brought human beings into an infinite and mysterious "small size, big world." Therefore, as an important tool for human beings to explore the microscopic world, the research and application of nanomaterials have been widely valued by many disciplines in recent years [1].

Nanomaterials are materials that have at least one dimension in three-dimensional space in the nanoscale range (1–100 nm, 1 nm = $10^{-9}$ m) or are composed of them as basic units [2, 3] and are known as "the most promising materials of the 21st century." As research progresses, scientists are gradually discovering that materials with dimensions at the nanoscale can exhibit unique properties that are superior to those of conventional materials in terms of physics, chemistry, optics, thermodynamics, and magnetism [4–6]. This is because the ratio of the number of atoms on the surface of nanomaterials to the total number of atoms increases dramatically as the particle size decreases. The special properties of nanomaterials are as follows.

### 1.1.1 Surface and Interfacial Effects

When the size of a material is reduced to the nanoscale, the number of surface atoms, the surface area, and the surface energy increase dramatically, and at the same time, a large number of unsaturated bonds, dangling bonds, and active centers

*Photofunctional Nanomaterials for Biomedical Applications*, First Edition.
Edited by Chunxia Li and Jun Lin.

appear in nanomaterials, and the surface defects of the material also increase. These defects introduce many surface states in the energy barrier band gap, which become traps for electrons or holes, seriously affecting the optical, photoelectrochemical, and nonlinear optical properties of the materials [7–10]. Therefore, many new properties of nanomaterials are inextricably linked to their surface and interfacial effects.

### 1.1.2 Small Size Effect

When the size of the material is comparable to or smaller than physical quantities, such as the wavelength of light waves (less than 100 nm), the radius of exciton bands of De Broglie wavelengths (1–10 nm), or the coherence length of superconductivity, the periodic boundary conditions of the internal crystals will be disrupted, and the density of atoms near the surface layer of the particles of amorphous nanoparticles will be reduced. This will lead to significant changes in the macroscopic physical and chemical properties (such as sound, light, electricity, magnetism, heat, and mechanics) of the nanomaterials [11–14].

### 1.1.3 Quantum Size Effect

When the size of the material is reduced to the nanometer scale, the electronic energy levels near the metallic Fermi energy level change from continuous to discrete, and the continuous energy band, valence band, and conduction band of semiconductors become discrete energy level structures, and the bandgap broadening phenomenon is called the quantum size effect [15–18]. When the energy level spacing is greater than the thermal, magnetic, electrostatic, photonic, or superconducting condensation energy, nanomaterials will exhibit a range of properties that are very different from those of bulk materials.

### 1.1.4 Macroscopic Quantum Tunneling Effects

When the scale of a material enters the nanometer range, certain macroscopic quantities of nanoparticles (such as particle magnetization intensity, magnetic flux in quantum coherent devices, and electric charge) exhibit tunneling effects that can cross the potential barriers of the macroscopic system and produce changes, known as macroscopic quantum tunneling effect [19–22]. Macroscopic quantum tunneling is the theoretical basis for future microelectronic and optoelectronic devices.

Because of the special properties mentioned above, nanomaterials have many more excellent physicochemical properties than macroscopic materials. Physically, nanomaterials have good electrical conductivity, dielectricity, magnetism, and mechanical properties. From a chemical point of view, nanomaterials are highly active on the surface and are particularly prone to adsorbing other atoms or chemically reacting with other atoms, which greatly improves the catalytic ability of the reaction. As a result, nanomaterials have broad application prospects in many fields such as optoelectronics, environmental science, and biomedicine.

## 1.2 Introduction and Classification of Photofunctional Nanomaterials

The development and application of materials are a sign of the progress of time and human civilization. The history of materials is as long as the history of mankind. Mankind has gone through a long period of Stone Age, Bronze Age, and Iron Age. Nowadays, with the continuous improvement of nanomaterial synthesis technology, research on nanomaterials has gradually shifted to refinement and functionalization. At the same time, with the growing demand for material functions in science and technology and living standards, as well as the cross-fertilization of the frontiers of various disciplines, a wide range of functionalized nanomaterials have emerged.

Functionalized nanomaterials are diverse and wide-ranging, and there are many ways to classify them. Functional nanomaterials can be classified into electrical nanomaterials, magnetic nanomaterials, optical nanomaterials, thermal nanomaterials, acoustic nanomaterials, chemical nanomaterials, invisible nanomaterials, and so on according to their performance, which is spectacular, and a large number of new functional nanomaterials have been introduced every year. Among them, a series of nanomaterials with unique optical properties (light-functional nanomaterials) have been successfully prepared [23–28], which has become one of the hotspots in the field of functionalized nanomaterials in recent years and has been widely applied in many fields, such as bioanalysis and sensing, illumination and display, environmental monitoring and purification, energy conversion and storage, biomedicine, anticounterfeiting, and information.

In fact, the understanding of optical phenomena in nature has a long history, and it can be said that human beings have progressed along with the knowledge of optical phenomena in nature. For example, fire is man's first perception of light, without which human society would not have survived. The propagation and absorption of light profoundly affect all aspects of nature, and without the phenomena of selective absorption, scattering, transmission, and reflection of light by matter, there would be no colors, no heat, no energy transformed by light, and no production of all biomass in nature. Photofunctional nanomaterials are light-driven functional materials that can effectively convert and utilize light energy, an inexhaustible source of clean and renewable energy. To date, the applications of photofunctional nanomaterials are very diverse, but essentially, the same physical and chemical processes take place and follow similar laws, including photon capture, photon absorption and utilization (conversion), and physicochemical processes at the surface interface [29].

### 1.2.1 Capture of Photons

Light has a fluctuating and particle duality (wave-particle duality), and when considering the energy conversion between light and electrons, light is treated as a particle called a photon. The trapping of photons is the first step in the process of light conversion and utilization by photofunctional nanomaterials, and the more

photons that are trapped, the greater the chance that they will be absorbed. It can also be assumed that the photon trapping ability of a material determines the upper limit of its light conversion efficiency. In general, the photon trapping capability of photofunctional nanomaterials can be increased in three directions: broadening the absorption spectral range of the material, reducing the loss of light after it has passed through the material, and increasing the optical range of light in the material.

### 1.2.2 Absorption and Conversion of Photons

In addition to trapping as many photons as possible, photofunctional nanomaterials must have the ability to absorb and convert the trapped photons into phonon vibrations, photogenerated electron-hole pairs, or other energies. When light is shone on a material, various physicochemical effects such as photothermal effect, photoluminescence, photoelectric effect, and photochemical effect, are produced due to electromagnetic vibrations of electromagnetic waves or inelastic collisions of photons.

Among them, the photothermal effect refers to the fact that photothermal materials, after absorbing the energy of light radiation, do not directly cause a change in the internal electronic state but convert the absorbed light energy into the vibration of the crystal point structure (which means the production of phonons), thus causing a temperature rise and the generation of thermal energy [30]. As the research progressed, it was found that the photothermal effect of photofunctional nanomaterials depends not only on the incident light but also on the absorption spectrum of the material itself. Materials are dense systems consisting of a large number of atoms and molecules, and thermal energy is the average kinetic energy of the irregular motion of these particles. In other words, the accelerated motion of atoms and molecules at the microscopic level corresponds exactly to the increased temperature of the material at the macroscopic level (known as heating). The characteristic frequencies of the continuous relative vibrations and rotations of the atoms and molecules in the material are similar to those of infrared light, so they can resonate with external infrared light. Therefore, when a material is irradiated with infrared light, the motion of the atoms and molecules of the material will be enhanced, and a large amount of heat will be emitted. In contrast, the material absorbs less blue-violet light, resulting in less heat generation and a poorer thermal effect.

Photoluminescence is the process by which a material absorbs photons and then re-radiates them [31]. When the material is irradiated with light of a certain wavelength, the electrons in the ground state of the material (mainly $\pi$ electrons and f and d electrons) are excited to a high-energy state, and when the external light stops, the electrons in the excited state will jump back to the ground state. In the process of the electron jump, some of the energy is emitted in the form of photons to accomplish the purpose of the light. Photoluminescence can be divided into two categories according to the delay time: fluorescence and phosphorescence [32]. Fluorescence is the emission of photons immediately after the substance is excited, and the luminescence time is $\leq 10^{-8}$ seconds. Phosphorescence can continue to emit light for a long time, and usually, the luminescence time is $\geq 10^{-8}$ seconds. According

to light excitation and emission, photoluminescent nanomaterials can be classified into upconversion luminescence or downconversion luminescence nanomaterials according to the nature of their light emission. Among them, upconversion luminescence is a photoluminescence phenomenon that violates Stokes' law, which is manifested by the conversion of several low-energy (long-wavelength) photons into one high-energy (short-wavelength) photon [33]. Downconversion luminescence is a photoluminescence phenomenon that obeys Stokes' law and is manifested by the conversion of a high-energy photon into one or more low-energy photons [34]. When one low-energy photon is emitted, it is commonly referred to as luminescence, and when two or more low-energy photons are emitted, it is referred to as quantum clipping of luminescence.

Photoelectric effect, which is the electrical effect of light, refers to the material in the light of the phenomenon of emission of electrons, the essence of photon excitation material to produce electrons and hole pairs; electrons migrate into the external circuit to do work, manifested as electrical energy [35]. Photochemical effect is the chemical effect of light, which refers to the material used in the photon excitation to produce electrons and hole pairs. They were with the reactant redox reaction, stored as chemical energy phenomenon [36].

### 1.2.3 Physical-chemical Processes at the Surface Interface

The physical processes at the surface interface of photofunctional nanomaterials mainly involve thermal radiation dissipation and relaxation quenching of photogenerated photons. In photothermal materials, by controlling the composition and structure of the nanomaterials, the radiation angle coefficients of the materials can be effectively reduced, thereby reducing the dissipation of thermal energy and improving the utilization of photothermal conversion energy. In luminescent materials, photons generated by photoluminescence can be recaptured by the material and achieve relaxation by nonradiative bonding, thus reducing the luminescence effect. In semiconductor nanomaterials, photoelectrons migrate to the surface of the material and return to the interior of the material to recombine with holes after work is done by the external circuit, achieving the conversion of light energy into electrical energy.

Surface interface chemical reactions of photofunctional nanomaterials usually occur during photocatalysis of the materials. Photogenerated electrons and holes migrate to the surface or interface of the material and combine with electron acceptors or donors adsorbed on the surface of the photocatalytic material to undergo a redox reaction, storing the energy in the chemical bonds of the products and realizing the conversion of light energy into chemical energy. The detailed process of the chemical reaction at the surface interface roughly involves the following processes. First, the reactants must diffuse around the material and pass through the Helmholtz layer to be adsorbed onto the active sites of the material. Next, the reactants undergo structural rearrangement at the active site and undergo redox reactions with photogenerated electron holes. Finally, the reaction products desorb from the surface of the material and return to the reaction solution. In the whole

process, a series of elementary reactions such as adsorption of reactants, charge exchange, and desorption of products together constitute the whole interfacial reaction process.

## 1.3 Introduction to Nanobiomedicine

In recent years, nanomaterials have been gradually integrated with biology and medicine in the development process, gradually forming a new discipline, namely "nanobiomedicine" (Figure 1.1) [38, 39]. Some people call the cooperation between nanomaterials and biomedicine "a great change" because it not only opens the door for nanobiology and nanomedicine but also brings new opportunities for biomedical research and clinical application. Governments around the world have increased the investment of funds and personnel in nanomedicine research, and nanobiomedicine has rapidly become a frontier and hot topic in the development of the biotechnology field in various countries, attracting more and more attention and expectations.

To be more precise, nanobiomedicine is an emerging discipline that applies nanomaterials to biomedical field, which involves materials science, physics, chemistry, biology, medicine, quantum science, and many other fields, and has very distinctive multidisciplinary cross characteristics. The research directions of nanobiomedicine include but are not limited to drug delivery and release [40–42], bioimaging [43], diagnosis and treatment of diseases (especially tumors) [44, 45], biosensing [46, 47], tissue engineering, and so on [48–50].

### 1.3.1 Nano-drug Delivery Systems

Through the design and preparation of nanocarriers such as nanoparticles, nanocapsules, nanofibers, and drugs are encapsulated in nanoscale structures to achieve precise drug delivery and release. Such nano-drug delivery systems can improve drug bioavailability, reduce side effects, and enable targeted therapy.

### 1.3.2 Nano-imaging Technology

High-resolution nano-imaging technology has been developed by exploiting the special optical, magnetic, and acoustic properties of nanomaterials. For example, nanoparticles can be used as contrast agents for fluorescence imaging, magnetic resonance imaging (MRI), and photoacoustic imaging (PAI) to achieve accurate imaging of biological tissues and lesions.

### 1.3.3 Nano-diagnostic Technologies

By exploiting the special properties of nanomaterials, nano-diagnostic technologies have been developed for biomarker detection, early diagnosis of diseases, and prognostic assessment. For example, nanoprobes can be used to detect the presence and activity state of specific molecules, enabling highly sensitive and selective diagnosis.

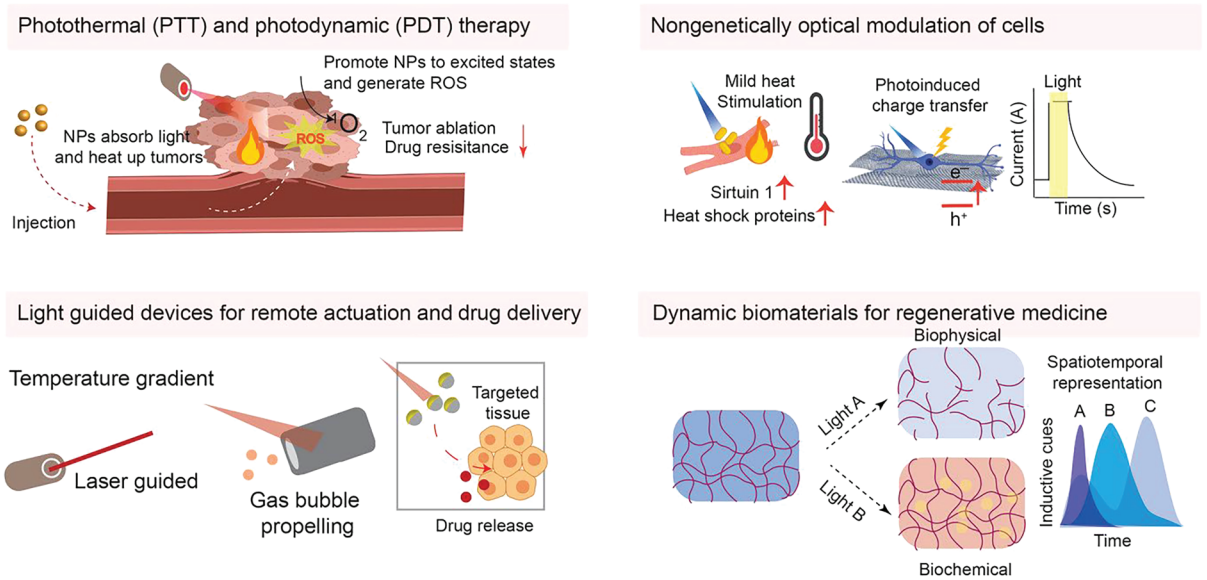


**Figure 1.1** Inorganic light-responsive nanomaterials have been widely applied to four main research fields of light-responsive biomaterials, which consist of PTT and PDT, light-guided devices for remote actuation and drug delivery, nongenetically optical modulation of cells, and dynamic biomaterials for regenerative medicine. Source: [51]/John Wiley & Sons/CC by 4.0.

### 1.3.4 Nanotherapeutic Technology

Using the special properties of nanomaterials, therapeutic methods have been developed for thermotherapy, phototherapy, drug release, and other therapeutic methods. For example, thermal therapy for tumors can be achieved by absorbing light energy from nanomaterials to produce thermal effects or by using nanoparticles with specific responsiveness to achieve targeted drug release.

### 1.3.5 Nano-biosensors

Using the special properties of nanomaterials and biorecognition molecules, nano-biosensors have been developed to monitor biomolecules, cellular activities, and biological processes. These sensors can monitor physiological and pathological changes in organisms in real time and provide timely diagnostic and therapeutic feedback.

### 1.3.6 Tissue Engineering

Nanotechnology can be used to create materials such as scaffolds, nanoparticles, and nanofibers with nanoscale structures to support and guide cell growth and differentiation. These nanomaterials can mimic the microstructure of human tissues and provide a suitable physical and chemical environment to promote cell adhesion, proliferation, and differentiation. In addition, nanotechnology can be used to prepare nanocarriers with controlled drug release to enhance the therapeutic efficacy of tissue-engineered constructs.

At present, nanobiomedicine has become an important direction in the development of nanotechnology, and its booming momentum will continue to provide new technologies and methods for modern biomedical research, open up new horizons for important biomedical problems at the nanoscale, and reveal the relevant new principles and possible practical applications.

In the biomedical field, the choice of light has unique requirements. As a common external stimulus with the advantages of noninvasiveness, high spatial and temporal resolution, and spatial and temporal controllability (including controllable light intensity and wavelength), light sources play an important role in biology and medicine [37, 51] and can induce organisms to perform or regulate many specific biological processes at a given site, such as gene transfection, cell function, signaling, ion channel opening, protein activity, molecular isolation, and tissue regeneration (Figure 1.2) [52]. However, most current photosensitive components respond only to ultraviolet or visible light, so the use of light as an excitation source for biomedical applications is subject to certain dilemmas that jeopardize its potential applications; for example, ultraviolet or visible light is readily absorbed and scattered in living tissues and has a very shallow tissue penetration depth [53, 54]. In addition, ultraviolet is phototoxic and is likely to damage biomolecules such as nucleic acids, proteins, and lipids. These issues need to be addressed from two perspectives. On the one hand, since biological tissues cannot efficiently absorb near-infrared (NIR) light

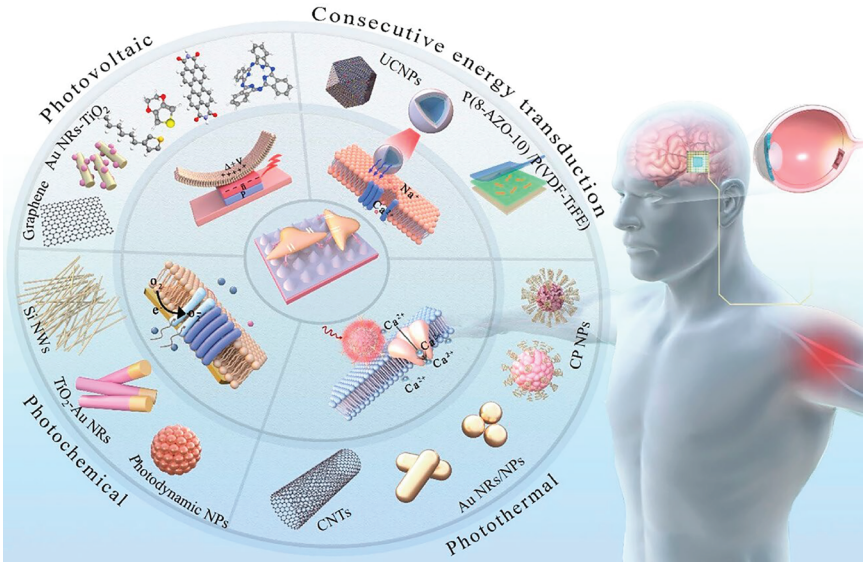


**Figure 1.2** Summary of photoactive nanomaterials for regulation of biomolecules, neurons, and nerve tissues. Source: Reproduced with permission from Ref. [52]; © 2022/American Chemical Society.

themselves, NIR light sources with lower tissue absorption, less light scattering, and deeper tissue penetration should be used to replace ultraviolet and visible light for biomedical research and applications [55]. On the other hand, there is a need to actively research and develop photofunctional nanomaterials or devices that can absorb NIR light and convert it into the desired signal or energy.

## 1.4 Classification of Photofunctional Nanomaterials

At this point, it should be stated in advance that due to the wide range of photofunctional nanomaterials, it is impossible to study them in detail one by one. Therefore, in connection with the theme of this book-"Photofunctional nanomaterials for biomedical applications," we will discuss the fluorescent, photothermal, photodynamic, photoelectrochemical, and photoacoustic parts of photofunctional nanomaterials and their research in biomedical fields such as biodetection [56], optogenetics [57], antibacterial [46], tumor diagnosis and treatment [45, 58], and other biomedical fields.

### 1.4.1 Fluorescent Nanomaterials

Fluorescent nanomaterials are nanoscale materials with special optical properties that absorb light energy at specific wavelengths and emit fluorescence at specific wavelengths. Compared with traditional organic dye fluorescent molecules, fluorescent nanomaterials have the advantages of better optical stability, higher

fluorescence intensity, and easy regulation of shape, size, and function [59, 60]. As a result, fluorescent nanomaterials have attracted great attention and have undergone rapid development in the biomedical field. At the cellular level, small-sized fluorescent nanomaterials can enter cells through endocytosis and infiltration and can be used as cellular fluorescent imaging probes to identify and localize specific cells or molecules in a highly selective manner. At the in vivo level, fluorescent nanomaterials can be passively and actively delivered to the lesion site after entering the bloodstream and can be used as fluorescent probes for early diagnosis of disease to provide structural and dynamic information of living samples [61]. In addition, the combination of fluorescent nanomaterials with antibacterial and antitumor drugs through nanotechnology can achieve the integration of diagnosis and treatment [62–65]. In conclusion, fluorescent nanomaterials have become a key link in the cross-integration of materials science, optics, biomedicine, and other disciplines, and they have great application value and prospects.

Fluorescent nanomaterials widely used in biomedicine mainly include quantum dot materials, silicon-based fluorescent nanomaterials, rare earth luminescent nanomaterials, organic fluorescent nanomaterials, and composite nanomaterials of different fluorescent materials.

#### 1.4.1.1 Quantum Dots

Quantum dots, also known as artificial atoms, are generally spherical or spheroidal in shape, and their diameters are often between 2-20 nm, with high crystallinity and micro-size being their typical features. When the size of quantum dots is less than or equal to the exciton Bohr radius, the electrons and holes inside them are quantum limited, and the continuous energy band structure becomes a discrete energy level structure with molecular properties, so the quantum dots produce strong light absorption and luminescence effects (Figure 1.3) [61]. As the size of the quantum dots decreases, the energy difference between the highest valence band and the lowest conduction band increases, which means that the quantum dots require more energy to excite, and at the same time, more energy is released when the crystal returns to the ground state. At this point, the wavelengths at which the quantum dots absorb and emit light are shifted toward shorter wavelengths of higher energy, known as the blue shift. This allows researchers to tune the optical properties of quantum dots according to their size for better applications in biology, medicine, and other fields. In addition to size tuning, the development of new methods for synthesizing quantum dots, such as core-shell structures, alloying, doping, surface ion modification, and voltage tuning, is likely to further facilitate the application of quantum dots in biomedical fields.

Quantum dots can be divided into semiconductor quantum dots (such as II–VI and III–V elements) [56], IV (carbon and silicon) quantum dots, and lead halide chalcogenide (perovskite) quantum dots according to the different constituent elements. Quantum dot materials used in biomedical applications do not contain toxic heavy metal elements such as cadmium or lead, and the most commonly used are carbon quantum dots, zinc-based quantum dots (ZnS, ZnO, and ZnSe), and Ag-based quantum dots ($Ag_2S$ and $Ag_2Se$) [65–68]. In addition, most of the current quantum

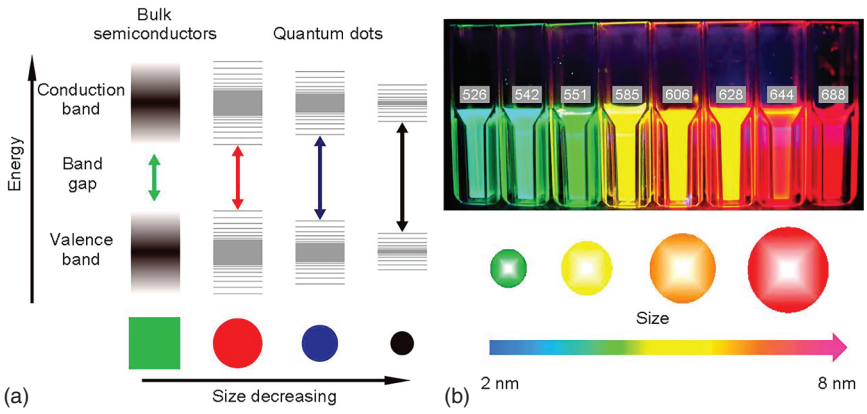


**Figure 1.3** (a) Energy diagrams for bulk semiconductor and QDs. (b) Example of cysteine-capped CdTe/ZnTe core/shell QDs synthesized in aqueous media, with a size-dependent luminescence. Upper panel: photographic images of CdTe/ZnTe QDs dispersed in water under UV irradiation. The emitted peak wavelength is marked in white numbers on the top of the image. Lower panel provides an illustration of the corresponding core/shell nanoparticle size from 2 to 8 nm. These core/shell QDs were prepared at the Institute for Lasers, Photonics, and Biophotonics, University at Buffalo. Source: Reproduced with permission from Ref. [39]; © 2016/American Chemical Society.

dots are mainly synthesized by the most classical high-temperature pyrolysis method and therefore their surfaces are often covered with alkyl chains. Achieving phase transfer (oil to water) of quantum dots is an important first step in their entry into biological applications. In addition, some quantum dots (like carbon quantum dots) can be synthesized directly in the aqueous phase, making their use in biological environments more convenient [69].

Since the first publication of research using quantum dots as bioprobes for fluorescence imaging of living cells in science in 1998, the exploration of quantum dots in the field of biomedical imaging has mushroomed [70]. Carbon quantum dots are widely used in cellular/bacterial imaging and in vivo imaging due to their high fluorescence stability, tunable optical properties, wide source of synthetic raw materials, low cost, and good biocompatibility. Depending on the variation of their fluorescence intensity, they can also be used to detect a wide range of anions and cations ($K^+$, $Al^{3+}$, $Fe^{3+}$, $ONOO^-$) [71], drug molecules (antibiotics, tetracycline, methotrexate), biomolecules (DNA, proteins, cysteine, hemoglobin, and cholesterol), bacteria, pH, and fingerprints. Tan and coworkers have used carbon dots encapsulated in organosilicon shells to achieve targeted specific capture of bacteria (Figure 1.4) [72]. The carbon dots@organosilicon surface was modified with anti-*Staphylococcus aureus* antibodies, which could selectively capture the target bacteria. At the same time, the bacteria were separated using antibody-modified magnetic nanoparticles. The organosilicon shell is then destroyed by reducing the sodium boron hydride ($NaBH_4$), releasing the carbon dots, and causing them to fluoresce. The fluorescence signal was significantly enhanced by the hundreds of carbon dots encapsulated in each organosilicon particle. The fluorescence signal of this

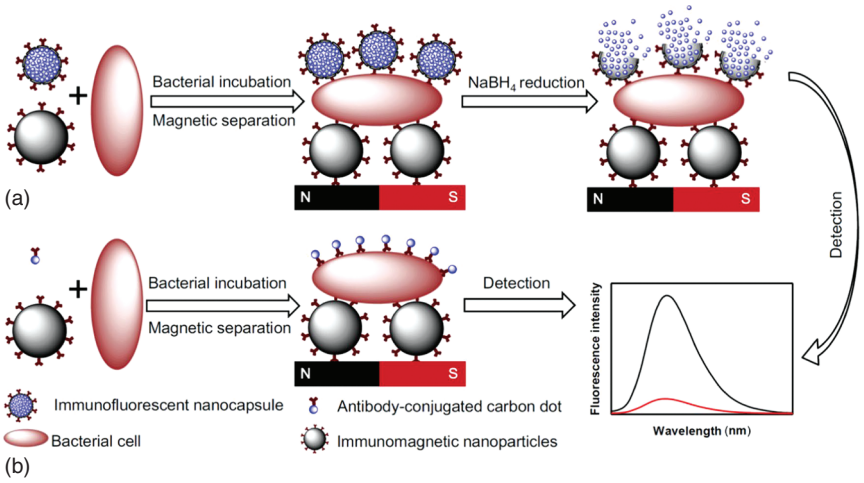


**Figure 1.4** (a) Illustration of the detection of pathogen bacteria with the proposed method and (b) conventional method. Source: Reproduced with permission from Ref. [72]; © 2018/American Chemical Society.

method is enhanced by a factor of 108 compared to the conventional assay using only carbon dots as markers. $Ag_2Se$ quantum dots with a narrow direct band gap (0.15 eV) are a new type of fluorescent probe in the NIR-II region that has received great attention in recent years [68]. To overcome the problem of low fluorescence quantum, yield due to a large number of cation vacancies and crystal defects caused by the high mobility of Ag ions, Wang and coworkers synthesized silver-gold-selenium (AgAuSe) quantum dots with tunable fluorescence emission spectra in the range of 820–1170 nm by alloying for the first time, which is an important impetus for the research of in vivo fluorescence imaging as well as therapeutic tracing [73].

#### 1.4.1.2 Silicon-Based Fluorescent Nanomaterials

Silicon is a fundamental building block of the human body. Silicon-based fluorescent nanomaterials exhibit good biocompatibility, attractive optical properties, and easy surface modification and have attracted widespread attention and research in the fields of biosensing, disease detection, and imaging. Fluorescence imaging based on silicon-based fluorescent nanomaterials enables long-range real-time imaging for the analysis of cancer, bacterial-related diseases, and ophthalmic diseases. In 2016, researchers in Japan developed a silicon-based fluorescent nanomaterial with a core-double-shell structure [74]. In this structure, crystalline silicon nanoparticles serve as the core, while hydrocarbon groups and surfactants are encapsulated on the surface. Two-photon excitation fluorescence imaging showed that the silicon nanoparticles would efficiently emit light when absorbing NIR light, while the hydrocarbon groups in the coating would increase the luminescence quantum yield. This work enabled the first successful bioimaging of silicon-based fluorescent nanomaterials under 650–1000 nm light irradiation, known as the "bio-optical window." As the research progressed, the scientists found that conventional fluorescent

probes suffered from the need to reintroduce probe molecules when changing labels and the difficulty of assessing the total concentration of probes at a target site, so color-switchable probes were developed to provide more reliable information at the cell or tissue level. Yang and coworkers recently reported a silicon-based color-switchable fluorescent nanomaterial that can successfully suppress oxidation-induced photoluminescence loss through a two-step surface passivation strategy to achieve a fluorescence jump from intrinsic NIR light on the microsecond scale to blue light on the nanosecond scale [75]. Specifically, red-emitting silicon nanocrystals are first passivated with acrolein and then interact with amines via a Schiff base reaction mechanism to achieve an in situ red-to-blue fluorescence transition in living cells. Taking the presence of abundant amino acids in the biological environment as an example, the blue fluorescence intensity displayed by the cells is dependent on the dosage of amino acids, suggesting that the silicon-based fluorescent nanomaterials can reflect the distribution and concentration of amino acids in different regions of living cells in real time and differentiate between living and dead cells. The silicon-based color-switchable fluorescent nanomaterials provide in situ multi-color imaging at the cell or tissue level for many fundamental life activities involving amino acids, proteins and nucleic acids, and have a wide range of development and application.

#### 1.4.1.3 Rare Earth Luminescent Nanomaterials

Rare earth luminescent nanomaterials refer to a kind of materials doped with rare earth ions or containing rare earth elements in the matrix. Rare earth elements are known as "vitamins of modern industry" and "luminescent treasures" (Figure 1.5). The luminescent properties of rare earth luminescent nanomaterials arise from the abundant electronic energy levels of rare earth elements and the unique 4f electron jump properties. Rare earth elements have unfilled 4f electron shell layer, and the arrangement of electrons on this electron layer will produce different energy levels. These electrons in the different energy levels between the jump will produce a large number of absorption and emission [57]. Rare earth luminescence can be divided into two categories: sharp line spectra (f–f transitions) and band spectra (f–d transitions). Rare earth luminescent nanomaterials are an important class of optical materials with the advantages of narrow emission spectral bands, high color purity, strong light absorption, high luminescence intensity, long fluorescence lifetime, and stable physicochemical properties [76]. By adjusting the type and proportion of doped rare earth ions, the full band of luminescence from ultraviolet to infrared can be realized under the excitation of a single excitation light source. Meanwhile, the low toxicity of rare earth luminescent nanomaterials has great potential for application in biofluorescent labeling and medical imaging and is now attracting the attention of researchers in the field of biomedicine.

Rare earth luminescent nanomaterials are generally composed of two parts: the matrix (the main body of the luminescent materials, mainly various compounds of Y, Gd, and Lu) and the activator (which is the dopant ion used as the luminescent centers, such as $Er^{3+}$, $Tm^{3+}$, $Ho^{3+}$, $Tb^{3+}$, $Sm^{3+}$, and $Eu^{3+}$) [33, 77]. The matrix provides a suitable crystalline environment for the activator ions, which

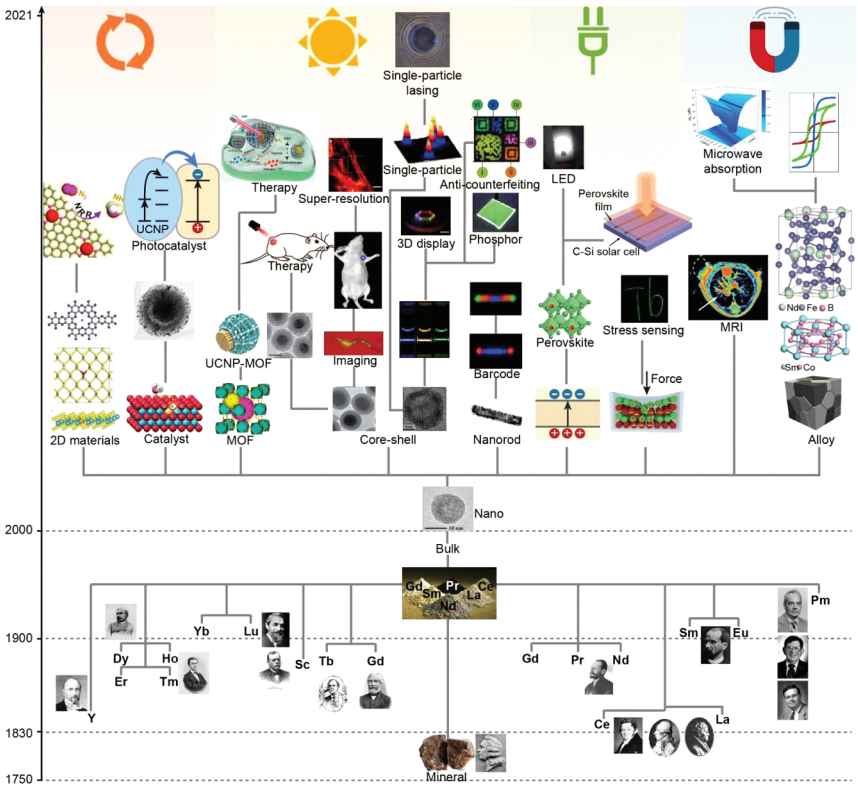


**Figure 1.5** Development and application of rare earth-based nanomaterials. The history of rare-earths begins with the discovery of rare earth minerals and their separation and purification by scientists. Since the advent of nanotechnology, doping of rare-earths in nanomaterials of different morphology and composition has enabled many technological applications. Source: Reproduced with permission from Ref. [57]; © 2022/American Chemical Society.

themselves usually constitute only a few luminescent energy levels. The activator acts as a luminescence inducer for the luminescent material. In addition, some sensitizers (such as $Yb^{3+}$ and $Nd^{3+}$) can be added to the material, which can be transferred to the neighboring luminescent centers by Foster resonance energy transfer (FRET), thus achieving efficient absorption of the excitation light and increasing the luminescence efficiency of the upconversion nanomaterials [78]. Based on the different luminescence mechanisms, rare earth luminescent nanomaterials can be classified into rare earth upconversion fluorescent nanomaterials and rare earth downconversion fluorescent nanomaterials. Downconversion luminescence follows Stokes' law, which refers to the process by which luminescent materials emit low-energy, long-wavelength light (e.g. visible light) after being excited by high-energy, short-wavelength light (e.g. ultraviolet light). Upconversion luminescence, also known as anti-Stokes luminescence, refers to the process by which a luminescent material absorbs low-energy long-wavelength light and emits high-energy short-wavelength light [76].

Rare earth luminescent nanomaterials have low toxicity and do not disrupt the normal physiological state of living organisms when imaged at the cellular, tissue, and in vivo levels. Rare earth luminescent nanomaterials have good photostability and chemical stability and can continue to emit light when excited by a light source, and their luminescence properties remain undisturbed even in acidic or alkaline chemical environments [39]. Rare earth luminescent nanomaterials used in biomedical fields are mostly excited by NIR light, which is highly penetrating and can be used for deep tissue imaging. At the same time, biological autofluorescence is not excited by NIR light (organisms basically do not produce fluorescence in the NIR region), which reduces the detection of background fluorescence and achieves a higher signal-to-noise ratio. In addition, the lower excitation energy of NIR light results in less photodamage to the organism and better safety, which is a unique advantage in biological applications [79]. As the study progressed, the researchers divided NIR light into NIR-I (650–950 nm) and NIR-II (1000–1700 nm). Compared to the visible range and NIR-I, NIR-II light, which is in the optically 'transparent' window of biological tissue, suffers from greatly reduced absorption and scattering effects as it propagates through biological tissues such as skin, fat, and bone, resulting in deeper tissue penetration and less energy attenuation in the delivery process [80]. At the same time, the autofluorescence of biological tissues is much lower in this band [81]. In particular, the imaging window at wavelengths of 1500–1700 nm is recognized as a promising window for noninvasive imaging of deep tissues, as the 'discount rate' caused by tissues is further reduced and autofluorescence from various pigments in the organism is almost eliminated, resulting in a further improvement in imaging depth and spatiotemporal resolution (Figure 1.6).

To date, a variety of imaging techniques based on rare earth luminescent nanomaterials have been successively developed, including upconversion luminescence imaging [82], downshifted luminescence imaging [83], time-resolved imaging [84], sustained luminescence imaging and multifunctional imaging [57], which have great potential for application in the fields of gene assay, immunoassay, fluorescent labeling, cellular imaging, biodetection, and biosensing. As shown in Figure 1.7, Lin and coworkers used the FRET phenomenon between $NaYF_4$:Yb/Er and gold nanoparticles to detect *Escherichia coli* [85]. The gold nanoparticles were modified with an aptamer of the target strain ATCC8739, and a cDNA nucleotide strand complementary to the target strain aptamer was modified on $NaYF_4$:Yb/Er. In the absence of *E. coli*, the complementary pairing of the cDNA nucleotide strand with the *E. coli* aptamer causes $NaYF_4$:Yb/Er to be in close proximity to the gold nanoparticles, and the fluorescence emitted by $NaYF_4$:Yb/Er is quenched. When *E. coli* is present, the aptamer dissociates from the cDNA and binds to *E. coli*, resulting in the dissociation of $NaYF_4$:Yb/Er from the gold nanoparticles and the recovery of upconversion fluorescence. Chen and coworkers synthesized a four-shell layer of upconversion nanoparticles co-doped with $Yb^{3+}$ and $Tm^{3+}$, achieved controllable regulation of the fluorescence lifetime by adjusting the thickness of the ion migrating layer and the concentration of rare earth ions doped in the upconversion energy transfer layer, and developed a time-resolved upconversion system based on

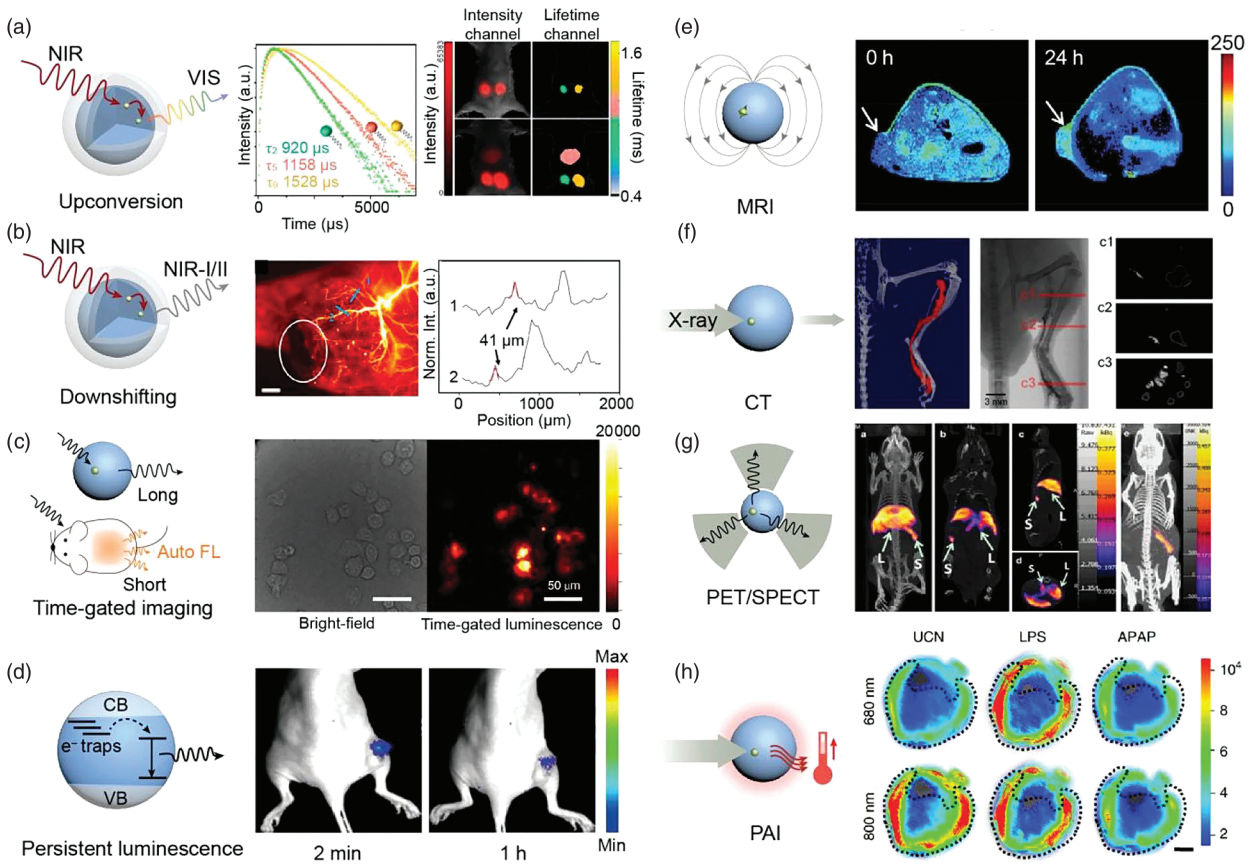


**Figure 1.6** Schematic illustration of the principles of imaging modes and corresponding (a) visible fluorescence imaging, (b) near-infrared fluorescence imaging (scale bar, 2 mm), (c) time-gated imaging (scale bars, 50 μm), (d) persistent luminescence imaging, (e) magnetic resonance imaging (MRI), (f) computed tomography (CT scale bar, 3 mm), (g) positron emission computed tomography/single-photon emission computed tomography (PET/SPECT), and (h) photoacoustic imaging (PAI) of rare earth doped nanomaterials. Source: Reproduced with permission from Ref. [57]; © 2022/American Chemical Society.

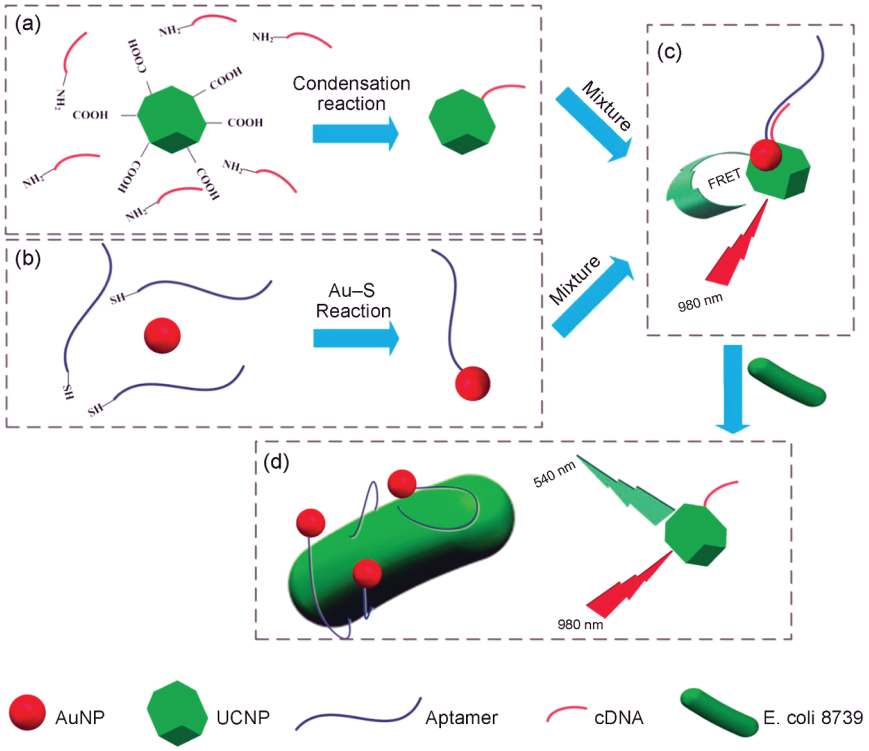


**Figure 1.7** Schematic illustration of upconversion nanoparticles based FRET aptasensor for rapid and ultrasensitive bacteria detection. (a) The amino-modified complementary DNA of the aptamer is attached to the carboxyl-functionalized UCNPs by condensation reaction (b) Conjugating thiol-modified aptamers to the AuNPs through Au-S chemistry. (c) The FRET system is established between a donor-acceptor pair: UCNPs-cDNA hybridized with AuNPs-aptamers. (d) By introducing target bacteria into the FRET system, aptamers preferentially bind to target bacteria, resulting in the dissociation of cDNA. Thereby, aptamers-DNA pairs are destroyed and the green fluorescence recovers. Source: Reproduced with permission from Ref. [85]; © 2016/Elsevier.

this, which was successfully applied to in vivo multiplexed pathway imaging [86]. Zhang and coworkers developed rare earth-alkali metal fluoride nanofluorescent probes based on $Tm^{3+}$, $Er^{3+}$, and $Ho^{3+}$-doped cubic crystal phases, which achieved different degrees of downshifted luminescence enhancement at 1632, 1530, and 1180 nm, respectively, with the excitation of 980 nm NIR light, further enriching the fluorescence emission of rare earth elements in the NIR-II and realizing real-time dynamic multiple in vivo imaging [87]. Meanwhile, rare earth doped nanomaterials can also be used as contrast agents; for example, $Gd^{3+}$ with seven unpaired electrons is suitable as a positive ($T_1$) contrast agent for MRI, and $Dy^{3+}$ and $Ho^{3+}$ are suitable as negative ($T_2$) contrast agents due to their high magnetic moments (~10.6 μB) and short electronic relaxation times (~0.5 ps) [88]. In addition, rare earth luminescent nanomaterials can also be used as contrast agents for X-ray computed tomography (CT) imaging due to the high atomic number and lanthanide contraction. Among

the lanthanides, lutetium (Lu) has the highest atomic number, and $NaLuF_4$ and $LiLuF_4$ have been shown to be effective CT contrast agents [89, 90]. Several research teams have also used rare earth-doped nanoparticles as contrast agents for PAI [91, 92].

#### 1.4.1.4 Organic Fluorescent Nanomaterials

Organic fluorescent nanomaterials are organic nanomaterials that can emit low-energy light waves after absorbing high-energy light waves. Through reasonable structural design, the luminescence performance of organic fluorescent nanomaterials can be effectively adjusted by changing the conjugation length and increasing the Stokes shift, which shows the characteristics of the material's structural diversity as well as its functional adjustability and predictability [93]. Meanwhile, organic fluorescent nanomaterials have good biocompatibility, which is of great concern to researchers at the intersection of materials, chemistry, and biomedicine. According to the different molecular structures, organic fluorescent nanomaterials can be classified into organic fluorescent small molecules and organic fluorescent polymers.

Organic fluorescent small molecules are an important class of fluorescent probe materials with the advantages of strong chemical modification, low synthesis cost, wide range of fluorescence emission, easy purification, and no heavy metal contamination. The structure of organic fluorescent small molecules is easy to design, and there are many types of them. Common fluorescent small molecules include fluorescein, rhodamine, coumarin, porphyrin, anthocyanin, fluoroborodipyrrole (BODIPY), and its derivatives. Recently, Lei and coworkers developed Chrodol-3, a hydroxyl-containing anthocyanin dye with NIR-II fluorescence with high quantum yield (0.34%) and low p$K_a$ (6.40), and prepared PN910, a NIR-II fluorescent probe for monitoring reactive oxygen species (ROS) and reactive nitrogen species, based on Chrodol-3 [94]. In vivo fluorescence imaging showed that PN910 could be used to accurately monitor cystitis and colitis. Smith and coworkers reported a modular synthetic approach to synthesize a series of high-performance ionic heptamethine cyanine dyes, which greatly enhanced the fluorescence emission and chemical stability of the dyes [95]. The produced NIR-I and NIR-II dyes can specifically bind to proteins and target specific sites in mice, enabling efficient in vivo tumor fluorescence imaging.

It is well-known that the application of most organic fluorescent molecules is limited by the aggregation-induced quenching (ACQ) phenomenon, which is manifested by the fact that they exhibit good fluorescence emission properties in dilute solutions [96, 97]. However, in the solid state or when the molecules are aggregated, their fluorescence emission intensity decreases or even disappears due to strong π–π interactions. It was only in 2001 that Tang and coworkers discovered a class of organic small-molecule fluorescent materials with special fluorescence properties, which are basically nonfluorescent in the solution state, while the fluorescence is significantly enhanced when they are prepared into nanoparticles or thin films, a phenomenon known as aggregation-induced luminescence (AIE) phenomenon (Figure 1.8) [98, 99]. The discovery of the AIE phenomenon opens up a new

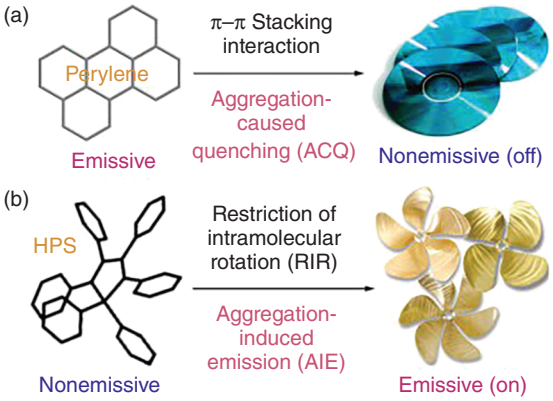


**Figure 1.8** (a) Planar luminophoric molecules such as perylene tend to aggregate as discs pile up due to the strong p–p stacking interactions between the aromatic rings, which commonly turns "off" light emission. (b) Nonplanar luminogenic molecules such as hexaphenylsilole (HPS) behave oppositely, with their light emissions turned "on" by aggregate formation due to the restriction of the intramolecular rotation (RIR) of the multiple phenyl rotors against the silole stator in the aggregate state. Source: Reproduced with permission from Ref. [98]; © 2011/The Royal Society of Chemistry.

avenue for applied research of organic functional optical materials. In 2016, AIE nanoparticles were listed in Nature as one of the four nanomaterials that will support the upcoming "nanolight revolution" [100]. Over the past two decades, research on AIE-emitting nanomaterials has made great progress, and many AIE molecules and probes have been designed and prepared for applications in cell- or organelle-specific imaging, single- or multiphoton imaging of blood vessels, disease sensing, in vivo drug distribution monitoring, long-term tracking, and fluorescence imaging-guided surgery [101–104]. For example, in the field of organelle-specific imaging, researchers have designed and synthesized DTPAP-P cationic polymers [105]. Due to anion–$\pi^+$ interactions, DTPAP-P exhibits excellent optical properties in the solid state and can be targeted to mitochondria or nuclei depending on the cellular state, enabling organelle-specific imaging and dynamic tracking at the nanoscale. In the field of in vivo tumor imaging, Liu and coworkers reported for the first time an NIR-II AIE nanoparticle for targeted NIR-II fluorescence and NIR-I PAI of brain tumors and evaluated in detail the penetration depth, spatial resolution, sensitivity, and imaging effect through in situ brain tumor models with intact scalp and skull, providing a powerful technical tool for monitoring and visualizing cerebrovascular and brain tissue abnormalities [106].

Organic fluorescent polymers can be divided into conjugated and nonconjugated fluorescent polymers according to their structural properties. The luminescence mechanisms of the two types of fluorescent polymers are different. Conjugated fluorescent polymers have a π–π conjugated structure with benzene rings or aromatic heterocycles as the main chain luminescent units, which have optical properties similar to those of semiconductor materials, and there are various photophysical processes between the ground state and the excited state. Nonconjugated

fluorescent polymers have more luminescence mechanisms, including luminescence induced by polymer side chain chromophores and luminescence induced by cochromophores such as aliphatic amines, ester groups, and carbonyl groups under certain conditions. In recent years, organic fluorescent polymers have shown great potential for application in a variety of fields such as sensor detection, drug screening, bioimaging, and pathological analysis, attracting the attention of more and more researchers. Tian and coworkers have synthesized a new type of organic luminescent "spherical nucleic acid," which can enhance the signal transduction of nucleic acid detection by exploiting the "light trapping antenna effect" of fluorescent π-conjugated polymers, thus realizing the detection of nucleic acids at ultra-low concentrations [107].

### 1.4.2 Photothermal Nanomaterials

Photothermal nanomaterials, also known as photothermal conversion nanomaterials, are a class of materials that can convert light energy into heat energy (Figure 1.9) [109]. When the size of the material reaches the nanoscale, the absorption of light changes significantly, and these nanomaterials can convert the absorbed light energy into thermal energy. By selecting suitable photothermal nanomaterials, surface modification, and functionalization to improve photothermal conversion efficiency, stability, and biocompatibility, they can be used in photothermal therapies for cancer treatment, antimicrobial, tissue repair, and so on. In photothermal therapy (PTT), photothermal reagents are used to increase the heating effect of the lesion area [110]. Depending on the degree of warming, it can be subdivided into irreversible damage therapy (above 48 °C), hyperthermia (41–48 °C, which is the PTT discussed in this chapter) and hypothermia (below 41 °C) [37, 111]. High temperatures can cause thermal damage or thermal lethality of the cells in the lesion to treat the disease. With the advantages of noninvasiveness, high selectivity, and localized thermal effect, PTT can effectively treat a wide range of diseases, including cancer, bacterial infections, and inflammation [112].

With the gradual deepening of research, the types of photothermal nanomaterials are becoming richer and richer, and at present, the more researched ones are mainly metal photothermal nanomaterials, semiconductor photothermal nanomaterials, organic photothermal nanomaterials, carbon matrix photothermal nanomaterials, certain 2D nanomaterials, and biomass photothermal nanomaterials, as well as the composite materials of these materials, and so on [108, 113–115].

#### 1.4.2.1 Metallic Photothermal Nanomaterials

The photothermal conversion process of metallic photothermal nanomaterials is highly dependent on the spatial motion of free electrons. When metal nanoparticles (such as gold, silver, copper, platinum, and palladium) are irradiated with light of a certain wavelength, the free electrons in the particles interact with the photons, absorb the energy of the photons, and are excited to form a periodic electron density oscillation [116]. This oscillation resonates with the electromagnetic field

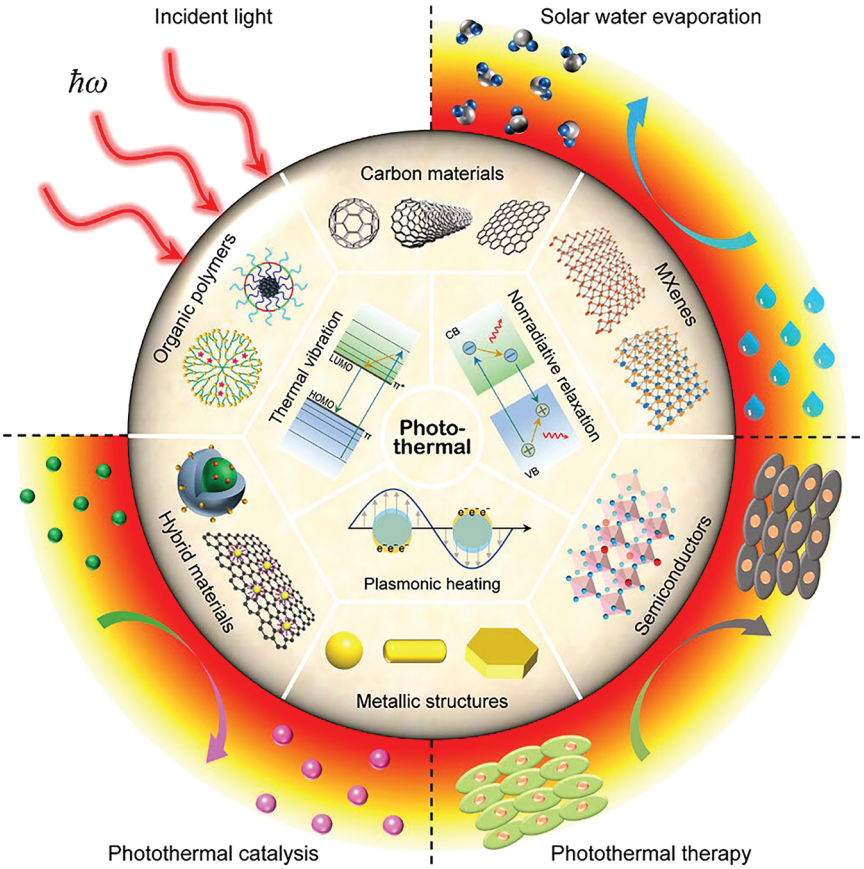


**Figure 1.9** Overview of the mechanisms, categories, and applications of photothermal nanomaterials. Source: [108]/American Chemical Society/CC BY 4.0.

of the incident light, giving rise to the localized surface plasmon resonance (LSPR) effect [117]. In this resonance process, the excited free electrons convert energy into heat by colliding with other electrons, which is a key step in the photothermal conversion process of metal nanoparticles. Furthermore, as the temperature of the metal nanoparticles increases, the heat is transferred to the surroundings through the interaction of electrons and metal lattice vibrations [108, 118]. In particular, the photothermal conversion process of metallic photothermal nanomaterials depends on factors such as the size and shape of the particles and the properties of the surrounding medium. Therefore, by finely controlling these parameters, it is possible to regulate the motion mode and energy level structure of free electrons, which in turn affects the strength and efficiency of the surface plasmon resonance effect, electron–electron, electron–photon, and electron–phonon interactions and achieves the regulation and optimization of the photothermal conversion performance.

#### 1.4.2.2 Semiconductor Photothermal Nanomaterials

Semiconductor nanomaterials with a fixed energy band gap, such as copper sulfide [119, 120], copper selenide [121, 122], and molybdenum disulfide [123], have excellent light absorption in the NIR region. Their energy band gap refers to the energy required for an electron to jump from the valence band (full electronic state) to the conduction band (empty electronic state). When semiconductor photothermal nanomaterials are irradiated by light, photons with energy greater than their energy band gap can excite electrons to jump from the valence band to the conduction band, forming electron-hole pairs. In the absence of an external electric field, the electrons in the excited state are unstable and will jump back to the valence band from the conduction band to compound with the holes. In this process, the electron releases energy equal to the energy band gap. The released energy is transferred to the crystal lattice in the form of vibrational energy (thermal energy), thus realizing the photothermal conversion. The photothermal conversion properties of semiconductor materials can be optimized by changing factors such as the type of material, crystal structure, defect state, particle size, shape, or external environment.

#### 1.4.2.3 Organic Photothermal Nanomaterials

Organic photothermal nanomaterials are a new type of materials that have attracted much attention in the field of photothermal conversion in recent years because their light absorption range is easy to regulate, and they can overcome the characteristics of inorganic materials that are not biodegradable, and they have been developed rapidly. Currently, common organic photothermal nanomaterials include small-molecule dyes, conjugated polymers, and organometallic complexes.

Small-molecule dyes with low quantum yields tend to have good photothermal conversion effects because low quantum yields mean that after absorbing a photon, only a small amount of the dye's energy is re-radiated in the form of fluorescence or phosphorescence, while more energy is released in a nonradiative way (e.g. thermal vibration). At present, small-molecule dyes that have been relatively well studied include indocyanine green (ICG), Prussian blue, and so on [124, 125]. In the case of ICG, for example, the presence of a large $\pi$-conjugated system in its molecule makes the absorption peak of this dye mainly in the range of 600–850 nm. When irradiated with laser light, the electron energy in the dye molecule will increase, and then the electrons will jump from the ground state to the excited state. When the electrons return to the ground state, the energy is released in the form of light and heat, allowing this dye to have the dual ability of fluorescence and photothermal conversion, giving it a wide range of applications in PTT, bioimaging, and biomarkers.

Conjugated polymers have received increasing attention from researchers due to their better photostability, biocompatibility, and temperature rise stability, as well as higher light absorption properties and photothermal conversion efficiencies compared to small-molecule dyes [126]. These conjugated polymers are typically derived from organic small-molecule monomers through polymerization reactions. Typical polymer-based photothermal agents mainly include

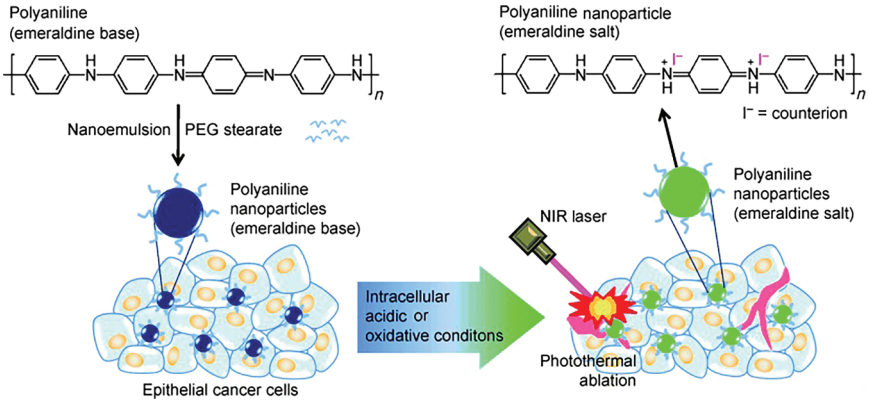


**Figure 1.10** Schematic illustration of the preparation of organic photothermal agents based on polyaniline nanoparticles and their application for the photothermal ablation of epithelial cancer cells by NIR laser irradiation. Source: Reproduced with permission from Ref. [127]; © 2011/John Wiley & Sons.

polyaniline, polypyrrole, polythiophene, and polydopamine, which have different photothermal conversion mechanisms due to their large structural differences [108]. Among them, polyaniline is a conductive polymer material with good biocompatibility, which has important applications in biomedical fields such as cell and tissue engineering due to its structural tunability, excellent electrical properties, and adaptability to the environment. In 2011, Haam and coworkers reported a novel organic photothermal agent based on polyaniline that induces hyperthermia for the treatment of epithelial cancer (Figure 1.10) [127]. Under the effect of protonation doping or the oxidative environment in cancer cells, a new bandgap state is created between the valence and conduction bands of polyaniline, inducing electron shifts and lowering the excited state energy level. At this point, the imine group on polyaniline is converted to an imine salt, and its absorption peak is significantly red-shifted, which can effectively ablate epithelial cancer cells under NIR light. Another representative class of polymer-based photothermal agents is polydopamine, a multifunctional biomimetic polymer material obtained by self-polymerization of dopamine monomer in a weakly alkaline environment [128–130]. On the one hand, polydopamine has broadband light-absorbing properties similar to those of natural melanin (broad light absorption throughout the ultraviolet, visible, and NIR regions), and on the other hand, it possesses nonselective and strong adhesion properties to the surfaces of a wide range of solid materials, mimicking the function of adsorbing proteins secreted by mollusks.

Organometallic complexes, such as metal phthalocyanine complexes and metal carbazole complexes, are compounds consisting of one or more metal ions and organic ligands. In such compounds, the metal ion usually acts as the central atom, while the organic ligand forms a chemical bond with the metal ion through an electron-donating group. The organometallic complexes have higher electron cloud density, better light absorption, and higher photothermal conversion efficiency, and their light absorption properties can be tuned by changing the type and structure of

the ligand, which has important application prospects in the field of photothermal conversion. Phthalocyanine is a planar macrocyclic conjugated system composed of four isoindole units, and there is a cavity with a diameter of about $2.70 \times 10^{-10}$ m in the center of its structure, and more than 70 metal elements can be chelated with phthalocyanine at the position of the cavity through two covalent bonds and two coordination bonds to form a highly stable metal phthalocyanine [131–133]. According to the aggregation leading to bursting effect, Zhang and coworkers synthesized special zinc phthalocyanine aggregates with better photothermal stability and photothermal conversion effect, which inhibited the fluorescence emission of zinc phthalocyanine and the inter-system jumping path and promoted the nonradiative jumping process to achieve higher photothermal conversion efficiency [134]. Zhang and coworkers synthesized a series of complexes with different rare earth centers (Ln = Gd, Yb, Er) based on NIR-absorbing carbazole porphyrin ligands [135]. These complexes have strong absorption in the phototherapy window of 650–850 nm.

Meanwhile, the fluorescence of the complexes was significantly burst due to the heavy atom effect and exhibited high photothermal conversion efficiency as well as singlet oxygen ($^1O_2$) generation capacity associated with the center metals.

#### 1.4.2.4 Carbon-Based Photothermal Nanomaterials

The photothermal conversion performance of carbon-based nanomaterials (e.g. carbon dots, fullerenes, carbon nanotubes [wires], graphene, and carbon nitride) is mainly due to the unique electronic structure and optical properties [123, 136–139]. Carbon-based nanomaterials have dense and sparse $\pi$-electron clouds with very close energy levels and generally exhibit broadband absorption, meaning that the vast majority of photon energy from the ultraviolet to the NIR can be absorbed by the electrons, placing them in an excited state. Meanwhile, thanks to the high thermal conductivity, the excited electrons in carbon-based nanomaterials fall back to the ground state and release heat, which can be quickly transferred to the surrounding materials and environment to avoid their own temperature being too high, thus improving the efficiency of light and heat conversion. In addition, carbon-based nanomaterials have good chemical stability, thermal stability, and photothermal tunability. By forming carbon nanostructures with different morphologies or by compositing carbon materials with other materials, it is possible to effectively maintain stable properties and modulate their photothermal properties [108, 140]. Carbon-based nanomaterials have been widely used in thermal therapy, imaging, and sensing platforms.

As shown in Figure 1.11, Tang and coworkers reported a graphene-functionalized magnetic microbead that can rapidly and sensitively detect tumor cells by using the magnetic effect of magnetic microbeads and the photothermal effect of graphene oxide, greatly solving the traditional problem of the difficulty of counting cells under the microscope [141]. Specifically, graphene oxide and magnetic beads are modified with specific antibodies and then combined to form a graphene-magnetic bead complex through antigen-antibody interaction. To identify cancer cells, the complex was incubated with the sample and then subjected to a membrane filtration

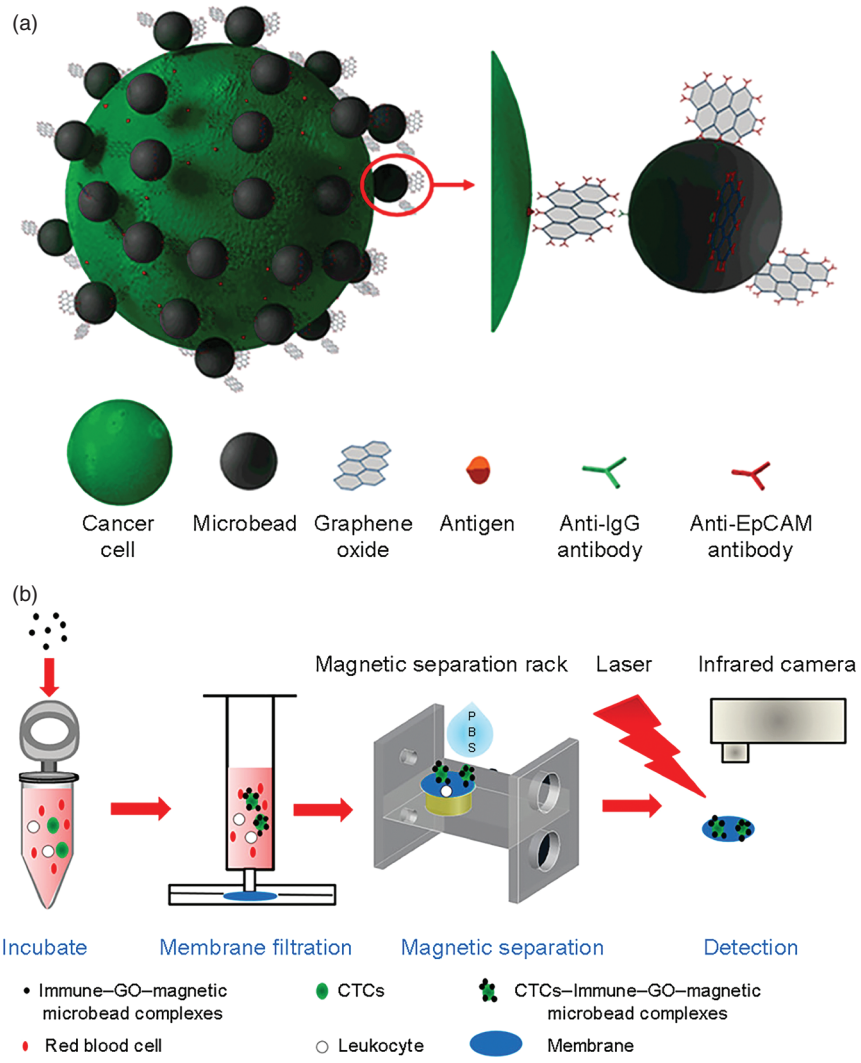


**Figure 1.11** (a) Schematic view of the cancer cells recognized by the immune-GO-magnetic microbead complexes. (b) Procedure of cell capture and thermal contrast detection based on the immune-GO-magnetic microbead complexes. Source: Reproduced with permission from Ref. [141]; © 2016/American Chemical Society.

and magnetic separation process to retain the cells attached to the graphene oxide-magnetic microbead complex and remove other contaminants. Finally, when a laser is used to irradiate graphene oxide on the cell-retaining membrane, graphene oxide, which has a photothermal effect, generates heat and causes a temperature change. A standard curve of temperature change versus number of cancer cells can therefore be established, and the number of cancer cells can then be determined by infrared thermography.

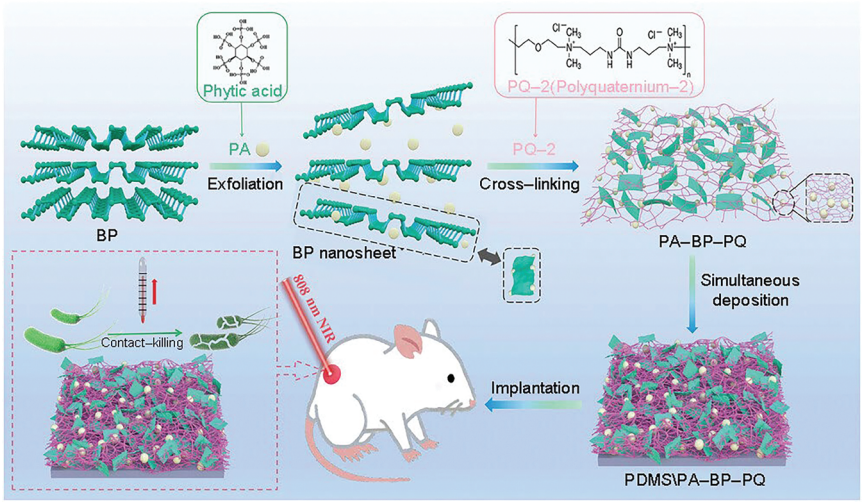


**Figure 1.12** Schematic representation of the preparation of PDMS-PA-BP-PQ nano-coating and evaluation of its contact-killing and antibacterial photothermal therapy (aPTT) effect. Source: Reproduced with permission from Ref. [150]; © 2023/John Wiley & Sons.

#### 1.4.2.5 Certain Two-Dimensional (2D) Nanomaterials

Black phosphorus and metal-carbon nitride/nitride materials are among the emerging two-dimensional nanomaterials that have rapidly attracted considerable attention from researchers since their discovery [142, 143]. As the most thermodynamically stable allotropic isomer of phosphorus [144], 2D semiconductor black phosphorus not only has a high specific surface area and excellent photothermal properties but also can be completely degraded in vivo to nontoxic phosphates, phosphites, and other phosphorus oxides [145, 146], which has excellent biocompatibility and safety and has a wide range of applications in the fields of drug carriers, antibacterial, and oncological therapy. The photothermal conversion efficiency of black phosphorus is higher than that of traditional photothermal agents, mainly due to its broadband light absorption properties, unique energy band structure, high thermal conductivity, and adjustable layer thickness. These properties enable black phosphorus to more effectively absorb light energy, convert it into heat energy and conduct it into the heat carrier, thereby improving the photothermal conversion efficiency [147, 148]. Wei et al. prepared a photothermal antibacterial hyaluronic acid-based nanocomposite injectable hydrogel for infected diabetic wound repair [149]. In this hydrogel, it is the functionalized black phosphorus nanosheets that exert the photothermal properties. Kang and coworkers prepared black phosphorus nanosheets by phytate-assisted ultrasonic stripping of black phosphorus powder, which were further deposited on the surface of polydimethylsiloxane with the participation of cationic polymers to form a stable functionalized coating (PA-BP-PQ) (Figure 1.12) [150]. The coating was found to have good contact bactericidal and photothermal antimicrobial activity against *S. aureus* and *E. coli* in anti-infection experiments.

2D transition metal carbon/nitride (MXene) is typically composed of $n+1$ layers of transition metal atoms (M) and n layers of carbon or nitrogen atoms (X) [151, 152]. Since it was first reported in 2011 [153], it has become a research hotspot due to its excellent properties such as broad wavelength absorption, high electrical conductivity, porous structure, excellent mechanical properties, and tunable chemical stability. In terms of photothermal conversion, MXene has good electromagnetic wave absorption capability and can absorb light in a wide range of wavelengths, including the visible and NIR spectra. Meanwhile, the high specific surface area and abundant free radical distribution are one of the important factors for its excellent photothermal conversion performance. In addition, the high density of surface charge carriers of MXene also plays an important role in their photothermal activities [154]. When MXene absorbs light energy, the photons excite the charge carriers on its surface, and the recombination of these charge carriers generates heat. Therefore, the excellent electromagnetic wave absorption capability, high specific surface area, abundant radical distribution and high density of surface carriers of MXene work together to give them strong light energy absorption capability and excellent photothermal conversion performance. The $Ti_3C_2$ MXene prepared by Hong and coworkers can quickly and efficiently kill a variety of drug-resistant bacteria and bacterial membrane structures within 20 minutes of NIR light irradiation [155]. Guo and coworkers developed a NIR light-activated photothermal-chemotherapeutic synergistic therapeutic platform by combining the nano-photothermal agent $Ti_3C_2TX$ MXene, the chemotherapeutic agent doxorubicin (DOX), and a thermoresponsive DNA hydrogel [156]. The heat generated by $Ti_3C_2TX$ in the presence of NIR light causes the double-stranded DNA cross-linking structure to unfold and release DOX, enabling the controlled release of photothermal and chemotherapeutic agents for the effective treatment of localized cancers.

#### 1.4.2.6 Biomass Photothermal Nanomaterials

Melanin and hemoglobin are two well-known biomass photothermal nanomaterials that are naturally produced by living organisms as biomolecules with chromophores that can absorb long-wavelength photons and convert them into heat [157–159]. Melanin, a biopolymer widely found in the skin, hair, feathers, and eyes of animals, is produced by melanocytes in living organisms. In general, melanin can be classified into eumelanin, pheomelanin, neuromelanin, allomelanin, and pyomelanin based on the chemical precursors in biosynthesis [160]. Polydopamine in conjugated polymers is a typical class of artificial melanin materials. In particular, the light absorption of melanin extends into the NIR region. As shown in Figure 1.13a, Yu et al. fabricated a hyaluronic acid-based microneedle that exploits the antioxidant and photothermal functions of natural melanin nanoparticles extracted from cuttlefish ink to scavenge ROS and enable PTT [161]. In addition, the amorphous silica shell formed by biomineralization on the surface of melanin nanoparticles continuously degrades to release $SiO_4^-$, which can control the inflammatory environment and stimulate the proliferation and differentiation of endothelial cells, thus promoting skin tissue regeneration. Therefore, this microneedle has multiple functions of tumor eradication and wound healing at the same time and

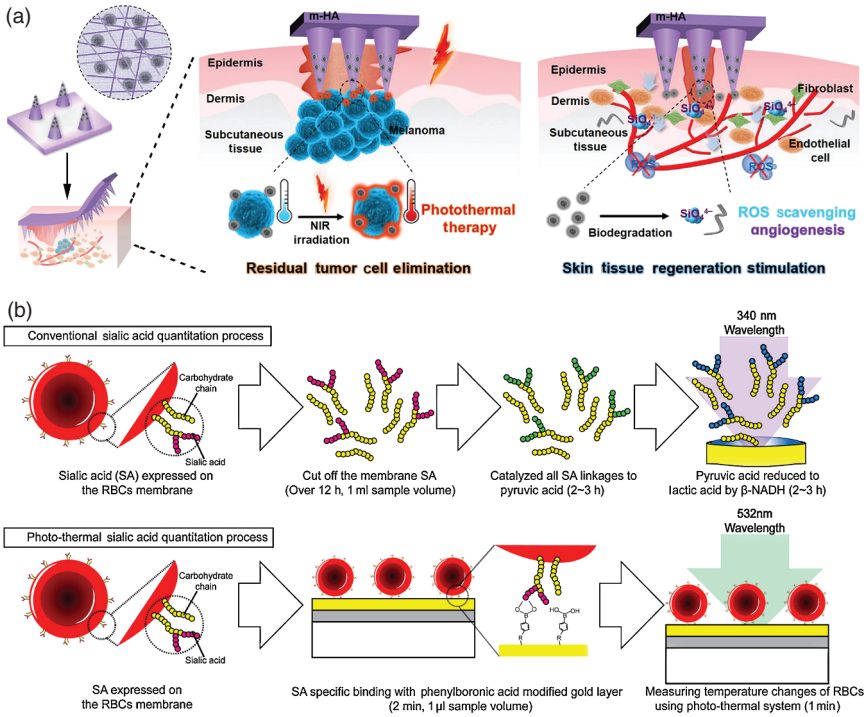


**Figure 1.13** (a) Schematic therapeutic process of the biomineralized melanin nanoparticles-loaded microneedle patches for the subcutaneous melanoma postoperative wound. Source: Reproduced with permission from Ref. [161]; © 2022, Wiley-VCH GmbH. (b) Comparison of SA analysis using a photothermal sensing system with a conventional method. Source: Reproduced with permission from Ref. [162]; © 2012/Elsevier.

is expected to be an effective adjunct to the postoperative treatment of skin tumor excision.

There are few reports on sensors based on biomass photothermal nanomaterials, which combine the good biocompatibility of biomass materials, the high precision and sensitivity of nanotechnology, and the special properties of the photothermal effect. A photothermal sensing system based on hemoglobin molecules in erythrocytes is presented here. Hemoglobin is a protein in erythrocytes that is mainly responsible for carrying and delivering oxygen [157]. Hemoglobin consists of four polypeptide chains, each containing a porphyrin ring structure with an iron ion in the center. The ability of hemoglobin to convert light energy into heat energy is primarily related to the porphyrin ring structure and its interaction with the iron ion. When light hits hemoglobin, the porphyrin ring can absorb some of the light energy, which excites electrons to jump from the ground state to the excited state. These electrons then release energy in a nonradiative way, known as heat, which returns the electrons to their ground state. Using this property of the hemoglobin molecule, Jung et al. developed a photothermal biosensor that can analyze the hemoglobin content of whole blood through temperature changes, making the

diagnosis of anemia easier and faster [163]. Building on this, they developed a new technique based on monitoring temperature changes in red blood cells to assess the concentration of sialic acid on their membranes (Figure 1.13b) [162]. A self-assembled monolayer of phenylboronic acid-modified thermoresponsive material was used to modify the sensor surface to detect red blood cells that overexpress sialic acid. Hemoglobin in the erythrocytes generates heat when irradiated with a 532 nm laser, which is used to determine the amount of sialic acid based on temperature changes on the sensor surface. The increase in erythrocyte temperature was found to be proportional to the level of sialic acid expression and laser intensity. The technique can directly measure the level of sialic acid in blood without complicated preprocessing steps (e.g. enzyme treatment and labeling), is easy to use, and can achieve sensitive detection of sialic acid, providing a new way of thinking about disease diagnosis.

### 1.4.3 Photodynamic Nanomaterials

Photodynamic nanomaterials are nanomaterials with specific structures and components that can act as carriers for photosensitizing small molecules, or that generate specific light responses and activities when irradiated with light, generating ROS for the realization of photodynamic therapy (PDT) [164, 165]. As a light-triggered therapy, the photodynamic nanomaterials are first injected or targeted to the diseased area and then irradiated by an external light, which activates the nanomaterials to generate a local chemical reaction, resulting in the destruction of tumor cells or disease-related tissues [166]. The treatment is noninvasive, highly selective, and localized and can reduce damage to normal tissues; it has been widely studied and applied in the treatment of tumors, bacterial infections, and some other chronic diseases.

As the core component of PDT, photodynamic nanomaterials are usually composed of nanoparticles or nanostructures whose surface or internal chemical components and structures are designed to have the ability to transport photosensitizers or to absorb, convert, and transmit light energy (Figure 1.14). Photodynamic nanomaterials can be divided into the following categories.

#### 1.4.3.1 Photosensitizer-Loaded Nanomaterials

At the current stage of research on small-molecule organic photosensitizers, most photosensitizers have poor stability and water solubility in vivo and are easily degraded or deactivated by agglomeration [167–169]. The use of nanocarrier materials can improve photosensitizer stability, biodistribution, and lifetime in vivo. In addition, the targeting of photosensitizers is poor, and it is difficult to achieve effective accumulation at lesion sites (such as tumors) [170]. By modifying ligands or antibodies on the surface of the vector materials, targeted delivery to the lesion site can be achieved, improving therapeutic efficacy and reducing damage to normal tissues. Carrier materials can also be used as storage and release platforms for photosensitizers, such as the orderly release of photosensitizers in response to in vivo environment (e.g. pH and temperature) or external stimuli (e.g. light and

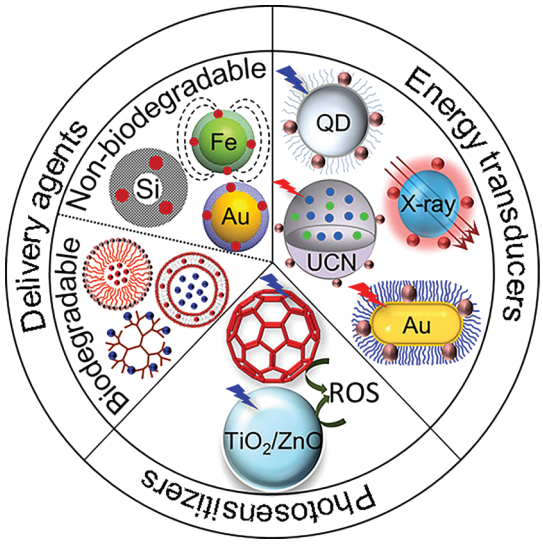


**Figure 1.14** Nanoparticles in photodynamic therapy. Source: Reproduced with permission from Ref. [164]; © 2015/American Chemical Society.

magnetic field). Nanomaterials used for photosensitizer loading are usually divided into two categories.

***Biodegradable Nanomaterials*** Biodegradable nanomaterials are made of natural biomaterials or synthetic polymeric nanomaterials with good biocompatibility and degradation properties that, after transporting the photosensitizer to the lesion site, undergo an enzymatic or hydrolytic reaction and release the photosensitizer, thereby improving the bioavailability and therapeutic efficacy of the photosensitizer and reducing the risk to normal tissues. Some common biodegradable nanocarrier materials are listed below.

**Liposomes** Liposomes are small nanoscale vesicles composed of phospholipids, cholesterol, etc., which can well encapsulate hydrophilic and hydrophobic drugs in their central lumen and membrane layer structures, respectively [171–174]. Liposomes can provide a stable environment to protect photosensitizers from the in vivo environment. Due to the presence of many active sites on the liposome membrane, their properties can be modified by attaching various functional ligands (such as antibodies, peptides, glycoprotein coupling, and folic acid) to enhance targeting to the lesion site. The metabolic properties and stability of liposomes can also be improved by tailoring their composition and structure. For example, the rate of drug release and stability can be controlled by adjusting the lipid fraction and the thickness of the membrane layer of liposomes, thereby improving the bioavailability and therapeutic efficacy of photosensitizers and making them more desirable carriers for photosensitizers.

**Polymeric Nanoparticles** Poly(lactic-*co*-glycolic acid) (PLGA) and polyethylene glycol (PEG) are both highly biocompatible and biodegradable polymers that

can be prepared as photosensitizer-loaded nanoparticles [175–178]. The surface of polymeric nanoparticles can also be chemically modified to improve their targeting and stability. It is worth noting that both PLGA and PEG have been approved by the US Food and Drug Administration (FDA). For PLGA, the FDA has approved it for use in a variety of areas including drug delivery (such as the preparation of nanoparticles and microspheres), tissue engineering, and medical devices. PEG is approved by the FDA as a pharmaceutical excipient for use as an inactive ingredient in drug formulations to improve drug solubility, stability and bioavailability [179].

**Nanogels** Nanogels are highly cross-linked polymers with a network structure and have excellent biocompatibility and biodegradability [180, 181]. This highly cross-linked network structure provides good stability with a large pore structure, allowing drugs (including photosensitizers) to be evenly distributed within the nanogel, preventing premature degradation or inactivation in vivo [182]. Another advantage of nanogels is that they can respond rapidly to changes in the in vivo environment and provide controlled drug release [183]. For example, when the nanogel is exposed to the low pH environment of tumor tissue, the cross-linked structure of the gel can be altered, leading to drug release [184, 185]. In addition, the temperature-sensitive properties of nanogels can be used to achieve temperature-sensitive drug release [186]. In conclusion, nanogels have promising applications in areas such as drug delivery and photosensitive therapy.

**Natural Macromolecules** Proteins, chitosan, DNA, gelatin, etc., which have good biocompatibility and biodegradability, can be loaded with photosensitizers in various ways (such as wrapping, adsorption, and chemical bonding) [187–190]. Among them, albumin has many advantages as a photosensitizer carrier [191–194]. Firstly, as a naturally occurring protein in living organisms, albumin can reduce adverse reactions to tissues and cells and reduce the toxicity and side effects of photosensitizer. Secondly, albumin has a long-circulating life and high stability, which allows it to carry and deliver photosensitizers stably in the body. Thirdly, albumin as a carrier can improve the stability of photosensitizers. Many photosensitizers are susceptible to inactivation by light and oxygen in the free state, and encapsulating them in albumin can provide protection and prolong the life of photosensitizers. In addition, albumin can modulate the activation state of photosensitizers by interacting with them, further improving their stability and efficacy. Fourthly, albumin has good targeting for drug delivery. Albumin can achieve targeted delivery to specific tissues or cells by binding to specific receptors or molecules. For example, by modifying the ligands on the surface of albumin, selective recognition and localization of tumor cells can be achieved, thereby improving the accumulation of photosensitizer in tumor tissues and the therapeutic effect. Fifthly, albumin as a carrier can also provide controlled drug release. By adjusting the structure of albumin or complexing it with other materials, it is possible to achieve a slow release of the photosensitizers or a controlled release in response to changes in the specific in vivo environment.

**Biodegradable Mesoporous Silica** Mesoporous silica nanoparticles are nanomaterials with regular pores and high specific surface area for efficient encapsulation of small-molecule photosensitizers. By introducing metal elements (e.g. elemental iron, manganese) or metal oxides (e.g. calcium oxide) as well as organic compounds (e.g. compounds containing disulfide or selenium bonds) into the –Si–O–Si– backbone of mesoporous silica [195–199], the degree of shrinkage of mesoporous silica nanoparticles' backbones can be reduced and porosity can be increased to enhance the dissolution rate of the mesoporous silica in the in vivo environment and to facilitate the release of the loaded substances. There are two main methods to regulate the degradation rate of mesoporous silica by doping with organic compounds, one of which is to bind noncovalently doped organic molecules (e.g. methylene blue) into the mesoporous silica backbone [200, 201], causing oligomerization of the silica nanoscale, thereby accelerating its hydrolysis/degradation process. The second is through the hydrolysis reaction of organosilanes [202, 203], which allows organic groups that can be cleaved in the physiological environment to participate in the formation of the silica skeleton.

***Nondegradable Nanomaterials*** Nondegradable nanomaterials, such as mesoporous silicon [204–208], have higher stability and longer lifetime than biodegradable nanomaterials and are less sensitive to pH and temperature. This enables them to stably carry and release photosensitizers in vivo, providing longer-lasting therapeutic effects. In addition, the stability of nondegradable nanomaterials reduces the loss and degradation of photosensitizers and increases their utilization. Another advantage of nondegradable nanomaterials is their high drug-loading capacity and more flexible surface modification capability. They typically have a large specific surface area and tunable pore structure, which can effectively encapsulate photosensitizers and chemically modify the surface for targeted delivery and controlled release of drugs. Therefore, nondegradable nanomaterials also have unique advantages in the field of photosensitizer carriers.

Overall, the choice of nondegradable or biodegradable nanomaterials for photosensitizers loading requires a comprehensive consideration of the specific application needs and objectives. If long-term stable drug release and high drug loading capacity are required, nondegradable nanomaterials may be more appropriate. If gradual drug release is required to reduce toxicity and side effects, or to achieve drug release at a specific time, biodegradable nanomaterials may be more competent. In addition, factors such as the cost of producing nanomaterials, scalability, and production safety also need to be considered.

#### 1.4.3.2 Nanomaterials with Intrinsic Photodynamic Effects

Some of the nanomaterials themselves can be used as downhconversion photosensitive reagents [119, 145, 164, 209–212]; for example, some nonmetallic semiconductor nanomaterials (e.g. fullerene nanoparticles and carbon nitride), metal oxide semiconductor nanomaterials (e.g. titanium dioxide nanoparticles and zinc oxide), metal sulfide semiconductor nanomaterials (e.g. copper sulfide), and metal nanoparticles (e.g. gold, platinum, and silver), which can be excited by light and

transfer the energy to the surrounding oxygen, exciting the triplet oxygen into $^1O_2$ (a type of ROS). Electron-hole pairs are also generated, and the electrons can reduce the oxygen to produce superoxide anion, which is also a ROS. Typically, metallic semiconductor nanomaterials generate ROS mainly through the superoxide anion generation mechanism, whereas nonmetallic semiconductor nanomaterials may generate ROS mainly through the monoclinic oxygen generation mechanism.

Among them, functionalized fullerenes have made promising progress in the field of antimicrobial photodynamic inactivation [213]. The amphiphilic C60 is obtained by introducing hydrophilic cationic groups through chemical substitution reaction, ion exchange reaction, photochemical reaction, or electrochemical method, etc. Since C60 itself weakly absorbs visible light, its ability to absorb visible light can be improved by introducing a light-trapping antenna on its core. C60 has good photostability and is not easily photobleached, and when excited by light, the light-trapping antenna absorbs the visible light and transfers the energy to the C60 molecule through a resonance energy transfer mechanism. Therefore, this process can more effectively excite C60 to participate in photochemical reactions and promote the occurrence of type I and type II photoreactions, which can form $^1O_2$ by energy transfer and superoxide anion radicals by electron transfer, thus exerting photodynamic effects. Photodynamic inactivation experiments have shown that the cationic C60 is an efficient photosensitizer and can be used as a broad-spectrum antimicrobial agent. In these structures, the hydrophobic nature of C60 enhances membrane permeability, while the presence of a positive charge increases the binding of fullerene derivatives to microbial cells, which greatly satisfies the antimicrobial requirement.

#### 1.4.3.3 Energy Conversion Nanomaterials for Photosensitizers

These nanomaterials do not have photosensitivity per se, but they can act as carrier materials and energy converters for photosensitizers and can transfer energy to photosensitizers after being activated by external energy, thus indirectly activating photosensitizers [164, 214]. In other words, this process causes the photosensitizer to produce ROS by changing the nature of the light (such as wavelength and intensity). The main advantage of these nanomaterials is that they change the UV or visible light absorption range of traditional photosensitizers and increase the light absorption of photosensitizers in the NIR range. They mainly include X-ray activated nanomaterials, luciferase quantum dot nanomaterials, two-photon absorption nanomaterials, and rare earth upconversion nanomaterials.

***X-Ray-activated Nanomaterials*** X-ray-activated nanomaterials generally have strong X-ray absorption and can convert it into UV or visible light. The photodynamic process is performed by activating surface-loaded photosensitizer molecules through energy transfer. The advantages of using this type of nanomaterial for PDT include the following [215–220]: X-rays have a strong penetrating ability compared to other photodynamic methods and have a better therapeutic effect on deep tissue lesions; X-rays work synergistically with PDT to produce a better therapeutic effect; X-ray-activated nanomaterials emit fluorescent light, which enables them to

achieve precise localization of the lesion and irradiated area to avoid unnecessary damage to normal tissues.

Chen et al. have achieved important research results in X-ray-induced PDT (Figure 1.15a) [221]. They successfully prepared mZGGOs long afterglow nanoparticles with uniform size and monodispersed spherical morphology using mesoporous silica template method. It was found that under low-dose X-ray irradiation, the mZGGOs could emit obvious NIR persistent luminescence. This fluorescence has a long lifetime and can penetrate 1 cm of muscle tissue, which can achieve an effective imaging function in mice. In addition, by loading silicon phthalocyanine (Si–Pc) photosensitizer, the X-ray excited persistent luminescence can effectively stimulate Si–Pc to generate ROS and kill cancer cells. Furthermore, in vivo luminescence imaging of in situ hepatocellular carcinoma showed that these nanoparticles accumulated in liver cancer tissues through a passive targeting mechanism. X-ray-activated PDT can effectively inhibit the growth of in situ liver tumors. Using organic phosphorescent nanoscintillators with dual roles as scintillators and photosensitizers, the deep-seated tumors can be effectively eliminated at a low dose of 0.4 Gy with almost no toxic side effects on normal tissues and cells (Figure 1.15b) [222]. The above study provides an important reference for the further development and application of X-ray-induced PDT in clinical applications.

***Luciferase Quantum Dot Nanomaterials*** The biofluorescent resonance energy transfer system based on luciferase quantum dot nanomaterials is a new type of energy converter that combines biotechnology and nanotechnology. The light produced by the reaction between luciferin and luciferase is called "molecular light" or "autofluorescence" [220, 223–225]. Although the total photon flux of molecular light is much lower than that of an external light source (for example, a laser), molecular light can operate within a few nanometers of the target and achieve relatively high photosensitivity efficiency at much lower photon fluxes through near-field energy transfer. Lai et al. synthesized a Renilla luciferase-immobilized quantum dot 655 (QD-RLuc8) for the realization of bioluminescence resonance energy transfer-mediated PDT [226]. Upon addition of coelenterazine, a substrate for the action of luciferase, QD-RLuc8 emitted autofluorescence at a wavelength of 655 nm, which in turn activated the photosensitizer Foscan to generate ROS.

Yun et al. have performed theoretical calculations of the photosensitization efficiency of molecular light using Chlorin e6 (Ce6) as a photosensitizer and bioluminescence resonance energy transfer from quantum dots as molecular light [227]. The calculations show that an irradiation intensity of up to $1\,mM\,cm^{-2}$ per Ce6 molecule is required in the minimum diffraction-limited region when irradiating with conventional physical light sources such as LED or laser. However, using bioluminescence resonance energy transfer-triggered photosensitization, one photon from a luciferin/luciferase reaction is sufficient to activate one Ce6 molecule if the bioluminescence resonance energy transfer efficiency is 100%. When the bioluminescence resonance energy transfer efficiency is about 50%, two photons can activate one Ce6 molecule. In comparison, the efficiency of activating Ce6 using bioluminescence resonance energy transfer is about 6830 times higher

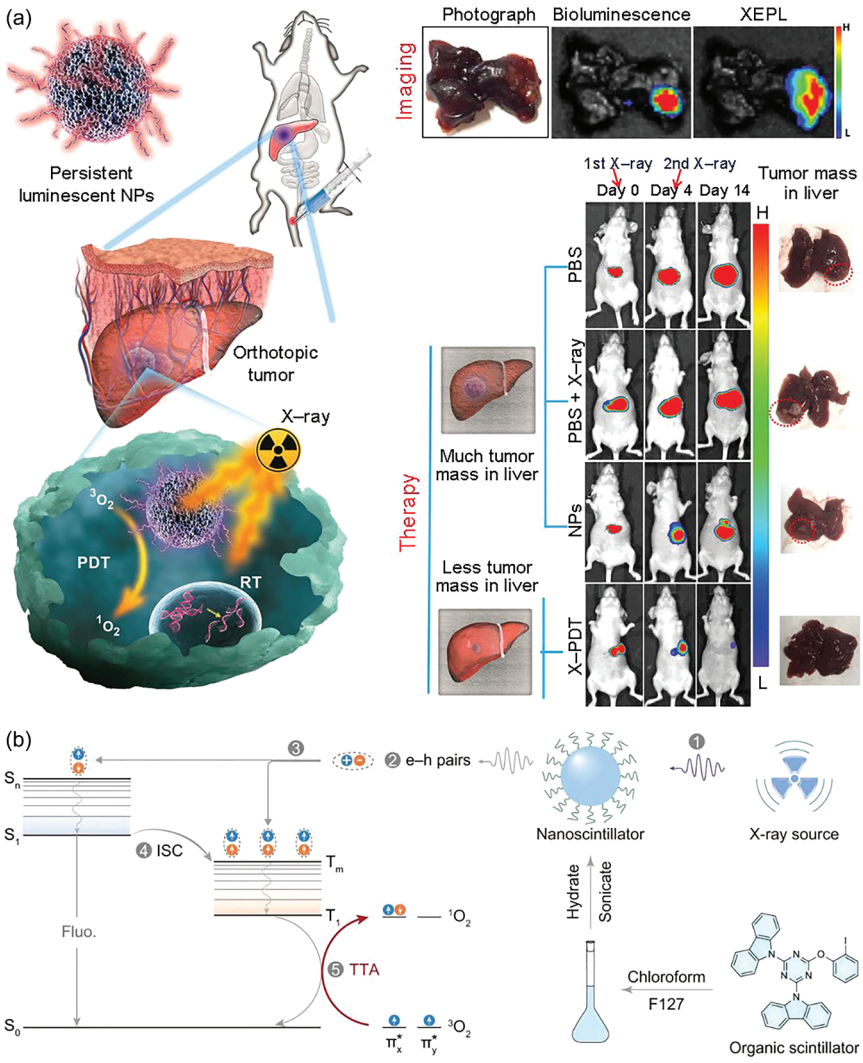


**Figure 1.15** (a) Schematic illustration demonstrates that X-ray-induced persistent luminescence promotes ultrasensitive imaging and effective inhibition of orthotopic hepatic tumors. Source: Reproduced with permission from Ref. [221]; © 2020/John Wiley & Sons. (b) Schematic illustration demonstrates X-ray-induced persistent luminescence promotes ultrasensitive imaging and effective inhibition of orthotopic hepatic tumors. Source: [222]/Springer Nature/CC BY 4.0.

than that of conventional LED or laser. Thus, the work provides good theoretical and computational evidence that molecular light can effectively activate photoreactions and in vivo photosensitization by near-field energy transfer.

***Two-photon Absorption Nanomaterials*** Two-photon absorbing nanomaterials are nanoscale materials that absorb two photons. Two-photon absorption is a nonlinear

optical process in which two photons are absorbed simultaneously by an atom or molecule, causing the atom or molecule to jump from an initial energy level to a higher energy level [228, 229]. This process requires the total energy of the two photons to be equal to or greater than the jump energy level difference. Photosensitizers based on two-photon excited nanoparticles, which combine two-photon absorption and nanotechnology to facilitate deep light penetration and reduce photobleaching of photosensitizers, have received much attention from researchers. A large number of photosensitizers have been developed, including mainly those based on two-photon excited quantum dots, two-photon excited carbon-based nanomaterials, two-photon excited silica nanomaterials, two-photon excited gold nanomaterials, and two-photon excited polymer nanomaterials. Regarding the related research progress in this field, Chen et al. have published a review entitled "Two-photon excitation nanoparticles for photodynamic therapy" in *Chemical Society Reviews* [230]. We will not repeat the contents here.

***Rare Earth Upconversion Nanoparticles (UCNPs)*** As mentioned above, UCNPs have the ability to absorb two or more low-energy photons and then "upconvert" them into a single high-energy photon, converting near-infrared light into visible or even ultraviolet light [231]. This is an inverse-Stokes-law process realized by a sequence of multiphoton absorption and energy transfer, and this unique property of UCNPs could not be better exploited to improve the efficiency of photosensitizers [76, 232, 233]. This is because conventional photosensitizers, such as dyes and organic compounds, typically absorb only a portion of the visible light spectrum, whereas UCNPs can absorb infrared or NIR light and convert it to visible or ultraviolet light, greatly expanding the spectral range of photosensitizer applications. Therefore, this unique optical property gives UCNPs a significant advantage in activating photosensitizers by overcoming the problems of short absorption of conventional photosensitizers in terms of wavelength and insufficient penetration depth of visible light, which can improve the efficiency of photosensitizers while reducing the potential damage to biological tissues from high-energy photons [234–237]. In addition, UCNPs are more stable to light and heat than conventional photosensitizers, making them ideal light energy converters, especially in biomedical applications. Overall, UCNPs offer a novel and efficient way of converting and harnessing light energy with a wide range of applications.

Ju et al. synthesized UCNPs with energy absorbing ($NaYF_4$:Nd,Yb), energy emitting ($NaYF_4$:Yb,Er), and inert ($NaYF_4$:Gd) core-shell structures, limiting energy absorption and transfer to a local space of 5 nm thickness on a single nanoparticle, and binding a NIR dye (800CW) to the surface of the $NaYF_4$:Nd,Yb layer for further sensitization (Figure 1.16a) [238]. Under NIR light irradiation, 800CW absorbs a large number of photons and then transfers the energy to $Nd^{3+}$ and $Er^{3+}$ sequentially via resonance energy transfer, which, coupled with the effect of inert nuclei blocking energy transfer to the interior of the nanomaterials, results in a 3600-fold increase in the emitted light intensity of $Er^{3+}$ compared to that of conventionally structured UCNPs. When a receptor molecule (such as the dye N719) is attached to the surface of UCNPs, the target to be measured substance, $Hg^{2+}$, reacts with N719,

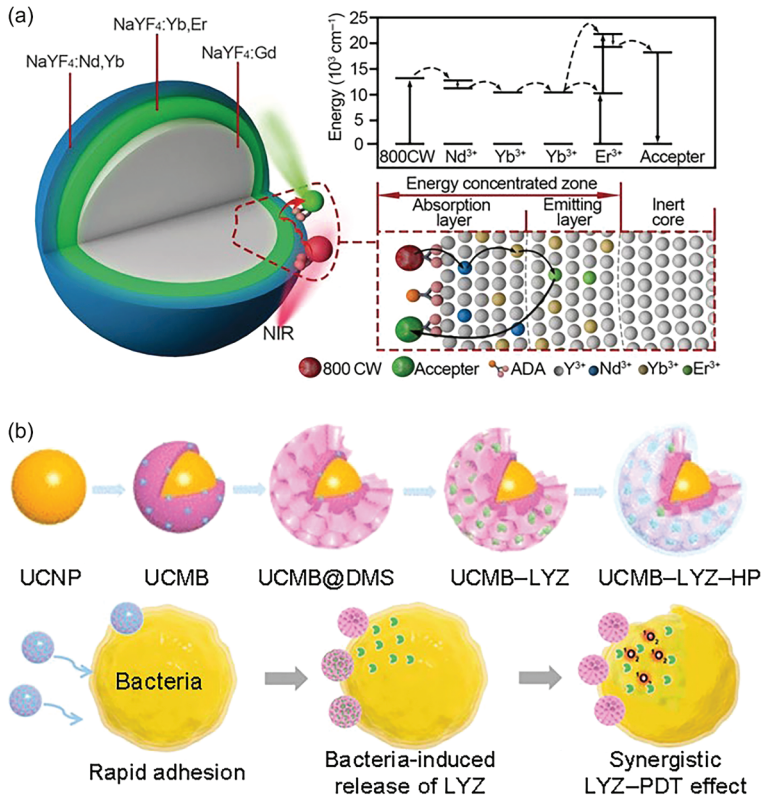


**Figure 1.16** (a) UCNPs structured with an energy-concentrating zone to boost energy transfer efficiency and a simplified energy level diagram. Source: Reproduced with permission from Ref. [238]; © 2019/John Wiley & Sons. (b) Illustration of the synthesis and mechanism of action of antibacterial nanohybrid UCMB-LYZ-HP. Source: Reproduced with permission from Ref. [239]; © 2021/John Wiley & Sons.

which in turn induces the recovery of $Er^{3+}$-emitting fluorescence, significantly improving the sensitivity of the bioanalysis and lowering the detection limit by three orders of magnitude. When the photosensitizer Rose Bengal was used as an energy acceptor molecule modified on the surface of the UCNPs, the ROS yield was also significantly improved, resulting in better tumor therapeutic outcomes even under anoxic conditions. This study provides an important option for the development of highly sensitive biochemical analysis methods and cancer therapeutic protocols.

Chen et al. reported a bioinorganic hybrid nanomaterial that presents a combined photodynamic and lysozyme antimicrobial therapy based on UCNPs, which successfully fights drug-resistant bacterial infections in deep tissues (Figure 1.16b) [239]. The key to this therapy is that they used a type of UCNP encapsulated by an oversized mesoporous silica layer that can be loaded with photosensitizers and lysozyme. They then modified the surface of the material by self-assembly of hyaluronic acid and polylysine to form a "valve" that responds to bacterial hyaluronidase, allowing intelligent release of lysozyme from the silica pore channels. Antimicrobial

experiments demonstrated the ability of this hybrid material to exert synergistic antimicrobial effects through bacterial cell wall disruption by releasing lysozyme and PDT, with significant disinfectant effects against methicillin-resistant *S. aureus*. The excellent therapeutic efficacy of the material against deep tissue infections with drug-resistant bacteria, without toxic side effects, was confirmed by experiments in mice models of wound infection. This work is instructive for the development of nonantibiotic antimicrobial agents and for mitigating the resistance crisis.

### 1.4.4 Photoelectrochemical Nanomaterials

Photoelectric nanomaterials are a class of energy-transforming functional materials that can convert light energy into electrical, chemical, or other energy [240–242]. There are various classification criteria for such materials, which can be divided into photoelectric conversion materials and photocatalytic materials in terms of their applications, and organic photoelectric functional materials, inorganic photoelectric functional materials, and organic–inorganic photoelectric complexes in terms of their compositions. Due to their unique physical and chemical properties, photoelectric nanomaterials have a wide range of applications in various fields such as photocatalysis, solar cells, light detection, optical communication, optical storage, lighting, and display technologies. Undoubtedly, photoelectric nanomaterials also play an important role in biomedical fields, such as biosensing and analytical detection, disease diagnosis, drug analysis, biomarkers and tracking, photothermal and photodynamic therapies, life analysis, and pathogenic microbial research [243, 244]. In this section, we will focus on the applications of photoelectrochemical nanomaterials in biosensing and analytical detection and nothing else.

Photoelectrochemical analysis is a new type of analytical method based on the photoelectric conversion properties of nanomaterials for detection, which has been established in recent years following the mature development of optical, photochemical, and electrochemical methods. This method is mainly based on the photoelectric conversion of photoelectrochemically active materials on the electrode surface and the recognition process of the target to be measured and is characterized by high sensitivity, simple equipment, low cost, fast detection speed, and easy miniaturization [245, 246]. As shown in Figure 1.17a, the photoelectrochemical sensors used in photoelectrochemical detection generally include, among other components, an excitation light source (laser, LED, xenon lamp, etc.), a monochromator, an electrolytic cell and an electrochemical detection device [247]. In the presence of the light source and the electron donor/acceptor, the photoelectrically active material on the working electrode undergoes charge jump and transfer, resulting in the formation of a stable photocurrent in the external circuit. Quantitative photoelectrochemical analysis is based on the relationship between the change in photocurrent or photovoltage and the concentration of the substance to be measured before and after the direct or indirect biorecognition interaction process. Since the photoelectrochemical process couples the photoexcitation process with electrochemical detection, the excitation and detection signals belong to different energy forms, which can significantly reduce the background noise compared

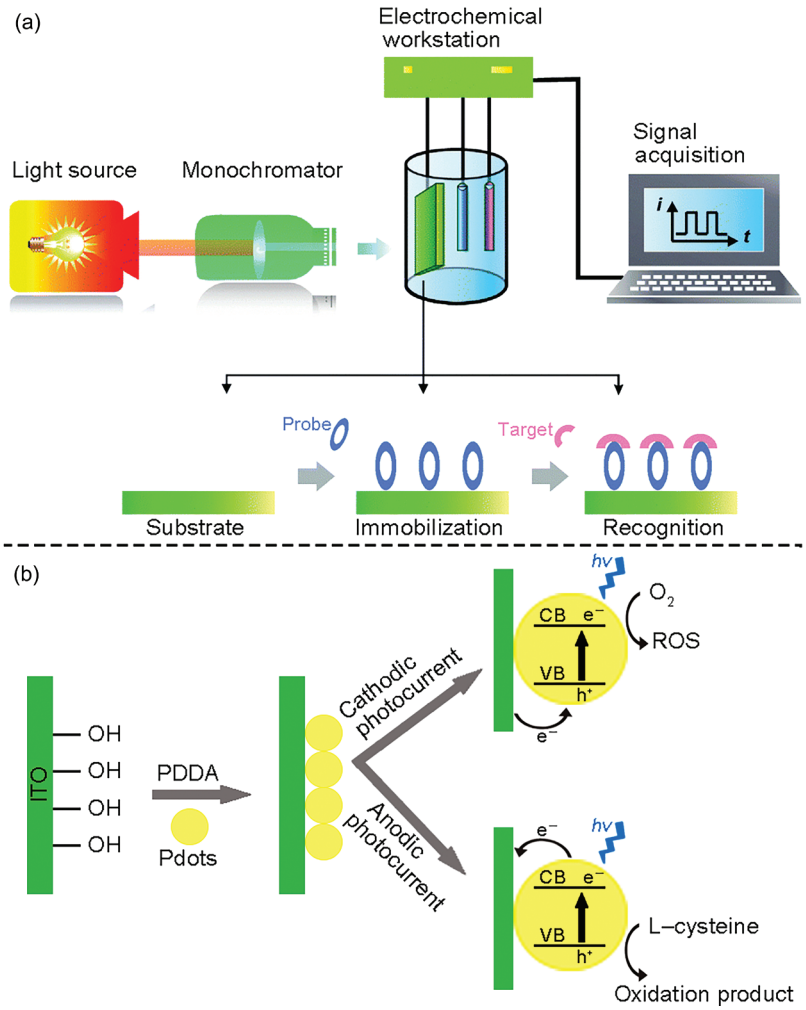


**Figure 1.17** (a) Schematic of the general instrumentation and working principle of PEC bioanalysis. Source: Reproduced with permission from Ref. [247]; © 2015/The Royal Society of Chemistry. (b) Schematic illustration for the preparation of TPP-doped PFBT Pdots and its application for the PEC detection of L-cysteine. Source: Reproduced with permission from Ref. [248]; © 2017/American Chemical Society.

to traditional detection methods (such as chromatography, enzyme labeling, and atomic absorption spectroscopy). At the same time, the lower signal-to-noise ratio helps to further reduce the detection limit [249].

#### 1.4.4.1 Photocurrent Signal Generation Mechanism

Polymer dots (Pdots) are used as an example to elucidate the mechanism by which the sensor exerts photoelectrochemical action (Figure 1.17b) [248]. When the energy of an incident photon ($h\nu$) is greater than the forbidden bandwidth of a photoelectrochemical material, electrons in the valence band of the material absorb the photon

energy and jump to the conduction band to form photogenerated electrons. At the same time, photogenerated holes are also formed in the valence band, resulting in electron-hole pairs (two types of carriers). The carriers have short lifetimes and are in an unstable excited state, so they must release energy to return to their steady state. In the case of excited photoelectrochemical materials, there are four main pathways for the de-activation energy process of photogenerated electron-hole pairs:

(I) Photogenerated electrons and photogenerated holes complex as they move through the material, known as in vivo complexation;
(II) Complexation occurs when photogenerated electrons and photogenerated holes migrate to the surface of the material, namely surface complexation;
(III) Photogenerated electrons migrate to the surface of the material and then react with electron acceptors in solution, that is, oxidized;
(IV) Photogenerated holes migrate to the surface of the material and then react with the electron donor in solution, which is reduced.

Of these four pathways, complexation of photogenerated electrons and photogenerated holes leads to bursting of the photocurrent signal, which is detrimental to the photocurrent signal and is therefore considered a side reaction. To inhibit the complexation of these two carriers, electron donors or electron acceptors can be added to the solution to deplete the photogenerated electrons or photogenerated holes accordingly, which is an effective method of achieving a continuous and stable photocurrent. When the electron donor in the electrolyte solution is consumed in large quantities, the photogenerated electrons become the main carriers, and an anodic photocurrent is generated in the external circuit. If the electron acceptor in the electrolyte solution is consumed in large quantities, the photogenerated holes become the main carriers, and a corresponding cathodic photocurrent is generated in the external circuit. It is not difficult to see that the presence of electron donors or electron acceptors can provide a stable and reliable signal output for carrying out sensing of living matter.

#### 1.4.4.2 Core Elements of Photoelectrochemical Biosensors

Photoelectrochemically active materials and biorecognition elements are the two core elements for the construction of photoelectrochemical biosensors, and both are indispensable [247]. They work together to enable the sensor to achieve high sensitivity, selectivity, and specificity for detecting target biomolecules. Photoelectrochemically active materials are materials that are capable of generating signals such as currents or potentials through photoexcitation or photocatalytic reactions and play the role of signal conversion in photoelectrochemical sensors [250]. So far, a variety of photoelectric conversion materials have been developed for the formation of photoelectrochemical biosensors, mainly in the following categories: inorganic photoelectric materials represented by $TiO_x$, ZnO, $SnO_2$, $Cu_2O$, $Bi_2S_3$, $Ag_2S$, CdTe, CdS, and so on; organic photoelectric materials, including organic small molecules, organometallic compatibilizers, polymer polymers, and part of COFs and MOFs; various types of composite photoelectric materials; and other photoelectric materials such as all-carbon materials, certain fluorescent proteins,

and so on. These materials have good photoelectrochemical properties and are able to convert light energy into electrical signals or chemical reactions, thereby achieving signal amplification and detection of target biomolecules. For reasons of space, this is not dealt with here. See Chapter 14 for details. Biometric elements are biomolecules or biomaterials capable of interacting specifically with a target substance [251].

#### 1.4.4.3 Types of Photoelectrochemical Biosensors

According to different classification methods, photoelectrochemical biosensors can be divided into different types. For example, according to different application fields, photoelectrochemical biosensors are mainly classified into photoelectrochemical small-molecule sensors, photoelectrochemical DNA sensors, photoelectrochemical immunosensors, photoelectrochemical enzyme sensors, and photoelectrochemical cell analysis. Based on the binding method of the target, photoelectrochemical biosensors can be classified into photoelectrochemical biosensors detected by direct method, photoelectrochemical biosensors detected by sandwich method, and photoelectrochemical biosensors detected by competition method. Based on the difference in the interaction between the biorecognition element and the target, photoelectrochemical biosensors can be further classified into two main categories: biocatalytic and biophilic. According to the type of photoelectrically active materials, photoelectrochemical sensors can be classified into photoelectrochemical sensors based on inorganic semiconductor nanomaterials, photoelectrochemical sensors based on organic semiconductor nanomaterials, and photoelectrochemical sensors based on composite semiconductor nanomaterials. According to the photocurrent signal change pattern of photoelectrochemical biosensors caused by the target, they can be classified into the following three types: signal enhancement type, signal burst type, and signal flip type. The classifications are as follows.

***Signal-enhanced Photoelectrochemical Biosensors*** Such sensors use the specific interaction of biomolecules with the target analyte to detect the presence of the target analyte by means of a current or potential signal generated by a photoelectrochemical reaction. Signal enhancement can be achieved in a variety of ways, including the use of enzymes, nanoparticles, multilayer structures, or signal-enhancing molecules. This approach can dramatically improve the sensor's ability to detect target molecules at low concentrations, thereby increasing the sensitivity and lower limit of detection. Xu et al. first proposed a strategy based on the combined enhancement of carrier directional mobility by piezoelectric and plasma excitons and successfully constructed a portable photoelectrochemical biosensor for the detection of low-abundance cancer markers in human plasma [252]. They simplified the basic building blocks of the photoelectrochemical biosensor, such as using a handheld UV flashlight instead of a physical excitation light source and a digital multimeter instead of an electrochemical workstation (Figure 1.18). The sensor performs the capture and immunoincubation process of the target PSA on a separate microtiter plate, where $H_2O_2$ produced by the enzyme immunoassay

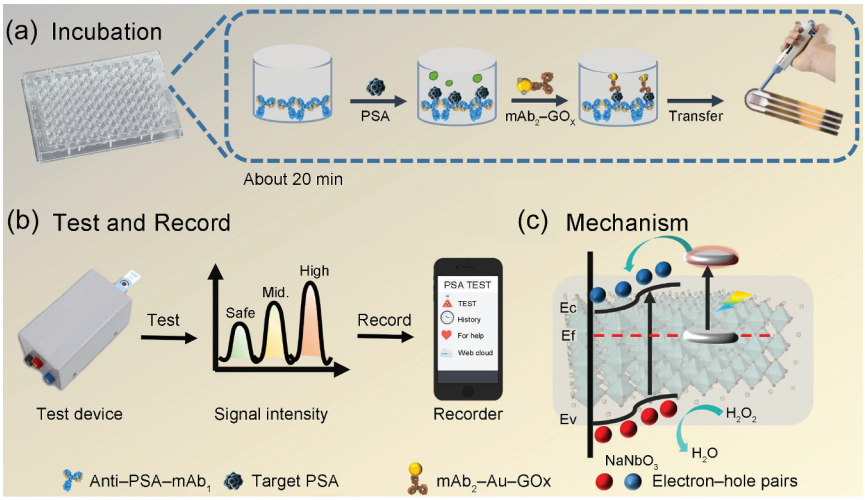


**Figure 1.18** Schematic diagram of PEC bioassay based on local surface plasmon resonance and piezoelectric co-enhancement. (a) Schematic diagram of the incubation process of target PSA in a microtiter plate. (b) Schematic diagram of the PEC recording platform for 3D printed micro devices, with results displayed on a smartphone. (c) Schematic diagram of the energy level structure and photoelectron transfer of the Ag/$NaNbO_3$ composites. Source: Reproduced with permission from Ref. [252]; © 2022/Elsevier.

induces the directional separation of electrons and holes under light excitation, thereby amplifying the photocurrent signal. A digital multimeter was used to monitor the photocurrent in real time. In addition, the effect of Ag nanoparticle deposition on the surface electronic states of the piezoelectric chalcogenide $NaNbO_3$ was investigated by density flood theory calculations. The results show that the photoelectrochemical biosensor exhibits an ultra-wide linear range and an ultra-low detection limit for the target PSA under optimized conditions. The performance is comparable to commercial ELISA kits at the 95% confidence level. This work provides new ideas for the preparation of improved photoelectrochemical biosensors for the rapid and accurate detection of cancer-related proteins.

***Signal-burst Photoelectrochemical Biosensors*** Unlike signal-enhanced sensors, signal-burst sensors cause a reduction in the detected signal when a specific biometric event occurs. This typically involves a biomolecule interacting with the sensor surface, resulting in a reduced photocurrent or current. Signal bursting can be achieved by physical or chemical mechanisms such as energy transfer, electron transfer, or competitive binding. Signal-bursting mechanisms are often used in detection strategies based on competition or site occupancy, and Yuan and coworkers have successfully prepared a signal-bursting photoelectrochemical biosensor for ultrasensitive DNA determination by using $SnO_2$/BiOBr complexes with ideal photoelectrochemical conversion efficiencies as the photoelectrically active substrate and $SiO_2$ as an effective signal quencher [253]. As shown in Figure 1.19, the $SnO_2$/BiOBr heterojunction was coated on the electrode surface

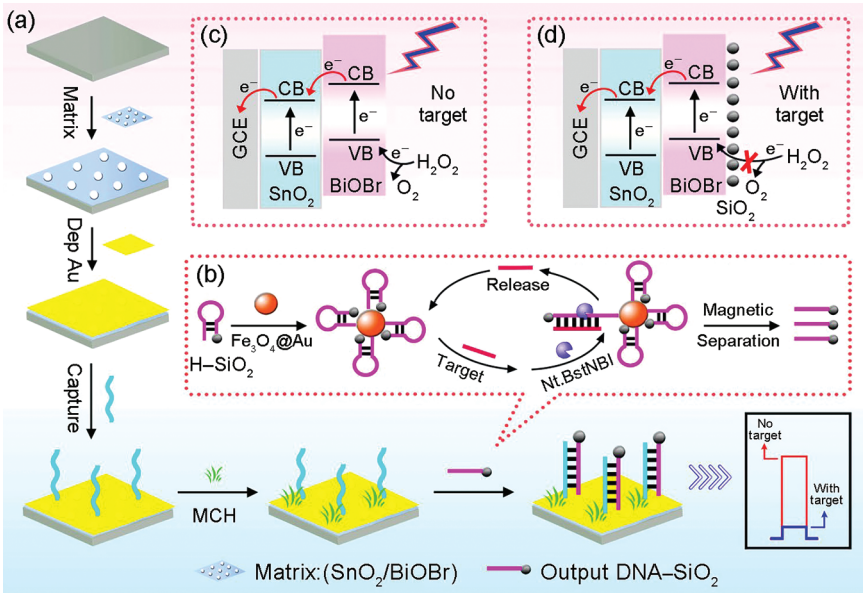


**Figure 1.19** Schematic illustration of this PEC assay for DNA detection based on the $SnO_2$/BiOBr heterostructure. (a) Biosensor assembly procedure. (b) Enzyme-assisted signal amplification process. (c,d) Photocurrent generation mechanism. Source: Reproduced with permission from Ref. [253]; © 2021/American Chemical Society.

to form a large built-in electric field, which not only inhibited the electron-hole recombination but also improved the light absorption ability in the UV-visible region and significantly enhanced the intensity of the initial photocurrent signal generation. Meanwhile, a gold nanoparticle coating was deposited on the surface of $SnO_2$/BiOBr to immobilize and capture DNA. The target DNA was then converted into a large amount of $SiO_2$-modified single-stranded output DNA through an enzymatic cyclic amplification process. Due to the strong steric hindrance effect of $SiO_2$ on electron transport, the initial photocurrent generated by the $SnO_2$/BiOBr heterojunction can be effectively burst, thus achieving highly sensitive detection of the target. Overall, this signal-bursting photoelectrochemical biosensor opens up a new way to monitor various biomarkers.

***Signal-flipping Photochemical Biosensors*** Signal flip-flop sensors are sensors in which the signal change triggered by a biometric event is reversed, i.e. flipped from one state to another. For example, a charge transfer process may occur after a photosensitive material or photoelectrode surface modification layer in a sensor interacts with a target analyte, resulting in a change in the intensity or polarity of the photoelectrochemical signal. This type of sensor may rely on complex biochemical or physical processes to translate a biometric event into a change in the electrical signal, a change that may be due to a change in conductivity, the opening or closing of ion channels, or the production, or consumption of electrochemically active substances. Dai and coworkers designed a signal-switchable photoelectrochemical

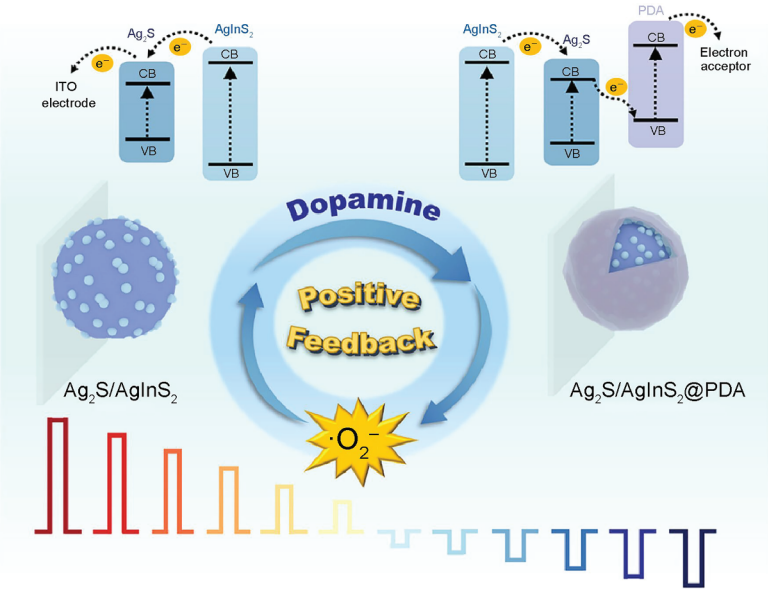


**Figure 1.20** Illustration of a signal-switchable photoelectrochemical biosensor for the detection of dopamine. Source: Reproduced with permission from Ref. [254]; © 2023/American Chemical Society.

biosensor for the detection of dopamine (Figure 1.20) [254]. The polarity switching of the $Ag_2S/AgInS_2$ heterojunction was regulated by free radical-induced positive feedback polydopamine adhesion. In particular, the $Ag_2S/AgInS_2$ complex exhibited extremely stable anodic photoelectrochemical activity. In the presence of light, it is capable of generating superoxide radical ($\cdot O_2^-$) and hydroxyl radical ($\cdot OH$) intermediates that lead to the oxidative polymerization of dopamine and the subsequent attachment of the generated polydopamine to the $Ag_2S/AgInS_2$ heterojunction. In this way, the presence of polydopamine creates a new electron transfer pathway that causes the polarity of $Ag_2S/AgInS_2$ to switch and the photoelectrochemical response to change from anodic to cathodic photocurrent.

In addition, polydopamine with stronger photoreductive activity promotes more radical intermediates, creating a positive feedback mechanism for polydopamine generation and greatly improving the sensitivity of photoelectrochemical biosensing. The applicability of the photocurrent polarity shift achieved by the sensor in real sample assays (e.g. determination of polydopamine in fetal bovine serum) was determined by comparison with commercial ELISA methods.

Different types of photoelectrochemical biosensors have their own advantages and applicability in different application scenarios. The choice of sensor usually depends on factors such as the nature of the target analyte, the desired detection sensitivity, and the complexity of the experimental design. With advances in materials science and biotechnology, the design of these sensors is becoming increasingly sophisticated, enabling higher detection performance and application flexibility.

### 1.4.5 Photoacoustic Nanomaterials

Photoacoustic nanomaterials are materials that can convert light energy into acoustic energy and emit it in the form of ultrasonic waves. Figure 1.21 shows that photoacoustic nanomaterials undergo three processes to produce a photoacoustic signal under the action of a laser: light absorption, photothermal conversion, and thermoacoustic conversion [256, 257]. Specifically, irradiating a material with a pulsed laser or a continuous beam of light that has undergone periodic intensity modulation creates periodic temperature changes within the material, causing that part of the material and its adjacent medium to thermally expand and contract to produce periodic changes in stress (or pressure) and thus generate an acoustic signal, known as a photoacoustic signal [255, 258]. The frequency of the photoacoustic signal is the same as the optical modulation frequency, and its intensity and phase depend on the optical, thermal, elastic, and geometrical properties of the material. This photoacoustic effect has important applications in biomedical imaging, detection, and analysis.

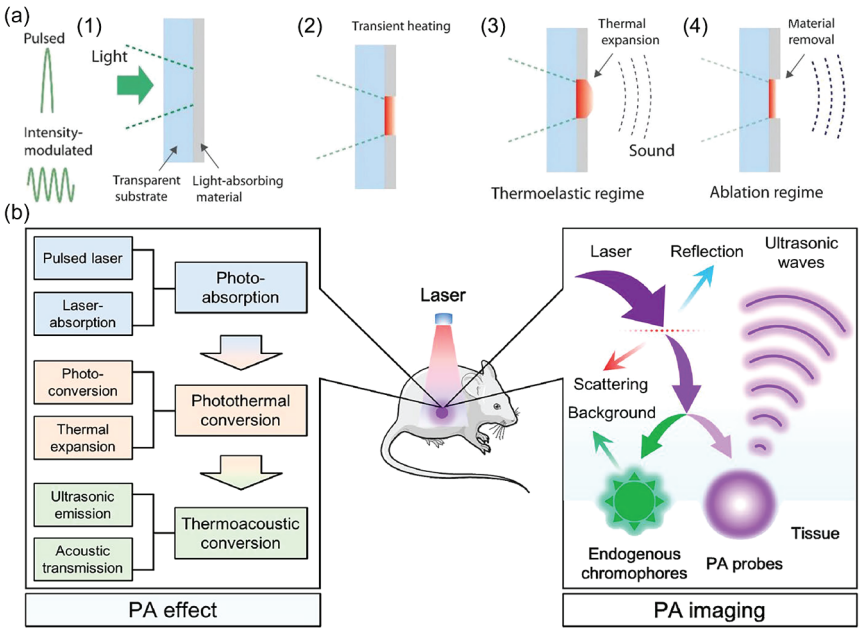


**Figure 1.21** (a) Photoacoustic generation. (1) Light absorption in a light-absorbing material. Light is illuminated in the form of pulsed or intensity-modulated waves. (2) Transient heating of the material by light absorption. Sound generation through two different regimes: (3) thermoelastic regime and (4) ablation regime. In the thermoelastic regime, sound is generated by thermal expansion of the heated material. In the ablation regime, the parts of the material are removed through phase change (invasive), producing much stronger sound intensity. Source: Reproduced with permission from Ref. [255]; © 2018/John Wiley & Sons. (b) Schematic diagram showing the three processes of PA generation and the interaction of laser and biological tissue in PA imaging. Source: Reproduced with permission from Ref. [256]; © 2022/American Chemical Society.

#### 1.4.5.1 Introduction to Photoacoustic Imaging

Photoacoustic imaging (PAI) is a noninvasive imaging technique developed based on the photoacoustic phenomenon, which uses photoacoustic detection to capture acoustic signals generated by biological tissues and then processes these signals through a computer to obtain an image of the internal structure of the biological tissues [259]. In PAI, photoacoustic detection, as an essential part of the process, is achieved by capturing and analyzing changes in the intensity of ultrasonic signals generated by laser energy absorbed by endogenous or exogenous photoacoustic probes to achieve the detection of the target analyte.

In PAI, not only can photoacoustic probes generate photoacoustic signals, but some endogenous pigments can also generate background signals [260–262]. At the same time, as the laser light passes through biological tissue, its intensity in the tissue is significantly reduced due to reflection and scattering at the surface and within the tissue, which can also affect the optical signal [260, 263]. However, the signal intensity in PAI is not represented by the optical signal but by ultrasound, and the scattering of ultrasound in biological tissue is much less than the optical signal. Therefore, although there is attenuation of the optical signal in biological tissue, this does not reduce the resolution of PAI [264]. PAI combines the high sensitivity and contrast of optical imaging with the deep penetration of ultrasound imaging and is therefore capable of imaging tissue up to several centimeters deep while maintaining high spatial resolution [265, 266]. This makes PAI promising for biomedical applications. For example, it can clearly depict the anatomical structure (e.g. melanin and lipid distribution) and physiological function (e.g. blood, blood flow, oxygen saturation, and metabolic rate) of tissues [256, 267–269]. PAI is therefore able to overcome the limitations of purely optical and purely ultrasonic imaging, opening up new possibilities in the field of biosensing and biomedical imaging.

#### 1.4.5.2 Selection of Photoacoustic Contrast Agents

Photoacoustic contrast agents are substances used in PAI to enhance the imaging contrast of tissues and organs. Depending on their source, photoacoustic contrast agents can be divided into endogenous and exogenous contrast agents.

***Endogenous Contrast Agents*** In the absence of external intervention, some biological tissues have the ability to absorb light energy and produce photoacoustic signals on their own, which are endogenous contrast agents. Some endogenous substances (such as water, hemoglobin, melanin, fat, collagen, etc.) have differential light absorption and can be used as endogenous contrast agents in PAI [267, 270, 271]. By modeling the propagation and detection of suitable photoacoustic signals, it is possible to image the structure and function of tissues and organs such as blood, skin, and the eye.

Endogenous contrast agents are substances that occur naturally in living organisms (namely nonspecific photoacoustic contrast agents) and do not require any additional introduction or special treatment, and are therefore highly biocompatible and less likely to cause immune or other adverse reactions. Certain endogenous contrast agents are present only in specific tissues or organs and can provide specific

imaging and contrast that can aid in the study and diagnosis of relevant tissues and lesions. For example, the aforementioned hemoglobin is a protein found only in red blood cells and can be used to image blood, blood vessels and the heart [272]. Melanin is a pigment found only in tissues such as skin, hair, and eyes and is helpful in imaging skin lesions, melanoma and the fundus of the eye [273]. Bilirubin is a yellow pigment metabolized by the liver and found mainly in bile, and is useful for imaging the gallbladder, bile ducts and gallstones [274]. Calcitonin is a calcium salt found in bones and calcified lesions and can be used to image bones, calcified tumors and atherosclerosis [275–277].

However, an unsatisfactory aspect of actual imaging is that certain diseases do not produce endogenous photoacoustic signals, or produce weak photoacoustic signals with relatively low contrast, and may therefore be difficult to detect by PAI in some cases [278]. In addition, the nature and distribution of endogenous contrast agents cannot usually be regulated, optimized, or tuned by external means. Therefore, the use of exogenous contrast agents is often necessary to enhance the contrast of PAI for the study and diagnosis of various diseases.

***Exogenous Contrast Agents*** Unlike endogenous contrast agents, exogenous contrast agents are the result of artificial intervention. These contrast agents are substances introduced into a living organism by injection or other means, which are then calibrated against specific biomarkers or diseased tissue to enhance the contrast of PAI. Exogenous contrast agents are usually light-absorbing nanomaterials such as nanoparticles and nano-dyes. These nanomaterials are capable of absorbing laser energy and generating photoacoustic signals, resulting in more pronounced contrast in imaging.

From an application point of view, tuning the absorption of exogenous contrast agents to the NIR region is key to enhancing image contrast and can improve the resolution and image output intensity of PAI. This is because, on the one hand, NIR light has a greater penetration depth and can better penetrate biological tissues to achieve a deeper imaging depth, enabling imaging of deep tissues and organs [257]. On the other hand, the wavelength range of NIR light is one of the least absorbing regions of biological tissues, and biological tissues absorb and scatter relatively less in this wavelength range, which can reduce the loss of light energy during the imaging process [53, 80]. In addition, the use of NIR light can avoid the damage and photothermal effect on biological organisms and reduce the adverse effects on biological organisms [53]. Therefore, adjusting the absorption of exogenous contrast agents to the NIR region can lead to more efficient generation and propagation of the photoacoustic signal, thereby increasing the intensity of the photoacoustic signal and improving image contrast.

In summary, exogenous photoacoustic contrast agents generally have the following advantages [279]: firstly, they provide a stronger photoacoustic signal, which enhances the contrast to tissues and organs, making subtle structures and functions more clearly visible. Secondly, their properties can be adapted and optimized to meet specific imaging requirements by changing their composition, size, surface modifications, etc. Thirdly, they can be appropriately modified and functionalized

to achieve targeted imaging of specific tissues or cells, improving the accuracy and specificity of imaging.

***Introduction to Photoacoustic Imaging Probes*** So far, many contrast agents (which can also be called PAI probes), for example, carbon-based nanomaterials, metal nanomaterials, transition metal sulfides, organic small molecules and polymers, and ionic liquids, have been widely used in PAI, which has greatly contributed to the development of this imaging technique [280]. In addition to the advancement of a part of PAI probes with strong light-absorbing properties, smart PAI probes triggered by the microenvironment at the lesion (e.g. tumor, Alzheimer's disease, and atherosclerosis) have also been gradually developed. The recent developments of these two types of PAI probes are summarized here.

**Photoacoustic Imaging Probes with Strong Light Absorption Properties** In general, photoacoustic contrast agents and photothermal converters share almost the same physicochemical properties, which means that nanomaterials used for PTT are usually effective for PAI [281, 282]. Such imaging probes can be appropriately modified and functionalized to allow targeted imaging of specific tissues or cells. Listed below are some PAI probes with strong light absorption properties.

A) *Gold-based nanoprobes*: Due to the LSPR effect, gold-based nanomaterials have high light-absorbing properties in the visible and NIR light range. In addition, the shape, size, and structure of gold nanoparticles can be tuned to optimize their light-absorbing properties and biocompatibility. Yao He and coworkers investigated the active endocytosis of glucose polymer-modified gold nanoparticles by different bacteria via the ATP-binding cassette transport pathway, and the small-sized gold nanoparticles after endocytosis could be aggregated under laser induction (Figure 1.22) [283]. The photoacoustic signal of the aggregates was enhanced about 15.2-fold compared to unaggregated gold nanoparticles, overcoming the difficulty of inaccessibility of large near-nanoparticles to bacteria and enabling high-resolution PAI of bacteria in deep tissues. Emelianov and coworkers synthesized hyperbranched gold nanoconstructs capable of acting as efficient photoacoustic contrast agents [284]. It was found that hyperbranched gold nanoconstructs exhibit superior optical properties, including strong NIR absorption, high absorption efficiency at different polarization angles, and excellent photostability, compared to conventional contrast agents based on equipartitioned excitations, such as gold nanorods and gold nanostars. In vitro and in vivo experiments confirm that hyperbranched gold nanostructures are well-suited for high-contrast imaging and stable PAI.
B) *Semiconductor nanoprobes*: These materials include metal sulfides, metal selenides, and metal carbides [285], which have important applications in the field of photoacoustic nanoprobes due to their unique physical and chemical properties such as high electrical conductivity, optoelectronic properties, and thermal stability. Tan and coworkers synthesized an ultrasmall single-layer of $MoS_2$ nanodots with metallic phase by *n*-butyllithium intercalation-assisted

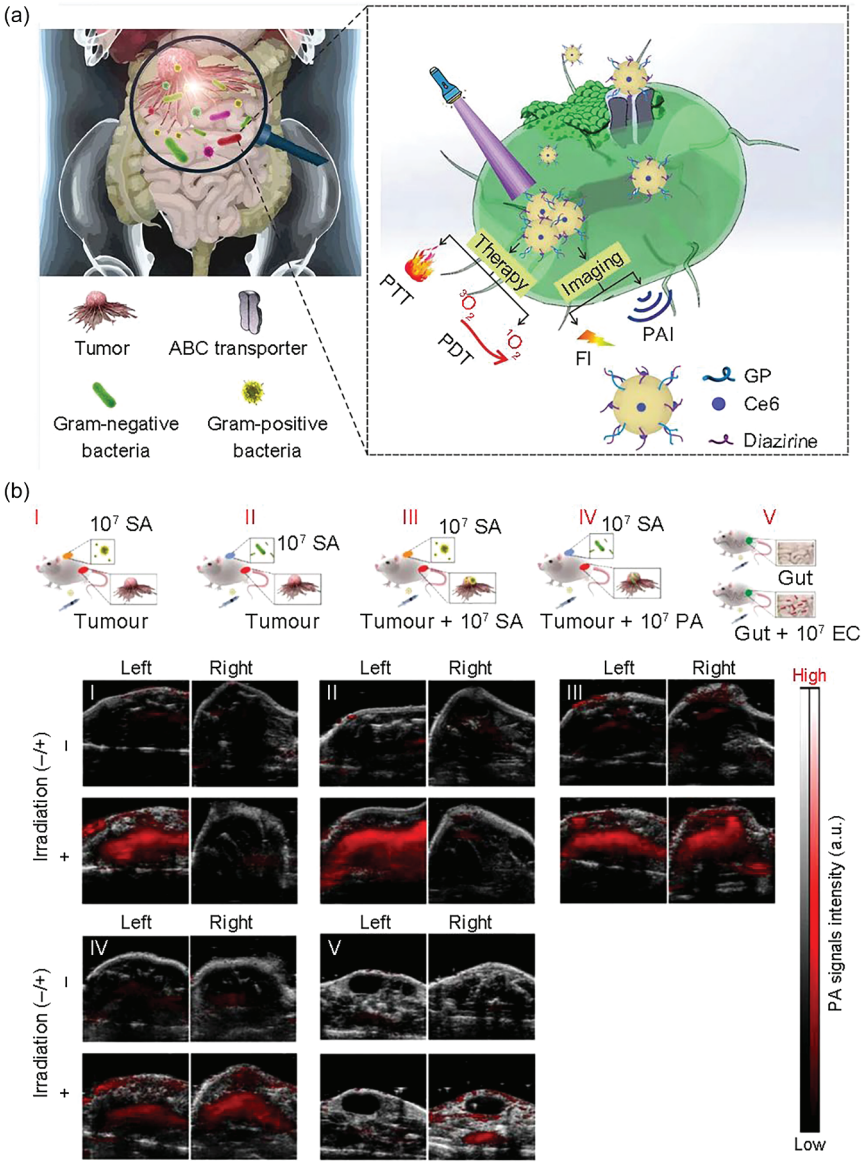


**Figure 1.22** (a) Schematic showing bacteria eating gold nanoparticles for aggregation-enhanced imaging and killing bacteria. The imaging models include fluorescence imaging (FI) and photoacoustic imaging (PAI). The therapeutic methods include PTT and PDT. (b) Schematic illustrating the mice with different treatments and corresponding photoacoustic imaging of photoacoustic intensity of different infected sites with or without the irradiation of 405 nm laser. Source: [283]/Springer Nature/CC by 4.0.

liquid-phase sonication [286]. The nanodots were found to have strong absorption and PAI signals in the NIR-II region and exhibit high extinction coefficients and photothermal conversion efficiency at 1064 nm, which can be used as PAI-mediated photothermal nanoformulations in the NIR-II region. Jiang and coworkers proposed a strategy for activatable PAI using in situ cation exchange of ultrathin zinc selenide (ZnSe) nanoplates to monitor copper levels in the brain of Alzheimer's disease mice [287]. They attached ultrathin ZnSe probes to peptide ligands that target the blood-brain barrier, allowing them to effectively cross it. Once in the brain, the nanoplatelet probe rapidly exchanges with endogenous copper ions, enabling activatable PAI of copper levels in the brain. Wu et al. obtained $MnO_x/Ta_4C_3$ nanocomposites by growing manganese oxide nanoparticles in situ on the surface of $Ta_4C_3$ MXene [288]. $Ta_4C_3$ has good photothermal conversion properties, making the synthesized material an ideal contrast agent for PAI both in vitro and in vivo.

C) *Carbon-based nanoprobes*: Carbon-based nanomaterials (e.g. carbon dots, carbon nanotubes, and graphene) serve as effective photoacoustic probes for biomedical imaging, such as tumor detection and vascular imaging, due to their high light absorption properties in the ultraviolet to NIR range and good biocompatibility [139, 289, 290]. Smith and coworkers have prepared ultra-selective Ly-$6C^{hi}$ carbon nanotubes for imaging and identification of inflammatory atherosclerotic plaques [291]. Since inflammatory cells such as macrophages and monocytes tend to accumulate on inflammatory patches, this specific carbon nanotube is preferentially taken up by macrophages and monocytes. In this technique, the vascular region of interest is irradiated with light, causing the carbon nanotubes to vibrate and emit an ultrasound signal. This photoacoustic effect makes it possible to visualize inflammatory plaques and identify which unstable patches are present in the body. This imaging technique is important for the early detection and localization of inflammatory atherosclerotic plaques.

D) *Black phosphorus-based nanoprobes*: Black phosphorus is a two-dimensional material with a special layered structure and tunable optoelectronic properties. Due to its wide band gap and high carrier mobility, black phosphorus has strong light absorption ability, which can effectively convert light into heat and produce a strong photoacoustic signal. Meanwhile, black phosphorus also has good biocompatibility and degradability. Therefore, black phosphorus-based nanoprobes have been widely studied and applied in the field of PAI and have potential applications in biomedical imaging and drug delivery disease diagnosis. Yu and coworkers successfully prepared a novel black phosphorus PAI contrast agent known as titanium ligand-modified black phosphorus quantum dots [292]. The quantum dots have excellent photoacoustic conversion properties and good stability in the physiological environment. Cell and animal in vivo tests have shown that the quantum dots can efficiently accumulate in tumor cells and absorb light pulses, resulting in detectable ultrasound signals. By analyzing these signals, high-resolution and high-contrast 3D tumor images can be generated. This study provides a new method for PAI of tumor tissue,

which enables accurate imaging and localization of tumors and is expected to provide more accurate and reliable imaging guidance for clinical diagnosis and treatment.

E) *Organic photothermal molecule-based nanoprobes*: There are many common dyes, such as pyrrolidine dyes, acridine dyes, phthalocyanine dyes, indocyanine, and rhodamine, which have strong light-absorbing properties, especially in the NIR region, and are used as PAI probes [293–295]. These organic photothermal molecules have high light absorption cross-sections and high photothermal conversion efficiencies, which can improve the generation and detection sensitivity of photoacoustic signals. In addition, these molecules can often be chemically modified or conjugated to other nanomaterials (e.g. gold nanoparticles or silicon nanoparticles) to improve their stability and targeting in vivo. Lin and coworkers have developed a new class of rhodamine-like photoacoustic dye called GX, which has controllable photoacoustic properties and function in the NIR-II region (Figure 1.23) [296].

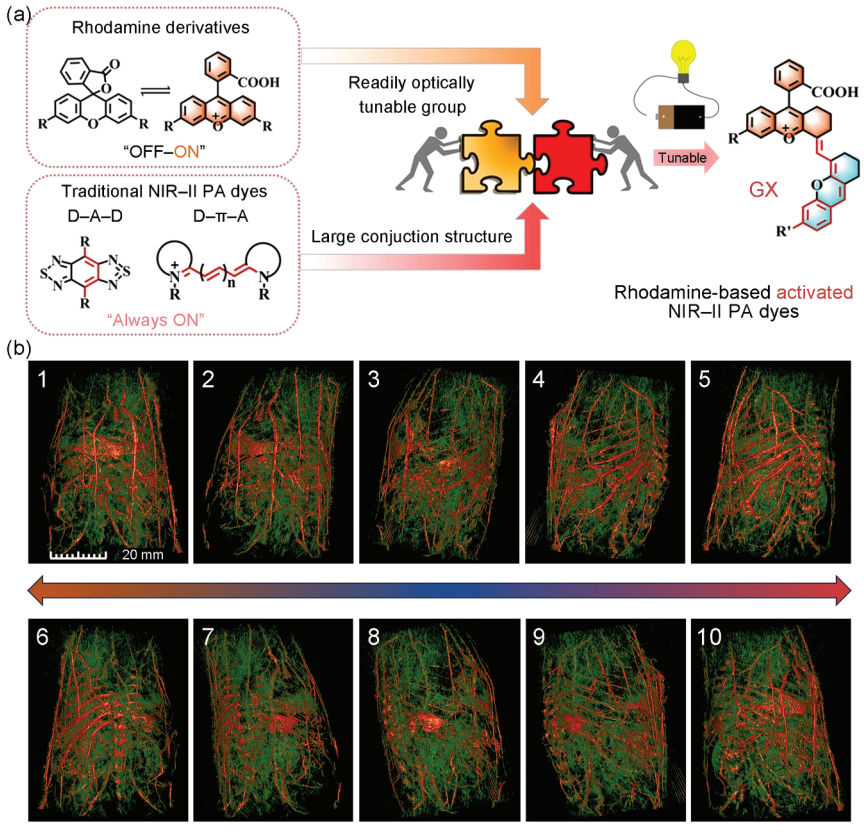


**Figure 1.23** (a) Rational design of dyes GX as a novel class-activated NIR-II PA platform. (b) Multi-angle NIR-II PA 3D imaging of mice vasculature by dye GX-5. Source: Reproduced with permission from Ref. [296]; © 2023/John Wiley & Sons.

These novel NIR-II photoacoustic dyes possess a robust optical switching mechanism similar to that of conventional rhodamine and have absorption and emission wavelengths suitable for the NIR-II region. Among them, the dye GX-5 has absorption and emission wavelengths up to 1082 and 1360 nm, respectively. They performed PAI experiments using GX-5 dye and successfully visualized the distribution and structure of the mouse vasculature in a three-dimensional perspective. In addition, using GX-5 as an activatable dye platform, they constructed the first NIR-II probe, GX-5-CO, for the specific detection of carbon monoxide. The probe has been shown to reveal carbon monoxide levels in hypertensive mice using NIR-II PAI, demonstrating the potential value of this novel NIR-II photoacoustic dye, which is expected to be a powerful tool for biomedical imaging and disease diagnosis, among other applications.

**Intelligent Photoacoustic Imaging Probes Triggered by the Lesion Microenvironment**
The lesion microenvironment refers to the specific environmental conditions surrounding the lesion area in diseases such as tumors, Alzheimer's disease, and atherosclerosis [297–302]. Lesion-triggered smart PAI probes are probes that respond and translate into photoacoustic signals based on the characteristics of the lesion microenvironment. These probes can provide a better understanding of the mechanisms of disease and the characteristics of the lesion area, and offer guidance and clues for the diagnosis and treatment of disease. The following are some common microenvironment-triggered smart PAI probes at lesions:

A) *pH-sensitive probes*: Diseases such as tumors and atherosclerosis are often associated with an acidic microenvironment [275, 303], so pH-sensitive probes are a common type of microenvironment-triggered photoacoustic probe at the site of a lesion. These probes typically consist of pH-sensitive organic dyes and carriers. In an acidic environment, these organic dyes undergo structural changes that alter their optical and photoacoustic properties and generate specific photoacoustic signals. pH-sensitive probes can achieve highly sensitive imaging and molecular diagnosis of the acidic microenvironment at the lesion site. Liu and coworkers reported a pH-responsive ratiometric photoacoustic probe obtained by self-assembly based on albumin, benzo[*a*]phenoxazine (BPOx), and the NIR dye IR825 [304]. It was found that IR825 could be used as an internal reference because its absorbance at 825 nm was not affected by pH changes. However, the photoacoustic signal at 680 nm of BPOx was significantly enhanced with decreasing pH. Therefore, the ratio of the intensity of the 680 nm to the 825 nm photoacoustic signal can be used to measure the pH of the tumor site. Using this pH-dependent ratio probe, immediate pH changes within the tumor can be detected.
B) *GSH-sensitive probes*: GSH is one of the major intracellular reductants involved in regulating intracellular redox reactions and maintaining intracellular redox homeostasis [305, 306]. However, the level of intracellular GSH is altered in some disease states, leading to dysregulation of redox homeostasis. In cancer, intracellular GSH levels are usually elevated due to factors such as high metabolic

activity, increased oxidative stress, and drug resistance in cancer cells [307, 308]. High levels of GSH help cancer cells resist oxidative stress and the toxicity of chemotherapeutic drugs, thereby promoting tumor growth and metastasis. In contrast, in some cardiovascular diseases, neurodegenerative disorders, and the aging process, GSH levels can decrease, making cells more susceptible to damage from oxidative stress [309–311]. Shi's team designed an intelligent pH/GSH dual-stimulation-responsive NIR probe, Cy-1, which can be activated by the synergistic effect of acidic pH and reducing GSH, followed by a bioorthogonal condensation reaction between the cyano group of 2-cyanobenzothiazole and 1,2-amino thiols to form amphiphilic cyclic dimers, which further self-assemble into nanoparticles with larger sizes [312]. The formed nanoparticles significantly enhanced the accumulation and retention of the probe in the tumor, enabling highly sensitive NIR/PAI.

C) *Hypoxia-sensitive probes*: Diseases such as tumors, atherosclerosis and Alzheimer's disease are often hypoxic [51, 313, 314], so hypoxia-sensitive probes are also a common microenvironment-triggered photoacoustic probe. These probes are usually nanoparticles or molecules containing specific fluorescent dyes or fluorescent proteins that undergo chemical or physical changes when exposed to an oxygen-deficient environment. This change can alter the way the probe absorbs light, which in turn affects the resulting acoustic signal. Hypoxia-sensitive probes provide information on the spatial distribution and temporal changes of oxygen deprivation, helping to understand disease mechanisms and guide therapeutic strategies. Nie and coworkers developed a hypoxia-sensitive molecular probe, HyP-650, for PAI [315]. The probe has an absorption peak at 650 nm, which is red-shifted in a hypoxic environment and converted to a substance red-HyP-650 with an absorption peak of 740 nm. Therefore, by simultaneously detecting the signal changes at both 650 and 740 nm, the conversion ratio of HyP-650 can be calculated, and the oxygen content in the tissue can be further inferred. This study overcomes some of the shortcomings of conventional methods of detecting tissue oxygen content and enables simultaneous imaging of tissue and blood oxygen content. This provides new ideas for hypoxia-related pathological analysis and disease detection. Using the HyP-650 probe, researchers can noninvasively detect hypoxia in tissues and obtain information about the extent and distribution of hypoxia. This is important for understanding the role of hypoxia in disease development, assessing disease severity, and guiding treatment.

D) *Enzyme-sensitive probes*: Diseases such as tumors and atherosclerosis usually exhibit high enzymatic activity [51, 275, 316]. Therefore, enzyme-sensitive photoacoustic probes can be used to accurately and sensitively detect the activity and distribution of specific enzymes in organisms by exploiting their molecular cleavage or structural rearrangement under the catalytic action of enzymes, which in turn changes the optical properties of the probes and affects the nature of the photoacoustic signals generated. Gao and coworkers have integrated a NIR fluorescent photoacoustic dye, a bone-targeting motif, and a histone K-responsive peptide sequence to prepare a histone K-activatable

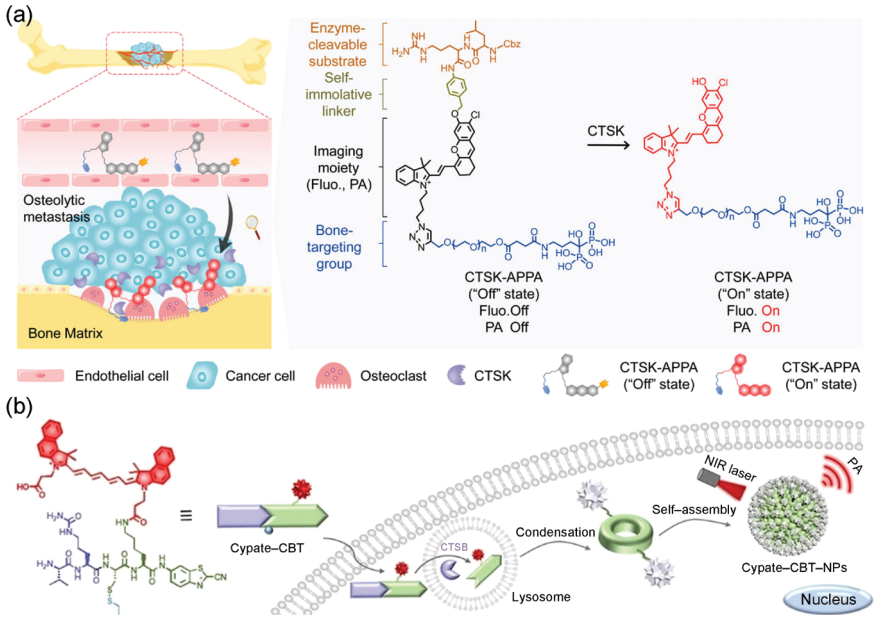


**Figure 1.24** (a) Schematic diagram showing the mechanism of CTSK-APPA for imaging osteolytic metastasis. Source: Reproduced with permission from Ref. [317]; © 2023, The Authors. Advanced Science published by Wiley-VCH GmbH. (b) CTSB-triggered self-assembly of Cypate-CBT-NPs for PAI of CTSB activity in vitro. Source: Reproduced with permission from Ref. [318]; © 2021/John Wiley & Sons.

bone-targeting fluorescent photoacoustic probe (Figure 1.24a) [317]. The probe could be targeted to bone tissue and activated by histone kinase K in the microenvironment of osteolytic bone metastatic tumors, and high-contrast and specific dual-modality photoacoustic and fluorescence imaging could be achieved under laser irradiation. Liang and coworkers developed a smart photoacoustic probe, Cypate-CBT, which responds to abundant GSH and histone B in tumor cells to self-assemble into nanoparticles containing the NIR fluorescent dye cypate, which in turn can be used for tumor-specific PAI of histone B activity (Figure 1.24b) [318].

E) *Temperature-sensitive probes*: Malignant tumors, Alzheimer's disease, and atherosclerosis, among others, usually exhibit higher temperatures. Therefore, the design of temperature-sensitive probes can provide information on temperature distribution and changes, which can help to understand temperature regulation mechanisms in biological processes and play an important role in medical diagnosis and treatment. By introducing about 4% tungsten into vanadium dioxide nanoparticles, a thermochromic material, Xing and coworkers not only reduced the phase-transition temperature of vanadium dioxide but also enhanced its absorption capability in the NIR region, which improved the performance of PAI [319]. Furthermore, the above materials were encapsulated with PEG to prepare body temperature-triggered phase-transition photoacoustic nanoprobes (W-$VO_2$@PEG), which have good convertible optical absorption

properties in the NIR region close to body temperature. This study provides a novel temperature-sensitive PAI nanoprobe with low phase-transition temperature and enhanced NIR absorption for high-resolution, high-contrast in vivo imaging.

F) *Metal ion-sensitive probes*: Metal elements play an important role in life processes, and they are involved in many key cellular processes such as enzyme catalysis, signal transduction, and regulation of gene expression. However, imbalances in metal ion homeostasis can severely disrupt these vital processes and lead to a variety of diseases [320]. Metal ion-sensitive probes allow the imaging of lesions through the binding of metal ions. These probes typically consist of metal ion-sensitive organic dyes and support that undergo structural changes when the metal ions are bound, thereby altering their optical properties and photoacoustic performance. He and coworkers developed a NIR absorbing photoacoustic probe (named HD-Zn) based on a merocyanine dye [321]. When the photoacoustic probe is not bound to $Zn^{2+}$, the lone pair of electrons on the amino group can freely flow into the dye, producing a $PA_{750}$ signal. In contrast, when $Zn^{2+}$ is present at the lesion, HD-Zn can sense $Zn^{2+}$ and produce a distinct blue-shifted $PA_{680}$ signal, together with a reduced absorbance at 750 nm. In in vivo experiments, the $PA_{680}/PA_{750}$ ratio was increased approximately 3.5-fold in mice injected with HD-Zn, demonstrating the successful implementation of $Zn^{2+}$-activated PAI. Zhang and coworkers reported a series of small-molecule probes, all with molecular weights below 440, that highly selectively bind $Cu^{2+}$ to form free radicals and exhibit strong NIR photoacoustic signals [322]. Among them, the screened RPS1 probe not only has high radical stability and photoacoustic intensity but also can easily cross the blood-brain barrier to achieve PAI of $Cu^{2+}$ in the brain. This study provides an effective tool for the study of Alzheimer's disease at the molecular level, drug screening, and evaluation of therapeutic effects.

## 1.5 Conclusion

Photofunctional nanomaterials have unique optical properties and can be used in a variety of scenarios in the biomedical field, such as drug delivery, bioimaging, optical information storage, cancer diagnosis, and therapy, as well as biosensing. In this book, we will introduce the basic background of photofunctional nanomaterials and their recent progress in various biomedical fields. Finally, the challenges and future opportunities for photofunctional nanomaterials are discussed.

## References

**1** Rivera-Gil, P., Jimenez De Aberasturi, D., Wulf, V. et al. (2012). The challenge to relate the physicochemical properties of colloidal nanoparticles to their cytotoxicity. *Accounts of Chemical Research* 46: 743–749.

2 Moriarty, P. (2001). Nanostructured materials. *Reports on Progress in Physics* 64: 297–381.
3 Rosei, F. (2004). Nanostructured surfaces: challenges and frontiers in nanotechnology. *Journal of Physics: Condensed Matter* 16: S1373–S1436.
4 Martin, C.R. (1994). Nanomaterials: a membrane-based synthetic approach. *Science* 266: 1961–1966.
5 Wang, Z.L. (2000). Probing the properties of individual nanostructures by novel techniques. *Progress in Natural Science: Materials International* 10: 481–496.
6 Yang, D. and Sun, W. (2003). Structural characters and special properties of nanomaterials. *Materials Review* 17: 7–10.
7 Bai, H.Y., Luo, J.L., Jin, D., and Sun, J.R. (1996). Particle size and interfacial effect on the specific heat of nanocrystalline Fe. *Journal of Applied Physics* 79: 361–364.
8 Chen, S., Tang, M., Zhang, Z. et al. (2013). Interfacial effect on the ferromagnetic damping of CoFeB thin films with different under-layers. *Applied Physics Letters* 103: 032402.
9 Nagashima, K., Yanagida, T., Klamchuen, A. et al. (2010). Interfacial effect on metal/oxide nanowire junctions. *Applied Physics Letters* 96: 073110.
10 Ni, M., Leung, M., Leung, D., and Sumathy, K. (2006). Theoretical modeling of $TiO_2$/TCO interfacial effect on dye-sensitized solar cell performance. *Solar Energy Materials and Solar Cells* 90: 2000–2009.
11 Buffat, P. and Borel, J.P. (1976). Size effect on the melting temperature of gold particles. *Physical Review A* 13: 2287–2298.
12 Huang, W.C. and Lue, J.T. (1994). Quantum size effect on the optical properties of small metallic particles. *Physical Review B* 49: 17279–17285.
13 Solliard, C. and Flueli, M. (1985). Surface stress and size effect on the lattice parameter in small particles of gold and platinum. *Surface Science* 156: 487–494.
14 Tounsi, A., Heireche, H., Berrabah, H.M. et al. (2008). Effect of small size on wave propagation in double-walled carbon nanotubes under temperature field. *Journal of Applied Physics* 104: 104301.
15 Ciraci, S. and Batra, I.P. (1986). Theory of the quantum size effect in simple metals. *Physical Review B* 33: 4294–4297.
16 Mikhailov, G.M., Malikov, I.V., and Chernykh, A.V. (1997). Influence of the quantum size effect for grazing electrons on the electronic conductivity of metal films. *JETP Letters* 66: 725–731.
17 Ohno, T., Numakura, K., Itoh, H. et al. (2009). Control of the quantum size effect of $TiO_2$–$SiO_2$ hybrid particles. *Materials Letters* 63: 1737–1739.
18 Xiong, Y., Yu, K.N., and Xiong, C. (1994). Photoacoustic investigation of the quantum size effect and thermal properties in $ZrO_2$ nanoclusters. *Physical Review B* 49: 5607–5610.
19 Hendry, P.C., Lawson, N.S., McClintock, P.V.E. et al. (1988). Macroscopic quantum tunneling of vortices in He II. *Physical Review Letters* 60: 604–607.
20 Ivanov, B.A. and Kireev, V.E. (2004). Macroscopic quantum tunneling in small antiferromagnetic particles: effects of a strong magnetic field. *Physical Review B* 70: 214430.

**21** Schwartz, D.B., Sen, B., Archie, C.N., and Lukens, J.E. (1985). Quantitative study of the effect of the environment on macroscopic quantum tunneling. *Physical Review Letters* 55: 1547–1550.

**22** Tejada, J., Ziolo, R.F., and Zhang, X.X. (1996). Quantum tunneling of magnetization in nanostructured materials. *Chemistry of Materials* 8: 1784–1792.

**23** West, J.L. and Halas, N.J. (2003). Engineered nanomaterials for biophotonics applications: improving sensing, imaging, and therapeutics. *Annual Review of Biomedical Engineering* 5: 285–292.

**24** Wang, J., Zhang, L., and Li, Z. (2021). Aggregation-induced emission luminogens with photoresponsive behaviors for biomedical applications. *Advanced Healthcare Materials* 10: 2101169.

**25** Ren, Y., Liu, H., Liu, X. et al. (2020). Photoresponsive materials for antibacterial applications. *Cell Reports Physical Science* 1: 100245.

**26** Li, J., Li, G., Lu, X. et al. (2023). Magnetically responsive optical modulation: from anisotropic nanostructures to emerging applications. *Advanced Functional Materials* 34: 2308293.

**27** Wang, C., Wang, H., Xu, B., and Liu, H. (2020). Photo-responsive nanozymes: mechanism, activity regulation, and biomedical applications. *View* 2: 20200045.

**28** Li, Z. and Yin, Y. (2019). Stimuli-responsive optical nanomaterials. *Advanced Materials* 31: 1807061.

**29** Wei, Y., Wang, Z., and Ranbo, Y. (2019). New media for efficient light energy conversion: hollow multi-shelled structures (HoMSs) (in chinese). *Chinese Science Bulletin-Chinese* 64: 3577–3593.

**30** Jung, Y., Kim, M., Kim, T. et al. (2023). Functional materials and innovative strategies for wearable thermal management applications. *Nano-Micro Letters* 15: 160.

**31** He, X.-P., Hu, X.-L., James, T.D. et al. (2017). Multiplexed photoluminescent sensors: towards improved disease diagnostics. *Chemical Society Reviews* 46: 6687–6696.

**32** Zhang, Z.-Y. and Liu, Y. (2019). Ultralong room-temperature phosphorescence of a solid-state supramolecule between phenylmethylpyridinium and cucurbit[6]uril. *Chemical Science* 10: 7773–7778.

**33** Zheng, K., Loh, K.Y., Wang, Y. et al. (2019). Recent advances in upconversion nanocrystals: expanding the kaleidoscopic toolbox for emerging applications. *Nano Today* 29: 100797.

**34** Yu, D., Yu, T., Lin, H. et al. (2022). Recent advances in luminescent downconversion: new materials, techniques, and applications in solar cells. *Advanced Optical Materials* 10: 2200014.

**35** Li, F., Shen, T., Wang, C. et al. (2020). Recent advances in strain-induced piezoelectric and piezoresistive effect-engineered 2d semiconductors for adaptive electronics and optoelectronics. *Nano-Micro Letters* 12: 106.

**36** Arroyo, P.C., David, G., Alpert, P.A. et al. (2022). Amplification of light within aerosol particles accelerates in-particle photochemistry. *Science* 376: 293–296.

**37** Lee, H.P. and Gaharwar, A.K. (2020). Light-responsive inorganic biomaterials for biomedical applications. *Advanced Science* 7: 2000863.

**38** Wang, Y., Xia, K., Wang, L. et al. (2021). Peptide-engineered fluorescent nanomaterials: structure design, function tailoring, and biomedical applications. *Small* 17: 2005578.

**39** Chen, G., Roy, I., Yang, C., and Prasad, P.N. (2016). Nanochemistry and nanomedicine for nanoparticle-based diagnostics and therapy. *Chemical Reviews* 116: 2826–2885.

**40** Kong, X., Qi, Y., Wang, X. et al. (2023). Nanoparticle drug delivery systems and their applications as targeted therapies for triple negative breast cancer. *Progress in Materials Science* 134: 101070.

**41** Wang, J., Ni, Q., Wang, Y. et al. (2021). Nanoscale drug delivery systems for controllable drug behaviors by multi-stage barrier penetration. *Journal of Controlled Release* 331: 282–295.

**42** Jiang, Q. and Zhang, S. (2023). Stimulus-responsive drug delivery nanoplatforms for osteoarthritis therapy. *Small* 19: 2206929.

**43** Mei, J. and Tian, H. (2021). Most recent advances on enzyme-activatable optical probes for bioimaging. *Aggregate* 2: e32.

**44** Fan, W., Yung, B., Huang, P., and Chen, X. (2017). Nanotechnology for multimodal synergistic cancer therapy. *Chemical Reviews* 117: 13566–13638.

**45** He, M., Chen, F., Shao, D. et al. (2021). Photoresponsive metallopolymer nanoparticles for cancer theranostics. *Biomaterials* 275: 120915.

**46** Huang, X., Li, L., Chen, Z. et al. (2023). Nanomedicine for the detection and treatment of ocular bacterial infections. *Advanced Materials* 35: 2302431.

**47** Lin, X., Zhao, M., Peng, T. et al. (2023). Detection and discrimination of pathogenic bacteria with nanomaterials-based optical biosensors: a review. *Food Chemistry* 426: 136578.

**48** Zhang, X., Liu, F., and Gu, Z. (2023). Tissue engineering in neuroscience: applications and perspectives. *BME Frontiers* 4: 0007.

**49** Bao, L., Cui, X., Mortimer, M. et al. (2023). The renaissance of one-dimensional carbon nanotubes in tissue engineering. *Nano Today* 49: 101784.

**50** Pardo, A., Gómez-Florit, M., Barbosa, S. et al. (2021). Magnetic nanocomposite hydrogels for tissue engineering: design concepts and remote actuation strategies to control cell fate. *ACS Nano* 15: 175–209.

**51** Sun, Q., Wang, Z., Liu, B. et al. (2022). Recent advances on endogenous/exogenous stimuli-triggered nanoplatforms for enhanced chemodynamic therapy. *Coordination Chemistry Reviews* 451: 214267.

**52** Zhao, D., Huang, R., Gan, J.-M., and Shen, Q.-D. (2022). Photoactive nanomaterials for wireless neural biomimetics, stimulation, and regeneration. *ACS Nano* 16: 19892–19912.

**53** Deng, K., Li, C., Huang, S. et al. (2017). Recent progress in near infrared light triggered photodynamic therapy. *Small* 13: 1702299.

**54** Liu, H., Zhao, J., Xue, Y. et al. (2023). X-ray-induced drug release for cancer therapy. *Angewandte Chemie International Edition* 62: e202306100.

**55** Zhang, X., Wang, S., Cheng, G. et al. (2022). Light-responsive nanomaterials for cancer therapy. *Engineering* 13: 18–30.

**56** Zheng, X., Wu, Y., Zuo, H. et al. (2023). Metal nanoparticles as novel agents for lung cancer diagnosis and therapy. *Small* 19: 2206624.

**57** Zheng, B., Fan, J., Chen, B. et al. (2022). Rare-earth doping in nanostructured inorganic materials. *Chemical Reviews* 122: 5519–5603.

**58** Zhao, W., Zhao, Y., Wang, Q. et al. (2019). Remote light-responsive nanocarriers for controlled drug delivery: advances and perspectives. *Small* 15: 1903060.

**59** Wu, G., Qiu, H., Liu, X. et al. (2023). Nanomaterials-based fluorescent assays for pathogenic bacteria in food-related matrices. *Trends in Food Science and Technology* 142: 104214.

**60** Zhao, D., Wang, C., Su, L., and Zhang, X. (2020). Application of fluorescence nanomaterials in pathogenic bacteria detection. *Progress in Chemistry* 33: 1482–1495.

**61** Pu, Y., Wang, D., Qian, J., and Chen, J. (2017). Fluorescent nanomaterials and their applications in bioimaging. *Materials China* 36: 103–111.

**62** Yang, M., Guo, X., Mou, F., and Guan, J. (2022). Lighting up micro-/nanorobots with fluorescence. *Chemical Reviews* 123: 3944–3975.

**63** Huang, J., He, B., Zhang, Z. et al. (2020). Aggregation-induced emission luminogens married to 2d black phosphorus nanosheets for highly efficient multimodal theranostics. *Advanced Materials* 32: 2003382.

**64** Han, H., Jin, Q., Wang, H. et al. (2016). Intracellular dual fluorescent lightup bioprobes for image-guided photodynamic cancer therapy. *Small* 12: 3870–3878.

**65** Li, C., Ma, M., Zhang, B. et al. (2022). A self-assembled nanoplatform based on $Ag_2S$ quantum dots and tellurium nanorods for combined chemo-photothermal therapy guided by $H_2O_2$-activated near-infrared-ii fluorescence imaging. *Acta Biomaterialia* 140: 547–560.

**66** Ding, C., Huang, Y., Shen, Z., and Chen, X. (2021). Synthesis and bioapplications of $Ag_2S$ quantum dots with near-infrared fluorescence. *Advanced Materials* 33: 2007768.

**67** Zhao, J., Chen, G., Gu, Y. et al. (2016). Ultrasmall magnetically engineered $Ag_2Se$ quantum dots for instant efficient labeling and whole-body high-resolution multimodal real-time tracking of cell-derived microvesicles. *Journal of the American Chemical Society* 138: 1893–1903.

**68** Yu, M., Yang, X., Zhang, Y. et al. (2021). Pb-doped $Ag_2Se$ quantum dots with enhanced photoluminescence in the NIR-II window. *Small* 17: 2006111.

**69** Chen, B., Liu, M., Gao, Y. et al. (2022). Design and applications of carbon dots-based ratiometric fluorescent probes: a review. *Nano Research* 16: 1064–1083.

**70** Gao, X., Cui, Y., Levenson, R.M. et al. (2004). In vivo cancer targeting and imaging with semiconductor quantum dots. *Nature Biotechnology* 22: 969–976.

**71** Yang, H., Bai, L., Geng, Z. et al. (2023). Carbon quantum dots: preparation, optical properties, and biomedical applications. *Materials Today Advances* 18: 100376.

**72** Yang, L., Deng, W., Cheng, C. et al. (2018). Fluorescent immunoassay for the detection of pathogenic bacteria at the single-cell level using carbon

dots-encapsulated breakable organosilica nanocapsule as labels. *ACS Applied Materials & Interfaces* 10: 3441–3448.

**73** Yang, H., Li, R., Zhang, Y. et al. (2021). Colloidal alloyed quantum dots with enhanced photoluminescence quantum yield in the NIR-II window. *Journal of the American Chemical Society* 143: 2601–2607.

**74** Chandra, S., Ghosh, B., Beaune, G. et al. (2016). Functional double-shelled silicon nanocrystals for two-photon fluorescence cell imaging: spectral evolution and tuning. *Nanoscale* 8: 9009–9019.

**75** Chen, H., Xu, J., Wang, Y. et al. (2022). Color-switchable nanosilicon fluorescent probes. *ACS Nano* 16: 15450–15459.

**76** Gai, S., Li, C., Yang, P., and Lin, J. (2014). Recent progress in rare earth micro/nanocrystals: soft chemical synthesis, luminescent properties, and biomedical applications. *Chemical Reviews* 114: 2343–2389.

**77** Zhou, J., Liu, Q., Feng, W. et al. (2015). Upconversion luminescent materials: advances and applications. *Chemical Reviews* 115: 395–465.

**78** Charron, D.M. and Zheng, G. (2018). Nanomedicine development guided by fret imaging. *Nano Today* 18: 124–136.

**79** Dong, H., Du, S.R., Zheng, X.Y. et al. (2015). Lanthanide nanoparticles: from design toward bioimaging and therapy. *Chemical Reviews* 115: 10725–10815.

**80** Xiang, H. and Chen, Y. (2020). Materdicine: interdiscipline of materials and medicine. *View* 1: 20200016.

**81** Xu, J., Fu, M., Ji, C. et al. (2023). Plasmonic-enhanced NIR-II downconversion fluorescence beyond 1500 nm from core–shell–shell lanthanide nanoparticles. *Advanced Optical Materials* 11: 2300477.

**82** Sun, G., Xie, Y., Wang, Y. et al. (2023). Cooperative sensitization upconversion in solution dispersions of co-crystal assemblies of mononuclear $Yb^{3+}$ and $Eu^{3+}$ complexes. *Angewandte Chemie International Edition* 62: e202304591.

**83** Xu, R., Liu, J., Cao, H. et al. (2023). In vivo high-contrast biomedical imaging in the second near-infrared window using ultrabright rare-earth nanoparticles. *Nano Letters* 23: 11203–11210.

**84** Wang, X., Han, X.-J., and Chen, G.-Y. (2020). Time-resolved imaging using lanthanide-doped nanomaterials. *Chinese Journal of Luminescence* 41: 1045–1057.

**85** Jin, B., Wang, S., Lin, M. et al. (2017). Upconversion nanoparticles based fret aptasensor for rapid and ultrasenstive bacteria detection. *Biosensors and Bioelectronics* 90: 525–533.

**86** Li, H., Tan, M., Wang, X. et al. (2020). Temporal multiplexed in vivo upconversion imaging. *Journal of the American Chemical Society* 142: 2023–2030.

**87** Yang, Y., Chen, Y., Pei, P. et al. (2023). Fluorescence-amplified nanocrystals in the second near-infrared window for in vivo real-time dynamic multiplexed imaging. *Nature Nanotechnology* 18: 1195–1204.

**88** Li, Y., Luo, Y., Wu, Z. et al. (2023). Research progress of $T_1$-$T_2$ dual-modal nano-magnetic resonance contrast agents. *Chinese Medicinal Biotechnology* 18: 516–522.

**89** Li, Y., Younis, M.H., Wang, H. et al. (2022). Spectral computed tomography with inorganic nanomaterials: state-of-the-art. *Advanced Drug Delivery Reviews* 189: 114524.

**90** Jin, Y., Ni, D., Gao, L. et al. (2018). Harness the power of upconversion nanoparticles for spectral computed tomography diagnosis of osteosarcoma. *Advanced Functional Materials* 28: 1802656.

**91** Ai, X., Wang, Z., Cheong, H. et al. (2019). Multispectral optoacoustic imaging of dynamic redox correlation and pathophysiological progression utilizing upconversion nanoprobes. *Nature Communications* 10: 1087.

**92** Wang, Z. and Xing, B. (2020). Near-infrared multipurpose lanthanide-imaging nanoprobes. *Chemistry--An Asian Journal* 15: 2076–2091.

**93** Ashoka, A.H., Aparin, I.O., Reisch, A., and Klymchenko, A.S. (2023). Brightness of fluorescent organic nanomaterials. *Chemical Society Reviews* 52: 4525–4548.

**94** Zhang, X., Chen, Y., He, H. et al. (2021). ROS/RNS and base dual activatable merocyanine-based NIR-II fluorescent molecular probe for in vivo biosensing. *Angewandte Chemie International Edition* 60: 26337–26341.

**95** Li, D., Gamage, R.S., Oliver, A.G. et al. (2023). Doubly strapped zwitterionic NIR-I and NIR-II heptamethine cyanine dyes for bioconjugation and fluorescence imaging. *Angewandte Chemie International Edition* 62: 202305062.

**96** Cheng, H., Li, Y., Tang, B., and Yoon, J. (2020). Assembly strategies of organic-based imaging agents for fluorescence and photoacoustic bioimaging applications. *Chemical Society Reviews* 49: 21–31.

**97** Shi, Y., Zhu, D., Wang, D. et al. (2022). Recent advances of smart aiegens for photoacoustic imaging and phototherapy. *Coordination Chemistry Reviews* 471: 214725.

**98** Hong, Y., Lam, J.W.Y., and Tang, B. (2011). Aggregation-induced emission. *Chemical Society Reviews* 40: 5361–5388.

**99** Luo, J.D., Xie, Z.L., Lam, J.W.Y. et al. (2001). Aggregation-induced emission of 1-methyl-1,2,3,4,5-pentaphenylsilole. *Chemical Communications* 1740–1741.

**100** Lim, X. (2016). The nanolight revolution is coming. *Nature* 531: 26.

**101** Cai, X. and Liu, B. (2020). Aggregation-induced emission: recent advances in materials and biomedical applications. *Angewandte Chemie International Edition* 59: 9868–9886.

**102** Mao, D. and Liu, B. (2021). Biology-oriented design strategies of AIE theranostic probes. *Matter* 4: 350–376.

**103** Wang, D., Su, H., Kwok, R.T.K. et al. (2018). Rational design of a water-soluble NIR aiegen, and its application in ultrafast wash-free cellular imaging and photodynamic cancer cell ablation. *Chemical Science* 9: 3685–3693.

**104** Zhang, J., He, B., Hu, Y. et al. (2021). Stimuli-responsive aiegens. *Advanced Materials* 33: 2008071.

**105** Xu, Y., Dang, D., Zhang, N. et al. (2022). Aggregation-induced emission (AIE) in super-resolution imaging: cationic AIE luminogens (AIEgens) for tunable organelle-specific imaging and dynamic tracking in nanometer scale. *ACS Nano* 16: 5932–5942.

**106** Sheng, Z., Guo, B., Hu, D. et al. (2018). Bright aggregation-induced-emission dots for targeted synergetic NIR-II fluorescence and NIR-I photoacoustic imaging of orthotopic brain tumors. *Advanced Materials* 30: 1800766.

**107** Xiao, F., Fang, X., Li, H. et al. (2022). Light-harvesting fluorescent spherical nucleic acids self-assembled from a DNA-grafted conjugated polymer for amplified detection of nucleic acids. *Angewandte Chemie International Edition* 61: 202115812.

**108** Cui, X., Ruan, Q., Zhuo, X. et al. (2023). Photothermal nanomaterials: a powerful light-to-heat converter. *Chemical Reviews* 123: 6891–6952.

**109** Chen, Y., Gao, Y., Chen, Y. et al. (2020). Nanomaterials-based photothermal therapy and its potentials in antibacterial treatment. *Journal of Controlled Release* 328: 251–262.

**110** Han, H.S. and Choi, K.Y. (2021). Advances in nanomaterial-mediated photothermal cancer therapies: toward clinical applications. *Biomedicine* 9: 305.

**111** Chang, M., Wang, M., Hou, Z., and Lin, J. (2022). Problems and solutions of nanomaterials in antitumor photothermal therapy. *Chinese Journal of Luminescence* 43: 995–1013.

**112** Xiong, Y., Rao, Y., Hu, J. et al. (2023). Nanoparticle-based photothermal therapy for breast cancer noninvasive treatment. *Advanced Materials* 33: 2305140.

**113** Cheng, L., Wang, X., Gong, F. et al. (2019). 2d nanomaterials for cancer theranostic applications. *Advanced Materials* 32: 1902333.

**114** Chen, J., Ning, C., Zhou, Z. et al. (2019). Nanomaterials as photothermal therapeutic agents. *Progress in Materials Science* 99: 1–26.

**115** Wang, Z., Wang, M., Wang, X. et al. (2023). Photothermal-based nanomaterials and photothermal-sensing: an overview. *Biosensors and Bioelectronics* 220: 114883.

**116** Zheng, L., Luo, Y., and Xu, W. (2018). Applications of optical and photothermal nanomaterials in biosensing, drug-targeted delivery and bioimaging. *Biotechnology Bulletin* 34: 79–89.

**117** Huang, X.H., El-Sayed, I.H., Qian, W., and El-Sayed, M.A. (2006). Cancer cell imaging and photothermal therapy in the near-infrared region by using gold nanorods. *Journal of the American Chemical Society* 128: 2115–2120.

**118** Yang, H., Zhang, Z., Liu, C., and Keming, J. (2022). Research progress of photothermal micro-nano materials. *Laser Journal* 43: 1–7.

**119** Wang, S., Riedinger, A., Li, H. et al. (2015). Plasmonic copper sulfide nanocrystals exhibiting near-infrared photothermal and photodynamic therapeutic effects. *ACS Nano* 9: 1788–1800.

**120** Ma, J., Li, N., Wang, J. et al. (2023). In vivo synergistic tumor therapies based on copper sulfide photothermal therapeutic nanoplatforms. *Exploration* 3: 20220161.

**121** Huang, Q., Zhang, S., Zhang, H. et al. (2019). Boosting the radiosensitizing and photothermal performance of $Cu_{2-x}Se$ nanocrystals for synergetic radiophotothermal therapy of orthotopic breast cancer. *ACS Nano* 13: 1342–1353.

**122** Chan, L., Liu, Y., Chen, M. et al. (2023). Cuproptosis-driven enhancement of thermotherapy by sequentially response $Cu_{2-x}Se$ via copper chemical transition. *Advanced Functional Materials* 33: 2302054.

**123** Chen, Y., Wu, Y., Sun, B. et al. (2017). Two-dimensional nanomaterials for cancer nanotheranostics. *Small* 13: 1603446.

**124** Wang, X. and Cheng, L. (2020). Multifunctional prussian blue-based nanomaterials: preparation, modification, and theranostic applications. *Coordination Chemistry Reviews* 419: 213393.

**125** Xue, P., Hou, M., Sun, L. et al. (2018). Calcium-carbonate packaging magnetic polydopamine nanoparticles loaded with indocyanine green for near-infrared induced photothermal/photodynamic therapy. *Acta Biomaterialia* 81: 242–255.

**126** Cheng, Y.J., Yang, S.H., and Hsu, C.S. (2009). Synthesis of conjugated polymers for organic solar cell applications. *Chemical Reviews* 109: 5868–5923.

**127** Yang, J., Choi, J., Bang, D. et al. (2010). Convertible organic nanoparticles for near-infrared photothermal ablation of cancer cells. *Angewandte Chemie International Edition* 50: 441–444.

**128** Wang, Z., Zou, Y., Li, Y., and Cheng, Y. (2020). Metal-containing polydopamine nanomaterials: catalysis, energy, and theranostics. *Small* 16: e1907042.

**129** Zheng, Y., Cao, T., Han, X. et al. (2022). Structurally diverse polydopamine-based nanomedicines for cancer therapy. *Acta Materia Medica* 1: 427–444.

**130** Ma, Z.-Y., Li, D.-Y., Jia, X. et al. (2023). Recent advances in bio-inspired versatile polydopamine platforms for "smart" cancer photothermal therapy. *Chinese Journal of Polymer Science* 41: 699–712.

**131** Yang, S., Yu, Y., Gao, X. et al. (2021). Recent advances in electrocatalysis with phthalocyanines. *Chemical Society Reviews* 50: 12985–13011.

**132** Nash, G.T., Luo, T., Lan, G. et al. (2021). Nanoscale metal–organic layer isolates phthalocyanines for efficient mitochondria-targeted photodynamic therapy. *Journal of the American Chemical Society* 143: 2194–2199.

**133** Gao, D., Wong, R.C.H., Wang, Y. et al. (2020). Shifting the absorption to the near-infrared region and inducing a strong photothermal effect by encapsulating Zinc(II) phthalocyanine in poly(lactic-co-glycolic acid)-hyaluronic acid nanoparticles. *Acta Biomaterialia* 116: 329–343.

**134** Gao, D., Chen, T., Chen, S. et al. (2021). Targeting hypoxic tumors with hybrid nanobullets for oxygen-independent synergistic photothermal and thermodynamic therapy. *Nano-Micro Letters* 13: 99.

**135** Zhu, M., Zhang, H., Ran, G. et al. (2021). Metal modulation: an easy-to-implement tactic for tuning lanthanide phototheranostics. *Journal of the American Chemical Society* 143: 7541–7552.

**136** Tian, Y., Zhao, D., Huang, X. et al. (2022). Extended π-conjugative carbon nitride for single 1064 nm laser-activated photodynamic/photothermal synergistic therapy and photoacoustic imaging. *ACS Applied Materials & Interfaces* 14: 7626–7635.

**137** Yin, P.T., Shah, S., Chhowalla, M., and Lee, K.B. (2015). Design, synthesis, and characterization of graphene-nanoparticle hybrid materials for bioapplications. *Chemical Reviews* 115: 2483–2531.

**138** Fusco, L., Gazzi, A., Peng, G. et al. (2020). Graphene and other 2D materials: a multidisciplinary analysis to uncover the hidden potential as cancer theranostics. *Theranostics* 10: 5435–5488.

**139** Wang, B., Cai, H., Waterhouse, G.I.N. et al. (2022). Carbon dots in bioimaging, biosensing and therapeutics: a comprehensive review. *Small Science* 2: 2200012.

**140** Xu, P. and Liang, F. (2020). Nanomaterial-based tumor photothermal immunotherapy. *International Journal of Nanomedicine* 15: 9159–9180.

**141** Zhang, H., Zhang, Z., Wang, Y. et al. (2016). Rapid and sensitive detection of cancer cells based on the photothermal effect of graphene functionalized magnetic microbeads. *ACS Applied Materials & Interfaces* 8: 29933–29938.

**142** Qu, G., Xia, T., Zhou, W. et al. (2020). Property–activity relationship of black phosphorus at the nano–bio interface: from molecules to organisms. *Chemical Reviews* 120: 2288–2346.

**143** Liu, S., Pan, X., and Liu, H. (2020). Two-dimensional nanomaterials for photothermal therapy. *Angewandte Chemie International Edition* 59: 5890–5900.

**144** Lei, W., Liu, G., Zhang, J., and Liu, M. (2017). Black phosphorus nanostructures: recent advances in hybridization, doping and functionalization. *Chemical Society Reviews* 46: 3492–3509.

**145** Yang, B., Chen, Y., and Shi, J. (2018). Material chemistry of two-dimensional inorganic nanosheets in cancer theranostics. *Chem* 4: 1284–1313.

**146** Wang, H., Zhong, L., Liu, Y. et al. (2018). A black phosphorus nanosheet-based sirna delivery system for synergistic photothermal and gene therapy. *Chemical Communications* 54: 3142–3145.

**147** Sun, Z., Xie, H., Tang, S. et al. (2015). Ultrasmall black phosphorus quantum dots: synthesis and use as photothermal agents. *Angewandte Chemie International Edition* 54: 11526–11530.

**148** Shao, J., Xie, H., Huang, H. et al. (2016). Biodegradable black phosphorus-based nanospheres for in vivo photothermal cancer therapy. *Nature Communications* 7: 12967.

**149** Yang, X., He, S., Wang, J. et al. (2023). Hyaluronic acid-based injectable nanocomposite hydrogels with photo-thermal antibacterial properties for infected chronic diabetic wound healing. *International Journal of Biological Macromolecules* 242: 124872.

**150** Wu, Z., Huang, T., Sathishkumar, G. et al. (2023). Phytic acid-promoted exfoliation of black phosphorus nanosheets for the fabrication of photothermal antibacterial coatings. *Advanced Healthcare Materials* 2302058.

**151** Zhang, Y.Z., El-Demellawi, J.K., Jiang, Q. et al. (2020). Mxene hydrogels: fundamentals and applications. *Chemical Society Reviews* 49: 7229–7251.

**152** Lukatskaya, M.R., Kota, S., Lin, Z. et al. (2017). Ultra-high-rate pseudocapacitive energy storage in two-dimensional transition metal carbides. *Nature Energy* 2: 17105.

**153** Naguib, M., Mashtalir, O., Carle, J. et al. (2012). Two-dimensional transition metal carbides. *ACS Nano* 6: 1322–1331.

**154** Hao, S., Han, H., Yang, Z. et al. (2022). Recent advancements on photothermal conversion and antibacterial applications over mxenes-based materials. *Nano-Micro Letters* 14: 178.

**155** Wu, F., Zheng, H., Wang, W. et al. (2020). Rapid eradication of antibiotic-resistant bacteria and biofilms by mxene and near-infrared light through photothermal ablation. *Science China Materials* 64: 748–758.

**156** He, P.P., Du, X., Cheng, Y. et al. (2022). Thermal-responsive mxene-DNA hydrogel for near-infrared light triggered localized photothermal-chemo synergistic cancer therapy. *Small* 18: 2200263.

**157** Zou, Q., Abbas, M., Zhao, L. et al. (2017). Biological photothermal nanodots based on self-assembly of peptide–porphyrin conjugates for antitumor therapy. *Journal of the American Chemical Society* 139: 1921–1927.

**158** Guo, K., Jiao, Z., Zhao, X. et al. (2023). Melanin-based immunoregulatory nanohybrids enhance antitumor immune responses in breast cancer mouse model. *ACS Nano* 17: 10792–10805.

**159** Zhang, Y., Wang, Q., Ji, Y. et al. (2022). Mitochondrial targeted melanin@m$SiO_2$ yolk-shell nanostructures for NIR-II-driven photo-thermal-dynamic/immunotherapy. *Chemical Engineering Journal* 435: 134869.

**160** Cao, W., Zhou, X., McCallum, N.C. et al. (2021). Unraveling the structure and function of melanin through synthesis. *Journal of the American Chemical Society* 143: 2622–2637.

**161** Lei, Q., He, D., Ding, L. et al. (2022). Microneedle patches integrated with biomineralized melanin nanoparticles for simultaneous skin tumor photothermal therapy and wound healing. *Advanced Functional Materials* 32: 2113269.

**162** Kwak, B.S., Kim, H.O., Kim, J.H. et al. (2012). Quantitative analysis of sialic acid on erythrocyte membranes using a photothermal biosensor. *Biosensors and Bioelectronics* 35: 484–488.

**163** Kwak, B.S., Kim, H.J., Kim, H.O., and Jung, H.-I. (2010). An integrated photo-thermal sensing system for rapid and direct diagnosis of anemia. *Biosensors and Bioelectronics* 26: 1679–1683.

**164** Lucky, S.S., Soo, K.C., and Zhang, Y. (2015). Nanoparticles in photodynamic therapy. *Chemical Reviews* 115: 1990–2042.

**165** Chen, J., Fan, T., Xie, Z. et al. (2020). Advances in nanomaterials for photodynamic therapy applications: status and challenges. *Biomaterials* 237: 119827.

**166** Xie, Z., Fan, T., An, J. et al. (2020). Emerging combination strategies with phototherapy in cancer nanomedicine. *Chemical Society Reviews* 49: 8065–8087.

**167** Ke, L., Wei, F., Xie, L. et al. (2022). A biodegradable iridium(III) coordination polymer for enhanced two-photon photodynamic therapy using an apoptosis–ferroptosis hybrid pathway. *Angewandte Chemie International Edition* 61: 202205429.

**168** Xiao, Q., Lin, H., Wu, J. et al. (2020). Pyridine-embedded phenothiazinium dyes as lysosome-targeted photosensitizers for highly efficient photodynamic antitumor therapy. *Journal of Medicinal Chemistry* 63: 4896–4907.

**169** Lin, W., Liu, Y., Wang, J. et al. (2023). Engineered bacteria labeled with iridium(III) photosensitizers for enhanced photodynamic immunotherapy of solid tumors. *Angewandte Chemie International Edition* 135: 202310158.

**170** Cui, M., Tang, D., Wang, B. et al. (2023). Bioorthogonal guided activation of cGAS-STING by AIE photosensitizer nanoparticles for targeted tumor therapy and imaging. *Advanced Materials* 35: 2305668.

**171** Yang, Z., Wang, Z., and Wei, P. (2020). Research advances on stimuli-responsive liposomes in the targeted drug delivery system. *Chinese Journal of Biochemistry and Molecular Biology* 36: 1395–1403.

**172** Liu, P., Chen, G., and Zhang, J. (2022). A review of liposomes as a drug delivery system: current status of approved products, regulatory environments, and future perspectives. *Molecules* 27: 1372.

**173** Beltrán-Gracia, E., López-Camacho, A., Higuera-Ciapara, I. et al. (2019). Nanomedicine review: clinical developments in liposomal applications. *Cancer Nanotechnology* 10: 11.

**174** Almeida, B., Nag, O.K., Rogers, K.E., and Delehanty, J.B. (2020). Recent progress in bioconjugation strategies for liposome-mediated drug delivery. *Molecules* 25: 5672.

**175** Hao, L., Li, J., Wang, P. et al. (2021). Spatiotemporal magnetocaloric microenvironment for guiding the fate of biodegradable polymer implants. *Advanced Functional Materials* 31: 2009661.

**176** Fan, J., Qin, Y., Xiao, C. et al. (2022). Biomimetic PLGA-based nanocomplexes for improved tumor penetration to enhance chemo-photodynamic therapy against metastasis of TNBC. *Materials Today Advances* 16: 100289.

**177** Xin, J., Deng, C., Zheng, M., and An, F. (2023). Amphiphilic photosensitizer polymer as a nanocarrier of cytotoxic molecule for carrier-free combination therapy. *MedComm - Biomaterials and Applications* 2: 28.

**178** Li, L., Shao, C., Liu, T. et al. (2020). An NIR-II-emissive photosensitizer for hypoxia-tolerant photodynamic theranostics. *Advanced Materials* 32: 2003471.

**179** Chen, W., Zhou, S., Ge, L. et al. (2018). Translatable high drug loading drug delivery systems based on biocompatible polymer nanocarriers. *Biomacromolecules* 19: 1732–1745.

**180** Qureshi, M.A. and Khatoon, F. (2019). Different types of smart nanogel for targeted delivery. *Journal of Science: Advanced Materials and Devices* 4: 201–212.

**181** Hajebi, S., Rabiee, N., Bagherzadeh, M. et al. (2019). Stimulus-responsive polymeric nanogels as smart drug delivery systems. *Acta Biomaterialia* 92: 1–18.

**182** Neamtu, I., Rusu, A.G., Diaconu, A. et al. (2017). Basic concepts and recent advances in nanogels as carriers for medical applications. *Drug Delivery* 24: 539–557.

**183** Preman, N.K., Barki, R.R., Vijayan, A. et al. (2020). Recent developments in stimuli-responsive polymer nanogels for drug delivery and diagnostics: a review. *European Journal of Pharmaceutics and Biopharmaceutics* 157: 121–153.

**184** Ma, H., Yu, G., Cheng, J. et al. (2023). Design of an injectable magnetic hydrogel based on the tumor microenvironment for multimodal synergistic cancer therapy. *Biomacromolecules* 24: 868–885.

**185** Zheng, Y., Lv, X., Xu, Y. et al. (2019). pH-sensitive and pluronic-modified pullulan nanogels for greatly improved antitumor in vivo. *International Journal of Biological Macromolecules* 139: 277–289.

**186** Zavgorodnya, O., Carmona-Moran, C.A., Kozlovskaya, V. et al. (2017). Temperature-responsive nanogel multilayers of poly(n-vinylcaprolactam) for topical drug delivery. *Journal of Colloid and Interface Science* 506: 589–602.

**187** He, J., Sun, Y., Gao, Q. et al. (2023). Gelatin methacryloyl hydrogel, from standardization, performance, to biomedical application. *Advanced Healthcare Materials* 12: 2300395.

**188** Tao, L., Huo, M., and Xu, W. (2020). Advances in the research of protein nanocarrier materials. *Journal of China Pharmaceutical University* 51: 121–129.

**189** Hu, Q., Li, H., Wang, L. et al. (2018). DNA nanotechnology-enabled drug delivery systems. *Chemical Reviews* 119: 6459–6506.

**190** Hejazi, R. and Amiji, M. (2003). Chitosan-based gastrointestinal delivery systems. *Journal of Controlled Release* 89: 151–165.

**191** An, F.F. and Zhang, X.H. (2017). Strategies for preparing albumin-based nanoparticles for multifunctional bioimaging and drug delivery. *Theranostics* 7: 3667–3689.

**192** Tao, H.-Y., Wang, R. -q., Sheng, W.-J., and Zhen, Y.-S. (2021). The development of human serum albumin-based drugs and relevant fusion proteins for cancer therapy. *International Journal of Biological Macromolecules* 187: 24–34.

**193** Bhushan, B., Khanadeev, V., Khlebtsov, B. et al. (2017). Impact of albumin based approaches in nanomedicine: imaging, targeting and drug delivery. *Advances in Colloid and Interface Science* 246: 13–39.

**194** Bern, M., Sand, K.M.K., Nilsen, J. et al. (2015). The role of albumin receptors in regulation of albumin homeostasis: implications for drug delivery. *Journal of Controlled Release* 211: 144–162.

**195** Wu, J., Williams, G.R., Niu, S. et al. (2019). A multifunctional biodegradable nanocomposite for cancer theranostics. *Advanced Science* 6: 1802001.

**196** Yang, B., Yao, H., Tian, H. et al. (2021). Intratumoral synthesis of nanometalchelate for tumor catalytic therapy by ligand field-enhanced coordination. *Nature Communications* 12: 3393.

**197** Yang, B. and Shi, J. (2020). Ascorbate tumor chemotherapy by an iron-engineered nanomedicine-catalyzed tumor-specific pro-oxidation. *Journal of the American Chemical Society* 142: 21775–21785.

**198** Yang, B., Guo, Y., Wang, Y. et al. (2022). Nanomedicine-leveraged intratumoral coordination and redox reactions of dopamine for tumor-specific chemotherapy. *CCS Chemistry* 4: 1499–1509.

**199** Li, X., Zhang, L., Dong, X. et al. (2007). Preparation of mesoporous calcium doped silica spheres with narrow size dispersion and their drug loading and degradation behavior. *Microporous and Mesoporous Materials* 102: 151–158.

**200** Zhao, S., Zhang, S., Ma, J. et al. (2015). Double loaded self-decomposable $SiO_2$ nanoparticles for sustained drug release. *Nanoscale* 7: 16389–16398.

**201** Zhang, S., Chu, Z., Yin, C. et al. (2013). Controllable drug release and simultaneously carrier decomposition of $SiO_2$-drug composite nanoparticles. *Journal of the American Chemical Society* 135: 5709–5716.

**202** Du, X., Kleitz, F., Li, X. et al. (2018). Disulfide-bridged organosilica frameworks: designed, synthesis, redox-triggered biodegradation, and nanobiomedical applications. *Advanced Functional Materials* 28: 1707325.

**203** Yang, Y., Chen, F., Xu, N. et al. (2022). Red-light-triggered self-destructive mesoporous silica nanoparticles for cascade-amplifying chemo-photodynamic therapy favoring antitumor immune responses. *Biomaterials* 281: 121368.

**204** Vallet-Regí, M., Schüth, F., Lozano, D. et al. (2022). Engineering mesoporous silica nanoparticles for drug delivery: where are we after two decades? *Chemical Society Reviews* 51: 5365–5451.

**205** Kankala, R.K., Han, Y.H., Na, J. et al. (2020). Nanoarchitectured structure and surface biofunctionality of mesoporous silica nanoparticles. *Advanced Materials* 32: 1907035.

**206** Cheng, Y.J., Hu, J.J., Qin, S.Y. et al. (2020). Recent advances in functional mesoporous silica-based nanoplatforms for combinational photo-chemotherapy of cancer. *Biomaterials* 232: 119738.

**207** Yang, Y., Zhang, M., Song, H., and Yu, C. (2020). Silica-based nanoparticles for biomedical applications: from nanocarriers to biomodulators. *Accounts of Chemical Research* 53: 1545–1556.

**208** Lin, F.-C., Xie, Y., Deng, T., and Zink, J.I. (2021). Magnetism, ultrasound, and light-stimulated mesoporous silica nanocarriers for theranostics and beyond. *Journal of the American Chemical Society* 143: 6025–6036.

**209** Younis, M.R., He, G., Qu, J. et al. (2021). Inorganic nanomaterials with intrinsic singlet oxygen generation for photodynamic therapy. *Advanced Science* 8: 202102587.

**210** Jin, L., Shen, S., Huang, Y. et al. (2021). Corn-like Au/Ag nanorod-mediated NIR-II photothermal/photodynamic therapy potentiates immune checkpoint antibody efficacy by reprogramming the cold tumor microenvironment. *Biomaterials* 268: 120582.

**211** Han, R., Zhao, M., Wang, Z. et al. (2019). Super-efficient in vivo two-photon photodynamic therapy with a gold nanocluster as a type I photosensitizer. *ACS Nano* 14: 9532–9544.

**212** Fatima, H., Jin, Z.Y., Shao, Z., and Chen, X.J. (2022). Recent advances in ZnO-based photosensitizers: synthesis, modification, and applications in photodynamic cancer therapy. *Journal of Colloid and Interface Science* 621: 440–463.

**213** Heredia, D.A., Durantini, A.M., Durantini, J.E., and Durantini, E.N. (2022). Fullerene C60 derivatives as antimicrobial photodynamic agents. *Journal of Photochemistry and Photobiology C: Photochemistry Reviews* 51: 100471.

**214** Chatterjee, D.K., Fong, L., and Zhang, Y. (2008). Nanoparticles in photodynamic therapy: an emerging paradigm. *Advanced Drug Delivery Reviews* 60: 1627–1637.

**215** Wang, Y., Zhang, H., Liu, Y. et al. (2022). Catalytic radiosensitization: insights from materials physicochemistry. *Materials Today* 57: 262–278.

**216** Xie, J., Wang, Y., Choi, W. et al. (2021). Overcoming barriers in photodynamic therapy harnessing nano-formulation strategies. *Chemical Society Reviews* 50: 9152–9201.

**217** Chen, X., Song, J., Chen, X., and Yang, H. (2019). X-ray-activated nanosystems for theranostic applications. *Chemical Society Reviews* 48: 3073–3101.

**218** He, L., Yu, X., and Li, W. (2022). Recent progress and trends in X-ray-induced photodynamic therapy with low radiation doses. *ACS Nano* 16: 19691–19721.

**219** Jiang, M., Deng, Z., Zeng, S., and Hao, J. (2021). Recent progress on lanthanide scintillators for soft X-ray-triggered bioimaging and deep-tissue theranostics. *View* 2: 20200122.

**220** Hu, J., Tang, Y., Elmenoufy, A.H. et al. (2015). Nanocomposite-based photodynamic therapy strategies for deep tumor treatment. *Small* 11: 5860–5887.

**221** Shi, T., Sun, W., Qin, R. et al. (2020). X-ray-induced persistent luminescence promotes ultrasensitive imaging and effective inhibition of orthotopic hepatic tumors. *Advanced Functional Materials* 30: 2001166.

**222** Wang, X., Sun, W., Shi, H. et al. (2022). Organic phosphorescent nanoscintillator for low-dose X-ray-induced photodynamic therapy. *Nature Communications* 13: 5091.

**223** Cui, X., Li, X., Peng, C. et al. (2023). Beyond external light: on-spot light generation or light delivery for highly penetrated photodynamic therapy. *ACS Nano* 17: 20776–20803.

**224** Ran, C. and Pu, K. (2023). Molecularly generated light and its biomedical applications. *Angewandte Chemie International Edition* 202314468.

**225** Zhang, Y., Hao, Y., Chen, S., and Xu, M. (2020). Photodynamic therapy of cancers with internal light sources: chemiluminescence, bioluminescence, and cerenkov radiation. *Frontiers in Chemistry* 8: 770.

**226** Hsu, C.-Y., Chen, C.-W., Yu, H.-P. et al. (2013). Bioluminescence resonance energy transfer using luciferase-immobilized quantum dots for self-illuminated photodynamic therapy. *Biomaterials* 34: 1204–1212.

**227** Kim, Y.R., Kim, S., Choi, J.W. et al. (2015). Bioluminescence-activated deep-tissue photodynamic therapy of cancer. *Theranostics* 5: 805–817.

**228** Hu, X., Wang, Z., Su, Y. et al. (2021). Metal–organic layers with an enhanced two-photon absorption cross-section and up-converted emission. *Chemistry of Materials* 33: 1618–1624.

**229** Su, Y., Dai, Y., Zeng, Y. et al. (2023). Interpretable machine learning of two-photon absorption. *Advanced Science* 10: 2204902.

**230** Shen, Y., Shuhendler, A.J., Ye, D. et al. (2016). Two-photon excitation nanoparticles for photodynamic therapy. *Chemical Society Reviews* 45: 6725–6741.

**231** Wang, D., Zhu, L., Chen, J.F., and Dai, L. (2016). Liquid marbles based on magnetic upconversion nanoparticles as magnetically and optically responsive miniature reactors for photocatalysis and photodynamic therapy. *Angewandte Chemie International Edition* 55: 10795–10799.

**232** Fan, Y., Liu, L., and Zhang, F. (2019). Exploiting lanthanide-doped upconversion nanoparticles with core/shell structures. *Nano Today* 25: 68–84.

**233** Liu, S., Yan, L., Huang, J. et al. (2022). Controlling upconversion in emerging multilayer core–shell nanostructures: from fundamentals to frontier applications. *Chemical Society Reviews* 51: 1729–1765.

**234** Ryu, K.A., Kaszuba, C.M., Bissonnette, N.B. et al. (2021). Interrogating biological systems using visible-light-powered catalysis. *Nature Reviews Chemistry* 5: 322–337.

**235** Zhang, C., Gu, Z., and Yan, L. (2019). Intelligent response-type medication system based on up-conversion fluorescent nanomaterials for the application of cancer therapy. *Scientia Sinica Chimica* 49: 1179–1191.

**236** Fan, W., Huang, P., and Chen, X. (2016). Overcoming the achilles' heel of photodynamic therapy. *Chemical Society Reviews* 45: 6488–6519.

**237** Wang, F., Banerjee, D., Liu, Y.S. et al. (2010). Upconversion nanoparticles in biological labeling, imaging, and therapy. *Analyst* 135: 1839–1854.

**238** Zhang, X., Chen, W., Xie, X. et al. (2019). Boosting luminance energy transfer efficiency in upconversion nanoparticles with an energy-concentrating zone. *Angewandte Chemie International Edition* 58: 12117–12122.

**239** Li, Z., Lu, S., Liu, W. et al. (2021). Synergistic lysozyme-photodynamic therapy against resistant bacteria based on an intelligent upconversion nanoplatform. *Angewandte Chemie International Edition* 60: 19201–19206.

**240** Ma, X., Kang, J., Wu, Y. et al. (2022). Recent advances in metal/covalent organic framework-based materials for photoelectrochemical sensing applications. *TrAC Trends in Analytical Chemistry* 157: 116793.

**241** Lv, J., Xie, J., Mohamed, A.G.A. et al. (2022). Photoelectrochemical energy storage materials: design principles and functional devices towards direct solar to electrochemical energy storage. *Chemical Society Reviews* 51: 1511–1528.

**242** Wang, S., Li, S., Wang, W. et al. (2019). A non-enzymatic photoelectrochemical glucose sensor based on bivo4 electrode under visible light. *Sensors and Actuators B: Chemical* 291: 34–41.

**243** Wang, Y., Rong, Y., Ma, T. et al. (2023). Photoelectrochemical sensors based on paper and their emerging applications in point-of-care testing. *Biosensors and Bioelectronics* 236: 115400.

**244** Devadoss, A., Sudhagar, P., Terashima, C. et al. (2015). Photoelectrochemical biosensors: new insights into promising photoelectrodes and signal amplification strategies. *Journal of Photochemistry and Photobiology C: Photochemistry Reviews* 24: 43–63.

**245** Zhang, J., Shang, M., Gao, Y. et al. (2020). High-performance VS2 QDs-based type II heterostructured photoanode for ultrasensitive aptasensing of lysozyme. *Sensors and Actuators B: Chemical* 304: 127411.

**246** Shang, M., Gao, Y., Zhang, J. et al. (2020). Signal-on cathodic photoelectrochemical aptasensing of insulin: plasmonic Au activated amorphous $MoS_x$ photocathode coupled with target-induced sensitization effect. *Biosensors and Bioelectronics* 165: 112359.

**247** Zhao, W.-W., Xu, J.-J., and Chen, H.-Y. (2015). Photoelectrochemical bioanalysis: the state of the art. *Chemical Society Reviews* 44: 729–741.

**248** Li, Y., Zhang, N., Zhao, W.-W. et al. (2017). Polymer dots for photoelectrochemical bioanalysis. *Analytical Chemistry* 89: 4945–4950.

**249** Zhao, C.-Q. and Ding, S.-N. (2019). Perspective on signal amplification strategies and sensing protocols in photoelectrochemical immunoassay. *Coordination Chemistry Reviews* 391: 1–14.

**250** Liu, T., Ouyang, X., Cheng, X. et al. (2023). Applications of photoelectrochemical sensors for the detection of emerging contaminants. *Energy Environmental Protection* 37: 12–19.

**251** Zhang, Z., Zhang, Y., Yu, H. et al. (2020). Types of biosensor recognition elements and their research progress in clinical testing. *Chinese Journal of Clinical Laboratory Science* 38: 767–771.

**252** Xu, M., Lin, L., Jin, G. et al. (2022). Two-in-one: portable piezoelectric and plasmonic exciton effect-based co-enhanced photoelectrochemical biosensor for point-of-care testing of low-abundance cancer markers. *Biosensors and Bioelectronics* 211: 114413.

**253** Long, D., Tu, Y., Chai, Y., and Yuan, R. (2021). Photoelectrochemical assay based on $SnO_2$/BiOBr p–n heterojunction for ultrasensitive DNA detection. *Analytical Chemistry* 93: 12995–13000.

**254** Li, Z., Lu, J., Wu, F. et al. (2023). Polarity conversion of the $Ag_2S/AgInS_2$ heterojunction by radical-induced positive feedback polydopamine adhesion for signal-switchable photoelectrochemical biosensing. *Analytical Chemistry* 95: 15008–15016.

**255** Lee, T., Baac, H.W., Li, Q., and Guo, L.J. (2018). Efficient photoacoustic conversion in optical nanomaterials and composites. *Advanced Optical Materials* 6: 1800491.

**256** Liu, Y., Teng, L., Yin, B. et al. (2022). Chemical design of activatable photoacoustic probes for precise biomedical applications. *Chemical Reviews* 122: 6850–6918.

**257** Fu, Q., Zhu, R., Song, J. et al. (2018). Photoacoustic imaging: contrast agents and their biomedical applications. *Advanced Materials* 31: 1805875.

**258** Wang, J., Xie, K., Ren, W. et al. (2022). Material composition and application progress of photoacoustic transducer. *Journal of Sensor Technology and Application* 10: 528–537.

**259** Park, B., Park, S., Kim, J., and Kim, C. (2022). Listening to drug delivery and responses via photoacoustic imaging. *Advanced Drug Delivery Reviews* 184: 114235.

**260** Hong, G., Antaris, A.L., and Dai, H. (2017). Near-infrared fluorophores for biomedical imaging. *Nature Biomedical Engineering* 1: 0010.

**261** Yang, Q., Ma, Z., Wang, H. et al. (2017). Rational design of molecular fluorophores for biological imaging in the NIR-II window. *Advanced Materials* 29: 1605497.

**262** Antaris, A.L., Chen, H., Cheng, K. et al. (2015). A small-molecule dye for NIR-II imaging. *Nature Materials* 15: 235–242.

**263** Lyu, Y. and Pu, K. (2017). Recent advances of activatable molecular probes based on semiconducting polymer nanoparticles in sensing and imaging. *Advanced Science* 4: 1600481.

**264** Upputuri, P.K. and Pramanik, M. (2020). Recent advances in photoacoustic contrast agents for in vivo imaging. *WIREs Nanomedicine and Nanobiotechnology* 12: 1618.

**265** Wang, L.V. and Hu, S. (2012). Photoacoustic tomography: in vivo imaging from organelles to organs. *Science* 335: 1458–1462.

**266** Liu, X., Duan, Y., and Liu, B. (2021). Nanoparticles as contrast agents for photoacoustic brain imaging. *Aggregate* 2: 4–19.

**267** Lin, L. and Wang, L.V. (2022). The emerging role of photoacoustic imaging in clinical oncology. *Nature Reviews Clinical Oncology* 19: 365–384.

**268** Park, B., Oh, D., Kim, J., and Kim, C. (2023). Functional photoacoustic imaging: from nano-and micro- to macro-scale. *Nano Convergence* 10: 29.

**269** Zhang, J., Qiao, Z., Yang, P. et al. (2014). Recent advances in near-infrared absorption nanomaterials as photoacoustic contrast agents for biomedical imaging. *Chinese Journal of Chemistry* 33: 35–52.

**270** Shan, T., Zhao, Y., Jiang, S., and Jiang, H. (2020). In-vivo hemodynamic imaging of acute prenatal ethanol exposure in fetal brain by photoacoustic tomography. *Journal of Biophotonics* 13: e201960161.

**271** Moreno, M.J., Ling, B., and Stanimirovic, D.B. (2020). In vivo near-infrared fluorescent optical imaging for CNS drug discovery. *Expert Opinion on Drug Discovery* 15: 903–915.

**272** Mukaddim, R.A., Rodgers, A., Hacker, T.A. et al. (2018). Real-time in vivo photoacoustic imaging in the assessment of myocardial dynamics in murine model of myocardial ischemia. *Ultrasound in Medicine & Biology* 44: 2155–2164.

**273** He, H., Schönmann, C., Schwarz, M. et al. (2022). Fast raster-scan optoacoustic mesoscopy enables assessment of human melanoma microvasculature in vivo. *Nature Communications* 13: 2803.

**274** Li, Y.-Y., Hu, Z.-B., Sun, H.-T., and Sun, Z.-R. (2020). Density functional theory studies on the excited-state properties of bilirubin molecule. *Acta Physica Sinica* 69: 163101.

**275** Björkegren, J.L.M. and Lusis and A.J. (2022). Atherosclerosis: recent developments. *Cell* 185: 1630–1645.

**276** Bai, S., Lan, Y., Fu, S. et al. (2022). Connecting calcium-based nanomaterials and cancer: from diagnosis to therapy. *Nano-Micro Letters* 14: 145.

**277** Thiabaud, G.D., Schwalm, M., Sen, S. et al. (2023). Texaphyrin-based calcium sensor for multimodal imaging. *ACS Sensors* 8: 3855–3861.

**278** Zhang, X., Wu, Y., Chen, L. et al. (2023). Optical and photoacoustic imaging in vivo: opportunities and challenges. *Chemical and Biomedical Imaging* 1: 99–109.

**279** Kruger, R.A., Liu, P., Fang, Y.R., and Appledorn, C.R. (1998). Photoacoustic ultrasound (PAUS)-reconstruction tomography. *Medical Physics* 22: 1605–1609.

**280** Wu, Y., Zeng, F., Zhao, Y., and Wu, S. (2021). Emerging contrast agents for multispectral optoacoustic imaging and their biomedical applications. *Chemical Society Reviews* 50: 7924–7940.

**281** Ouyang, J., Xie, A., Zhou, J. et al. (2022). Minimally invasive nanomedicine: nanotechnology in photo-/ultrasound-/radiation-/magnetism-mediated therapy and imaging. *Chemical Society Reviews* 51: 4996–5041.

**282** Liu, Y., Yu, W., Wang, J. et al. (2021). Application of bismuth-based nanomaterials in imaging diagnosis and therapy for cancer. *Chinese Journal of Inorganic Chemistry* 37: 1–15.

**283** Yang, Y., Chu, B., Cheng, J. et al. (2022). Bacteria eat nanoprobes for aggregation-enhanced imaging and killing diverse microorganisms. *Nature Communications* 13: 1255.

**284** Kim, M., VanderLaan, D., Lee, J. et al. (2023). Hyper-branched gold nanoconstructs for photoacoustic imaging in the near-infrared optical window. *Nano Letters* 23: 9257–9265.

**285** Gong, F., Cheng, L., and Liu, Z. (2020). Application of nanoprobes in photoacoustic cancer imaging. *Laser and Optoelectronics Progress* 57: 180004.

**286** Zhou, Z., Li, B., Shen, C. et al. (2020). Metallic 1t phase enabling $MoS_2$ nanodots as an efficient agent for photoacoustic imaging guided photothermal therapy in the near-infrared-II window. *Small* 16: 2004173.

**287** Han, Y., Yi, H., Wang, Y. et al. (2022). Ultrathin zinc selenide nanoplatelets boosting photoacoustic imaging of in situ copper exchange in Alzheimer's disease mice. *ACS Nano* 16: 19053–19066.

**288** Dai, C., Chen, Y., Jing, X. et al. (2017). Two-dimensional tantalum carbide (MXenes) composite nanosheets for multiple imaging-guided photothermal tumor ablation. *ACS Nano* 11: 12696–12712.

**289** Li, J., Lu, X., Fu, Y. et al. (2021). Research progress of novel graphene-like two-dimensional nanomaterials applied in photoacoustic imaging of tumor. *Chinese Bulletin of Life Sciences* 33: 479–489.

**290** Yang, Z., Xu, T., Li, H. et al. (2023). Zero-dimensional carbon nanomaterials for fluorescent sensing and imaging. *Chemical Reviews* 123: 11047–11136.

**291** Gifani, M., Eddins, D.J., Kosuge, H. et al. (2021). Ultraselective carbon nanotubes for photoacoustic imaging of inflamed atherosclerotic plaques. *Advanced Functional Materials* 31: 2101005.

**292** Sun, Z., Zhao, Y., Li, Z. et al. (2017). $TiL_4$-coordinated black phosphorus quantum dots as an efficient contrast agent for in vivo photoacoustic imaging of cancer. *Small* 13: 1602896.

**293** Zeng, Y., Dou, T., Ma, L., and Ma, J. (2022). Biomedical photoacoustic imaging for molecular detection and disease diagnosis: "always-on" and "turn-on" probes. *Advanced Science* 9: 2202384.

**294** Liu, Y., Teng, L., Liu, H.-W. et al. (2019). Recent advances in organic-dye-based photoacoustic probes for biosensing and bioimaging. *Science China Chemistry* 62: 1275–1285.

**295** Jiang, Y. and Pu, K. (2017). Advanced photoacoustic imaging applications of near-infrared absorbing organic nanoparticles. *Small* 13: 1700710.

**296** Li, J., Wang, J., Xu, L. et al. (2023). A class of activatable NIR-II photoacoustic dyes for high-contrast bioimaging. *Angewandte Chemie International Edition* 202312632.

**297** Ahmadi, S., Rabiee, N., Bagherzadeh, M. et al. (2020). Stimulus-responsive sequential release systems for drug and gene delivery. *Nano Today* 34: 100914.

**298** Jack, C.R. (2022). Advances in Alzheimer's disease research over the past two decades. *The Lancet Neurology* 21: 866–869.

**299** Song, Y., Jing, H., Vong, L.B. et al. (2022). Recent advances in targeted stimuli-responsive nano-based drug delivery systems combating atherosclerosis. *Chinese Chemical Letters* 33: 1705–1717.

**300** Overchuk, M. and Zheng, G. (2018). Overcoming obstacles in the tumor microenvironment: recent advancements in nanoparticle delivery for cancer theranostics. *Biomaterials* 156: 217–237.

**301** Khattab, M., Mansour, H., Fawzy, H., and El-Khatib, A. (2022). Repurposed anti-cancer epidermal growth factor receptor inhibitors: mechanisms of neuroprotective effects in Alzheimer's disease. *Neural Regeneration Research* 17: 1913.

**302** Zhao, L., Meng, F., Li, Y. et al. (2023). Multivalent nanobody conjugate with rigid, reactive oxygen species scavenging scaffold for multi-target therapy of Alzheimer's disease. *Advanced Materials* 35: 2210879.

**303** Peng, S., Xiao, F., Chen, M., and Gao, H. (2021). Tumor-microenvironment-responsive nanomedicine for enhanced cancer immunotherapy. *Advanced Science* 9: 2103836.

**304** Chen, Q., Liu, X., Chen, J. et al. (2015). A self-assembled albumin-based nanoprobe for in vivo ratiometric photoacoustic pH imaging. *Advanced Materials* 27: 6820–6827.

**305** Wang, X., Wang, X., Jin, S. et al. (2019). Stimuli-responsive therapeutic metallodrugs. *Chemical Reviews* 119: 1138–1192.

**306** Jiao, Y.T., Kang, Y.R., Wen, M.Y. et al. (2023). Fast antioxidation kinetics of glutathione intracellularly monitored by a dual-wire nanosensor. *Angewandte Chemie International Edition* 62: e202313612.

**307** Niu, B., Liao, K., Zhou, Y. et al. (2021). Application of glutathione depletion in cancer therapy: enhanced ROS-based therapy, ferroptosis, and chemotherapy. *Biomaterials* 277: 121110.

**308** Hecht, F., Zocchi, M., Alimohammadi, F., and Harris, I.S. (2023). Regulation of antioxidants in cancer. *Molecular Cell* 11: 001.

**309** Matuz-Mares, D., Riveros-Rosas, H., Vilchis-Landeros, M.M., and Vázquez-Meza, H. (2021). Glutathione participation in the prevention of cardiovascular diseases. *Antioxidants* 10: 1220.

**310** Verkhratsky, A., Butt, A., Li, B. et al. (2023). Astrocytes in human central nervous system diseases: a frontier for new therapies. *Signal Transduction and Targeted Therapy* 8: 396.

**311** Park, S., Kim, Y.A., Lee, J. et al. (2023). 4-Hydroxycinnamic acid attenuates neuronal cell death by inducing expression of plasma membrane redox enzymes and improving mitochondrial functions. *Food Science and Human Wellness* 12: 1287–1299.

**312** Wang, A., Mao, Q., Zhao, M. et al. (2020). pH/reduction dual stimuli-triggered self-assembly of NIR theranostic probes for enhanced dual-modal imaging and photothermal therapy of tumors. *Analytical Chemistry* 92: 16113–16121.

**313** Somaa, F. (2021). A review of the application of hyperbaric oxygen therapy in Alzheimer's disease. *Journal of Alzheimer's Disease* 81: 1361–1367.

**314** Liang, X., Li, H., Li, X. et al. (2023). Highly sensitive $H_2O_2$-scavenging nano-bionic system for precise treatment of atherosclerosis. *Acta Pharmaceutica Sinica B* 13: 372–389.

**315** Chen, M., Knox, H.J., Tang, Y. et al. (2019). Simultaneous photoacoustic imaging of intravascular and tissue oxygenation. *Optics Letters* 44: 3773.

**316** de Visser, K.E. and Joyce, J.A. (2023). The evolving tumor microenvironment: from cancer initiation to metastatic outgrowth. *Cancer Cell* 41: 374–403.

**317** Song, Z., Miao, J., Miao, M. et al. (2023). Cathepsin K-activated probe for fluoro-photoacoustic imaging of early osteolytic metastasis. *Advanced Science* 10: 2300217.

**318** Wang, C., Du, W., Wu, C. et al. (2021). Cathespin B-initiated cypate nanoparticle formation for tumor photoacoustic imaging. *Angewandte Chemie International Edition* 61: 202114766.

**319** Li, L., Chen, H., Shi, Y., and Xing, D. (2022). Human-body-temperature triggerable phase transition of W-$VO_2$@PEG nanoprobes with strong and switchable NIR-II absorption for deep and contrast-enhanced photoacoustic imaging. *ACS Nano* 16: 2066–2076.

**320** Swartchick, C.B. and Chan, J. (2023). Leveraging coordination chemistry to visualize metal ions via photoacoustic imaging. *Current Opinion in Chemical Biology* 74: 102312.

**321** Fang, H., Wang, C., Chen, Y. et al. (2021). A photoacoustic $Zn^{2+}$ sensor based on a merocyanine/xanthene-6-ol hybrid chromophore and its ratiometric imaging in mice. *Inorganic Chemistry Frontiers* 8: 3402–3410.

**322** Wang, S., Sheng, Z., Yang, Z. et al. (2019). Activatable small-molecule photoacoustic probes that cross the blood–brain barrier for visualization of copper(II) in mice with Alzheimer's disease. *Angewandte Chemie International Edition* 58: 12415–12419.